Physiological responses of goldfish and naked mole-rats to chronic hypoxia: Membrane, mitochondrial and molecular mechanisms for metabolic suppression

Elie Farhat

Thesis submitted to the University of Ottawa
in partial Fulfillment of the requirements for the Doctorate in Philosophy degree in Biology

Department of Biology

Faculty of Science

University of Ottawa

Table of Content

Acknowledgements

I want to first and foremost thank my supervisor, Dr. Jean-Michel Weber, for his exceptional guidance and mentorship during my 5 years in his lab. Your constructive criticism and your faith in my abilities inspired me to become a better biologist. I want to thank you for always being there for a chat, whether it was science-related or not. I enjoyed our talks on science, football, music, movies, travel and food. I want to also thank you for opening the door for me to travel and collaborate with some fantastic researchers during my PhD.

I would also like to thank my committee members, Dr. Matthew Pamenter and Dr. Kenneth Storey for their continued support and availability. It has been a privilege to collaborate with Dr. Pamenter on two chapters of my thesis in addition to other projects that are not included here.

Special thanks also go to Dr. Jan Mennigen, Dr. Caroline Romestaing and Dr. Loic Teullier for their support during my time collaborating with them. Thank you Loic for your generous hospitality in Lyon. Your whole group at the Unviersité de Lyon made my 3-months stay in France extremely fun, productive and memorable.

I want to also thank all my lab members that I have had the pleasure of sharing space with since joining in May, 2016 as well as the biograds. In particular, I want to thank Eric Turenne, Johnathon Forbes, Daniel Kostyniuk, Rawan Merhi, Hang Cheng, Mais Jubbouri, Giancarlo Talarico and Liam Eaton who all remain good friends.

Furthermore, I want to thank Bill Fletcher and all the animal care personnel for ensuring the animals were well taken care of.

I want to thank some of my closest friends in Canada, Lebanon, The Netherlands, USA, Italy and France. Your constant support and love despite the distance between some of us has always kept me in good spirits. You were always there to help pick me up if I was feeling down and I am extremely grateful for that. I am proud to say that I am blessed to have you all in my life.

I am also thankful for my family members in Montreal, Gatineau, Ottawa and Lebanon for their love and support. To my family in Montreal, thank you for helping me settle in when I returned to Canada. I will always be grateful for your generous hospitality that made the start of this phase of my life easier. To my family in Gatineau and Ottawa, thank you for making me feel at home. To my family in Lebanon, thank you for your love and support. I will always keep your kind words of encouragement in my heart.

Last, but certainly not least, I want to thank my father and best friend, Farhat “Frank” Farhat for always being there for me. You have always been my idol and the closest person to my heart. You have always inspired me to be confident and persevering in accomplishing my goals. Words will never be enough to explain my gratitude to you. I am incredibly lucky and blessed to have you as my dad.

Abstract

Chronic hypoxia is a state of oxygen limitation that is common in many aquatic and terrestrial environments. Metabolic suppression is an essential strategy that is used by hypoxia-tolerant champions such as goldfish and naked mole-rats to cope with prolonged low oxygen. This thesis examines the physiological processes used by goldfish and naked mole-rats to survive in low oxygen environments. It proposes a novel mechanism - the remodeling of membrane lipids - to reduce ATP use and production. Temperature (homeoviscous adaptation), diet (natural doping in migrant birds) and body mass (membrane pacemaker of metabolism) have an impact on the lipid composition of membranes that, in turn, modulates metabolism. In chapters 2 and 3 of this thesis, I demonstrate that vertebrate champions of hypoxia tolerance undergo extensive changes in membrane lipid composition upon *in vivo* exposure to low oxygen. These changes and those observed in hibernating mammals can promote the downregulation of Na^+/K^+-ATPase (major ATP consumers), mitochondrial respiration capacity [OXPHOS (phosphorylating conditions), proton leak (non-phosphorylating conditions), cytochrome c oxidase], and energy metabolism (β-oxidation and glycolysis) as discussed in chapters 3 and 4. A common membrane signal regulating the joint inhibition of ion pumps and channels could be an exquisite way to preserve the balance between ATP supply and demand in hypometabolic states. In chapter 5, I show that the reduction in ATP turnover is also orchestrated by mechanisms that involve post-translational and post-transcriptional modifications and epigenetic changes. Membrane remodeling, together with these more traditional molecular mechanisms, could work in concert to cause metabolic suppression.

Résumé

L'hypoxie chronique est un état de manque en oxygène commun dans de nombreux environnements aquatiques et terrestres. La suppression métabolique est une stratégie essentielle utilisée par les champions de la tolérance à l'hypoxie tels que les poissons rouges et les rats-taupes nus pour faire face à un manque d'oxygène prolongé. Cette thèse examine les processus physiologiques utilisés par les poissons rouges et les rats-taupes nus pour survivre dans des environnements à faible teneur en oxygène. Elle propose un nouveau mécanisme - le remodelage des lipides membranaires - pour réduire l'utilisation et la production d'ATP. La température (adaptation homéovisqueuse), le régime alimentaire (dopage naturel chez les oiseaux migrateurs) et la masse corporelle (théorie du pacemaker membranaire du métabolisme) ont un impact sur la composition lipidique des membranes qui, à son tour, module le métabolisme. Dans les chapitres 2 et 3 de cette thèse, je démontre que les vertébrés champions de la tolérance à l'hypoxie subissent des changements importants dans la composition de leurs lipides membranaires lors d'une exposition *in vivo* à un manque d'oxygène. Ces changements et ceux observés chez les mammifères hibernateurs peuvent favoriser l'inhibition de la Na^+/K^+-ATPase (un consommateur important d'ATP), de la capacité respiratoire mitochondriale [OXPHOS (conditions de phosphorylation), de la fuite de protons (conditions non phosphorylantes), de la cytochrome c oxydase] et du métabolisme énergétique (β-oxydation et glycolyse) comme discuté dans les chapitres 3 et 4. Un signal membranaire commun régulant l'inhibition conjointe des pompes et des canaux ioniques pourrait être un excellent moyen de préserver l'équilibre entre l'offre et la demande d'ATP dans les états hypométaboliques. Au chapitre 5, je montre que la réduction du taux de renouvellement

de l'ATP est aussi orchestrée par des mécanismes impliquant des modifications post-traductionnelles et post-transcriptionnelles et des changements épigénétiques. Le remodelage membranaire, de concert avec ces mécanismes moléculaires plus traditionnels, pourraient fonctionner ensemble pour causer la suppression métabolique.

List of Figures

List of Tables

List of Abbreviations

14:0 Myristic acid

16:0 Palmitic acid

16:1 Palmitoleic acid

18:0 Stearic acid

18:1 Oleic acid

18:2 Linoleic acid

18:3 α-Linolenic acid

20:0 Arachidic acid

20:2 Eicosadienoic acid

20:4 Arachidonic acid

20:5 Eicosapentaenoic acid

22:0 Behenic acid

22:3 Docosatrienoic acid

22:5 Docosapentaenoic acid

22:6 Docosahexaenoic acid

24:0 Lignoceric acid

ago2a argonaute-2

AMPK 5'-AMP-activated protein kinase

ANOVA Analysis of variance

ATP Adenosine triphosphate

β-oxidation Beta-oxidation

BSA Bovine serum albumin

Ca^{2+}-ATPase Calcium adenosine triposphatase

Ca^{2+}-dependent K^{+} channel Calcium-dependent potassium channel

(Ca^{2+}, Mg^{2+})-ATPase (Calcium, magnesium)-adenosine triposphatase

CCCP Carbonyl cyanide m-chlorophenyl hydrazine

COX Cytochrome c oxidase

CPT Carnitine palmitoyltransferase

CS Citrate synthase

cyp7a cholesterol 7alpha-hydroxylase gene

DBI Double Bond Index

DHA Docosahexaenoic acid

egln Egl nine gene

ETC Electron Transport Chain

FA Fatty acid

GABA Gamma aminobutyric acid

HIF Hypoxia Inducible Factor

HK Hexokinase

hmgcs1 hydroxymethylglutaryl-CoA synthase gene

HOAD 3-hydroxyacyl CoA dehydrogenase

LDH Lactate dehydrogenase

LEAK Nonphosphorylating respiration

lxr liver X receptor gene

miRNA micro ribonucleic acid

mRNA Mature ribonucleic acid

MUFA Monounsaturated fatty acid

Na^+/K^+-ATPase Sodium/potassium-adenosine triposphatase

NMR Naked mole-rat

OXPHOS Oxidative phosphorylation

PCM Palmitoylcarnitine/malate

PEP Phosphoenolpyruvate

PFK Phosphofructokinase

PK Pyruvate kinase

PL Phospholipid

PM Pyruvate/malate

PUFA Polyunsaturated fatty acid

RCR Respiratory control ratio

RM-ANOVA: repeated-measures two-way analysis of variance

ROS Reactive oxygen species

s.e.m: Standard error of the mean

SERCA Sarcoplasmic reticulum Ca2+-adenosine triposphatase

SFA Saturated fatty acid

State 3 OXPHOS in the presence of substrates and ADP

State 4 LEAK after ADP depletion

TCA Tricarboxylic acid cycle

tet ten-eleven translocation

$\dot{V}CO_2$ Carbon dioxide production

$\dot{V}O_2$ Oxygen consumption

Chapter 1

General Introduction

This chapter and chapter 6 are based on a manuscript titled “Hypometabolic responses to chronic hypoxia: a potential role for membrane lipids”

Written by

Elie Farhat and Jean-Michel Weber

And published in

Metabolites

https://doi.org/10.3390/metabo11080503

Statement of contribution: I performed the literature search and wrote the manuscript. Dr. Weber edited the manuscript with me.

1.1. Hypoxia

Hypoxia is a ubiquitous state of low oxygen (O_2) common to many aquatic and terrestrial environments. It occurs in warm waters where O_2 solubility is low, in ice-covered lakes and streams where exchange through the surface is restricted, at high altitude, and in deep underground burrows (Diaz and Rosenberg, 2008; Lutz and Storey, 2010; Richards et al., 2009). Global warming is exacerbating the problem, particularly in oceans, where oxygen minimum “dead” zones are expanding rapidly (Stramma et al., 2008). Except for a few unusually tolerant species, hypoxia is lethal to most animals as they eventually fail to match ATP supply with demand (Hochachka, 1986). Champions of hypoxia tolerance like some cyprinid fish, freshwater turtles and African mole rats can easily withstand several weeks of low O_2 by suppressing their metabolic rate (Bickler and Buck, 2007; Pamenter et al., 2018). This critical response can only be achieved through the parallel downregulation of ATP-consuming processes (Hochachka, 1986) and energy metabolism (Martínez et al., 2006; Solaini et al., 2010; Storey, 1997). The simultaneous reduction in ATP supply and demand is realized via post-translational and post-transcriptional modifications involving phosphorylation/dephosphorylation reactions, association of enzymes with subcellular structures (Storey and Storey, 1990), activation of 5’-AMP-activated protein kinase (AMPK), an inhibitor of protein synthesis (Pamenter, 2014), and epigenetic mechanisms (Storey, 2015).

1.2. Membranes

Membranes are essential structures that define cellular boundaries. Membranes of eukaryotic cells are present externally (plasma membrane surrounding the cell) and

internally (membranes surrounding cellular organelles such as mitochondria). Membranes are indispensable for life because they isolate and protect cellular organelles from the environment, and they organize selective intracellular pathways. Biological membranes are fluid in nature and are primarily composed of phospholipids, cholesterol and proteins (Spector and Yorek, 1985). Together they form the fluid mosaic model where the phospholipid polar head groups face the outside surfaces of the bilayer and the hydrophobic fatty acid tails face each other (Singer and Nicolson, 1972). The fatty acid tails can be saturated (no double bonds), monounsaturated (one double bond) or polyunsaturated (two or more double bonds) hydrocarbon chains of lengths varying from 14 to 22 carbons (Hulbert, 2003). Eukaryotic membranes have a desaturase enzyme system that introduces double bonds to the acyl chains. Most vertebrates can obtain these desaturases from their diets because they lack the enzymes needed to produce the omega-3 (n-3) and omega-6 (n-6) desaturases (Tocher et al., 1998). The double bonds of polyunsaturated fatty acids cause the fatty acids to kink. This means that the saturated fatty acids are packed up closely together in contrast to unsaturated fatty acids that are more loosely packed (Hazel, 1995; Raynard and Cossins, 1991). Cholesterol intercalates between phospholipids in the bilayer causing a change in the membrane permeability depending on the temperature. Moreover, cholesterol disrupts fatty acid interactions causing an increase in membrane fluidity depending on the temperature (Crockett and Hazel, 1995; Crockett, 1998; Robertson and Hazel, 1995). Membrane proteins can be present anywhere on the bilayer, and they are essential for selectively controlling the transport of molecules between compartments (Cockburn et al., 2004). Examples of membrane proteins

include ion channels (Katz et al., 1982), enzymes like ATP synthase and carnitine palmitoyltransferase (CPT) (Guo et al., 2005; Yoshida et al., 2001) as well as ion pumps like Na^+/K^+ - ATPase that establish gradients (Glitsch, 2001). The activity of these membrane proteins contribute to the bulk of the cellular-generated metabolic rate (Hulbert and Else, 2000). Membrane protein activity can be modulated by changes in the lipid composition of membranes (Murphy, 1990). Compositional changes which can affect protein activity include changes in fatty acid composition and cholesterol (Seebacher et al., 2010). This can include changes in the degree of unsaturation, the ratio of n-3 to n-6 polyunsaturated fatty acids (Murphy, 1990), the chain lengths of membrane phospholipids (Lee, 2004) as well as cholesterol content that modulates the activity of Na^+/K^+ - ATPase (Crockett and Hazel, 1997; Garcia et al., 2019; Yeagle, 1989; Yeagle et al., 1988). The interactions between membrane proteins and cholesterol can form lipid rafts whereby the function of some proteins is affected (Turk and Chapkin, 2013). The lipid rafts increase the thickness of the lipid bilayer, leading to an increase in the fatty acid chain length of the phospholipids. Lipid rafts also recruit proteins with long transmembrane domains resulting in the activation of signaling cascades (Simons and Toomre, 2000). Specialized membranes can be differentiated from each other by the presence of certain lipids. For example, cardiolipin is a phospholipid that is commonly found in inner mitochondrial membranes (Fernandez et al., 2004).

1.2.1. Membrane lipids: response to environmental stress and how they affect metabolism, ion pumps and channels

1.2.1.1. Temperature and toxins

Membrane fluidity varies with temperature (Hulbert and Else, 1999), but most animals manage to maintain it constant by altering their lipid constituents - phospholipids and cholesterol - through a mechanism known as homeoviscous adaptation (Cossins et al., 1981; Hazel, 1995). This response is most common in ectotherms (Crockett, 1998; Hazel, 1995; Seebacher et al., 2009), but has also been reported in isolated mammalian cells (Anderson et al., 1981). Animals counteract the effects of increasing temperature on membrane fluidity by decreasing the degree of unsaturation and/or increasing the fatty acid chain length of phospholipids (Hulbert and Else, 1999). Because cholesterol affects the interactions between phospholipids, changes in its abundance can be used to stabilize membrane fluidity and cope with a variety of environmental stresses. Cholesterol promotes an “intermediate state” in phospholipids that causes an increase in fluidity below and a decrease in fluidity above the liquid-gel phase transition temperature (Lewis and McElhaney, 1992). It also interacts with the polar head groups of phospholipids to decrease membrane permeability (Crockett, 1998; Demel and De Kruyff, 1976). Interestingly, homeoviscous adaptation can even occur in response to environmental pollutants. For example, goldfish chronically exposed to a membrane fluidizer like PCB-153 can use changes in cholesterol abundance to counteract the effects of the toxin and maintain constant fluidity (Gonzalez et al., 2013).

1.2.1.2. Diet

Membranes are known to be affected by the lipid composition of the diet in various animal groups including fish (Martin et al., 2013), birds (Nagahuedi et al., 2009; Pierce et al., 2005) and mammals (Abbott et al., 2010). Some species use this mechanism strategically to prepare for hibernation (Ruf and Arnold, 2008) or long-distance migration (Weber, 2009). The likelihood of golden-mantled ground squirrels to enter and survive hibernation is greatly increased when they switch from a high polyunsaturated fatty acid (PUFA) diet in the summer to a low PUFA diet in the fall before entering torpor (Frank, 2002). Specific fatty acids such as the omega 6 (n-6) PUFA linoleic acid (n-6 18:2) have been shown to enhance hibernation capacity (Giroud et al., 2018; Ruf and Arnold, 2008). Similarly, some birds drastically improve their ability for aerobic metabolism by feeding on diets high in long-chain n-3 PUFAs. Semipalmated sandpipers double their body mass just before migrating across the Atlantic Ocean between Canada and Brazil by eating large amounts of n-3 PUFA (mud shrimps loaded with eicosapentaenoic acid (n-3 20:5) and docosahexaenoic acid (n-3 22:6)). This “natural doping” strategy greatly improves the aerobic capacity of the long-distance migrant (Maillet and Weber, 2006; Maillet and Weber, 2007), and has been further demonstrated experimentally in sedentary quails (Nagahuedi et al., 2009). Therefore, animals can manipulate the lipid composition of their membranes by selecting particular diets to prime basal metabolism or aerobic capacity for successful hibernation or long-distance migration.

1.2.2. Membrane pacemaker theory of metabolism

The membrane pacemaker theory of metabolism stipulates that the fatty acid composition of membrane phospholipids sets the basal metabolic rate of organisms (Hulbert and Else, 2005). Its original formulation was based on the combined observations that: (i) the mass-specific metabolic rate of animals decreases with body size, (ii) the average number of double bonds in membrane fatty acids also decreases with size, and (iii) integral proteins are activated when membrane unsaturation increases (Hulbert and Else, 2005). This theory was inferred from the correlation between the lipid composition of membranes and body size discovered in mammals (Hulbert and Else, 1999), and was subsequently supported by multiple other studies (Calhoon et al., 2015; Hulbert, 2007). The validity of the pacemaker theory has been questioned, however, because the relationship between body size and membrane composition first characterized in mammals disappears when the effects of phylogeny are taken into account (Valencak and Ruf, 2007). More recently, analyses using orchid bees (Rodriguez et al., 2015) and cypriniform fish (Gonzalez et al., 2015) provide support for the theory, even after correction for phylogeny. If the metabolic rate of organisms can be set by membrane composition on an evolutionary time scale, the same mechanism could be used to suppress metabolism in hypoxia within an animal's lifespan.

1.2.3. Membrane lipids affect enzymes involved in ATP production and utilization

The main pitfall faced by organisms exposed to prolonged hypoxia is their ultimate failure to match ATP supply with demand (Hochachka, 1986). Thus, it is imperative to downregulate ATP-consuming and ATP-supplying processes to survive in

low O_2 environments. This can be achieved by modulating enzymes that play essential roles in regulating ATP use (ATPases) and ATP production (energy metabolism). Current evidence shows that the activities of several such enzymes are affected by their local lipid environment, in particular by the relative abundance of specific fatty acids and cholesterol. Multi-species comparisons for birds and mammals show that Na^+/K^+-ATPase activity is positively correlated with membrane 22:6 abundance (Turner et al., 2003), and a clear functional link between these parameters has been demonstrated with cross-species experiments. Na^+/K^+-ATPase taken from an ectotherm is activated when reconstituted in a mammalian membrane that is richer in 22:6, and the reverse experiment has confirmed that 22:6 is an activator of this essential pump (Else and Wu, 1999; Wu et al., 2004). N-3 PUFAs are also known to downregulate sarcoplasmic reticulum Ca^{2+}-ATPase (SERCA), and n-6 PUFA such as 18:2 upregulate the calcium pump (Arnold et al., 2015). ATPases are also sensitive to the presence of cholesterol. Changing intrinsic cholesterol abundance downregulates Na^+/K^+-ATPase in humans, rabbits, guinea pigs and rats (Crockett and Hazel, 1997; Garcia et al., 2019; Yeagle, 1989; Yeagle et al., 1988), while high levels of the sterol downregulate rabbit (Ca^{2+}, Mg^{2+})-ATPase (Bastiaanse et al., 1997).

Specific membrane fatty acids influence the activities of many enzymes of energy metabolism. N-3 PUFA levels are positively correlated with the activities of tricarboxylic acid (TCA) cycle and β-oxidation enzymes (Arnold et al., 2015). This is evident in sedentary quails (Nagahuedi et al., 2009) and migrant sandpipers (Maillet and Weber, 2007) that activate citrate synthase (CS), 3-hydroxyacyl-CoA dehydrogenase (HOAD) and carnitine palmitoyl transferase (CPT) after eating long-chain n-3 PUFA for a few

weeks. The activity of CPT also increases in the presence of more n-3 20:5 in the membranes of adipocytes (Guo et al., 2005). Fast glycolytic muscles contain more palmitic acid (16:0) and n-6 18:2, but less long-chain PUFA (Alasnier et al., 1996) than slow oxidative muscles, suggesting that glycolytic enzymes are downregulated by long-chain PUFA. No information is currently available about whether modulating membrane cholesterol has similar repercussions on energy metabolism pathways as it does on ATPases. Overall, however, there is strong evidence that altering membrane phospholipids and cholesterol affects ATP supply and demand by activating or inhibiting key enzymes in these processes.

1.2.4. Membrane lipids and ion channels

Reducing ion pump activity in hypoxia is only possible with a matching decrease in ion leak so that vital transmembrane ion gradients are preserved. Therefore, it is essential to examine whether ion channels can also be downregulated by changing the lipid composition of membranes. Ion channels are integral membrane proteins surrounded by lipids and they contain a transmembrane domain that moves within the bilayer (Poveda et al., 2014). Membrane lipids are known to modulate ion channels directly or indirectly via specific lipid-protein interactions. This section reviews known mechanisms whereby changes in membrane PUFAs and cholesterol alter the function of Ca^{2+}, K^{+} and Na^{+} channels as well as nicotinicoid receptors (Poveda et al., 2014; Tillman and Cascio, 2003). Depleting cholesterol experimentally causes an increase in Ca^{2+} uptake through the Ca^{2+} channel and the Na^{+}/Ca^{2+} exchanger of the sarcolemma, whereas cholesterol enrichment decreases conductance of the Ca^{2+}-dependent K^{+} channel (Bastiaanse et al., 1997; Poveda et al., 2014). Negatively charged long chain

fatty acids upregulate Ca^{2+}-activated K^+ channels with the strongest effect observed for cis unsaturated fatty acids (Tillman and Cascio, 2003). Modifying membrane cholesterol from normal levels inhibits K^+ channels (Levitan et al., 2010; Tillman and Cascio, 2003). Moreover, voltage-gated Na^+ channels are inhibited by PUFAs (D'Avanzo, 2016; Kang and Leaf, 1996) and cholesterol (Levitan et al., 2010). This occurs by shifting the steady-state inactivation kinetics of this voltage-gated ion channel in the direction of hyperpolarization, possibly via selective binding to the inactive site of the channel (Kang and Leaf, 1996).

Membrane lipids also impact the function of ligand-gated ion channels such as nicotinicoid receptors. They include the excitatory acetylcholine and serotonin receptors as well as the inhibitory gamma-aminobutyric acid (GABA) receptors that are required to propagate neuronal signals. Functional acetylcholine receptors depend on the presence of both cholesterol and negatively charged phospholipids to support ion flux. On its own, cholesterol also alters the function of GABA, serotonin and acetylcholine receptors because this sterol is necessary for maintaining their optimal activity (Poveda et al., 2014; Tillman and Cascio, 2003). It has also been suggested that a decrease in hippocampal cholesterol levels could reduce N-methyl-D-aspartate receptor signaling (Palomer et al., 2016). Overall, current information clearly shows that membrane lipids do not only modulate ion pumps, but also ion channels.

1.3. Effects of chronic hypoxia on key enzymes regulating ATP supply and demand

Continuing to match ATP supply with demand during hypoxia can be achieved by (i) downregulating aerobic pathways and/or (ii) activating anaerobic metabolism.

Animals that tolerate long-term hypoxia favor selecting the first option because anaerobic glycolysis relies entirely on small carbohydrate stores and has very low efficiency. These two important limitations mean that glycolysis can only proceed for a very short time (Weber, 2011). Reducing overall ATP turnover by downregulating multiple enzymes is therefore essential for survival. This section deals with how chronic hypoxia affects Na^+/K^+-ATPase and key enzymes of energy metabolism.

1.3.1 Na^+/K^+-ATPase

Na^+/K^+-ATPase is an integral protein that is responsible for approximately 25% of total ATP consumption (Rolfe and Brown, 1997). This enzyme requires constant ATP supply to maintain transmembrane Na^+ and K^+ gradients. When ATP production is reduced under O_2-limiting conditions, Na^+/K^+-ATPase becomes the dominant cellular energy sink (Hochachka et al., 1996). This pump is particularly important in the brain where it drives action potentials by regulating Na^+ and K^+ currents. Any failure of its normal function eventually causes a spike in intracellular calcium that can lead to cell death (Hochachka, 1986). Surprisingly, only a handful of studies have examined the effects of chronic hypoxia on Na^+/K^+-ATPase (see Table 1.1) because the bulk of previous research has focused on acute hypoxia or anoxia instead. The hypoxia tolerant crucian carp as well as the rat downregulate Na^+/K^+-ATPase when exposed to chronic hypoxia. Unfortunately, the limited information available does not allow to determine if tolerant and sensitive species show different Na^+/K^+-ATPase responses. Previous studies have mostly examined Na^+/K^+-ATPase in the vertebrate brain, and it will also be important to characterize the effects of chronic hypoxia on other tissues from both, hypoxia-sensitive and -tolerant animals. The general downregulation of Na^+/K^+-ATPase

observed to date (see Table 1.1) suggests that ion channels are also inhibited by prolonged hypoxia to prevent a harmful increase in intracellular calcium.

Table 1.1. Effects of chronic hypoxia (minimum 1 week) on the maximal activity of Na^+/K^+-ATPase in various animals.

Species	Tissue	Na^+/K^+-ATPase response	Reference
Mouse (*Mus musculus)*	Brain	-	(Cáceda et al., 2001)
Rat (*Rattus norvegicus)*	Brain	~30-40% ↓	(Benzi et al., 1994)
Crucian carp (*Carassius carassius)*	Heart	33% ↓	(Paajanen and Vornanen, 2003)

1.3.2. Glycolysis

The overall effects of chronic hypoxia on all glycolytic enzymes are variable, but some trends can be observed in endotherms (Tables 1.2-1.4). No pattern can be found for the glycolytic response of ectotherms, and it is presently unclear whether a general response to chronic hypoxia exists for this group of animals. However, endotherms generally upregulate hexokinase (HK; Table 1.2), maintain phosphofructokinase (PFK; Table 1.3), and downregulate pyruvate kinase (PK; Table 1.4). Because PFK plays a dominant role in the regulation of glycolytic flux (Berg et al., 2007) and is not affected, it appears that endotherms do not modulate glycolysis to cope with chronic hypoxia. The opposite responses shown by HK (activation) and PK (inhibition) also support the notion that hypoxic endotherms simply maintain normal glycolytic supply of ATP. As the last

enzyme of the glycolytic pathway, lactate dehydrogenase (LDH) activity is often used as an indicator of tissue capacity for anaerobic ATP production. The lack of a clear activation or downregulation of LDH by chronic hypoxia in ecto- and endotherms measured to date (Table 1.5) indicates that animals do not generally rely on anaerobic metabolism to survive in hypoxic environments. Moreover, there is no indication that the glycolytic supply of pyruvate to the TCA cycle is reduced to help metabolic suppression in chronic hypoxia.

Table 1.2. Effects of chronic hypoxia (minimum 1 week) on the maximal activity of hexokinase (HK) in various animals.

Species	Tissue	HK response	Reference
Deer mouse (*Peromyscus maniculatus)*	Gastrocnemius	35% ↑	(Lau et al., 2017)
	Gastrocnemius	-	(Lau et al., 2017)
Mouse (*Mus musculus)*	Brain	-	(Cáceda et al., 2001)
Rat (*Rattus norvegicus)*	Gastrocnemius, soleus, heart, brain	8-105% ↑	(Daneshrad et al., 2000; Low et al., 1986; Pastoris et al., 1995; Waskova-Arnostova et al., 2014)
Gulf killifish (*Fundulus grandis)*	Heart, brain	16-28% ↑	(Martínez et al., 2006)
	Liver	-	(Martínez et al., 2006)
	White muscle, red muscle, liver	-	(van den Thillart and Smit, 1984)
Tench (*Tinca tinca)*	White muscle	67% ↓	(Johnston and Bernard, 1982)
	Red muscle, liver	-	(Johnston and Bernard, 1982)
Chinese shrimp (*Fenneropenaeus chinensis)*	pancreas, pleopod, abdominal	24-26% ↓	(Li et al., 2018)

Table 1.3. Effects of chronic hypoxia (minimum 1 week) on the maximal activity of phosphofructokinase (PFK) in various animals.

Species	Tissue	PFK response	Reference
Deer mouse (*Peromyscus maniculatus)*	Gastrocnemius	-	(Lau et al., 2017)
Rat (*Rattus norvegicus)*	Heart, soleus, gastrocnemius, caudal nerve	-	(Daneshrad et al., 2000; Low et al., 1986; Pastoris et al., 1995)
Gulf killifish (*Fundulus grandis)*	White muscle	25% ↓	(Martínez et al., 2006)
	Liver	63% ↑	(Martínez et al., 2006)
	Heart, brain	-	(Martínez et al., 2006)
Nile tilapia (*Oreochromis niloticus)*	Liver, white muscle	59-123 ↑	(Mahfouz et al., 2015)
Tench (*Tinca tinca)*	White muscle	-	(Johnston and Bernard, 1982)
	Red muscle, liver	98-120% ↑	(Johnston and Bernard, 1982)
Chinese shrimp (*Fenneropenaeus chinensis)*	hepatopancreas, pleopod, abdomen	16-31% ↓	(Li et al., 2018)

Table 1.4. Effects of chronic hypoxia (minimum 1 week) on the maximal activity of pyruvate kinase (PK) in various animals.

Species	Tissue	PK response	Reference
Deer mouse (*Peromyscus maniculatus)*	Gastrocnemius	-	(Lau et al., 2017)
Rat (*Rattus norvegicus)*	Heart, soleus	-	(Daneshrad et al., 2000)
	Gastrocnemius	-	(Pastoris et al., 1995)
Mouse (*Mus musculus)*	Liver	65% ↓	(Dukhande et al., 2011)
Northern shrimp (*Pandalus borealis)*	White muscle	-	(Pillet et al., 2016)
Greenland halibut (*Reinhardtius hippoglossoides)*	White muscle	46% ↓	(Pillet et al., 2016)
Common carp (*Cyprinus carpio)*	White muscle	-	(Zhou et al., 2000)
Nile tilapia (*Oreochromis niloticus)*	Liver	61-96% ↑	(Mahfouz et al., 2015)
	White muscle	-	(Mahfouz et al., 2015)
Gulf killifish (*Fundulus grandis)*	White muscle	23% ↓	(Martínez et al., 2006)
	Heart	24% ↑	(Martínez et al., 2006)
	Liver, brain	-	(Martínez et al., 2006)
Goldfish (*Carassius auratus)*	White and red muscle, liver	-	(van den Thillart and Smit, 1984)
Tench (*Tinca tinca)*	White and red muscle	-	(Johnston and Bernard, 1982)
	Liver	86% ↑	(Johnston and Bernard, 1982)
Chinese shrimp (*Fenneropenaeus chinensis)*	hepatopancreas, pleopod, abdominal muscle	14-39% ↓	(Li et al., 2018)

Table 1.5. Effects of chronic hypoxia (minimum 1 week) on the maximal activity of lactate dehydrogenase (LDH) in various animals.

Species	Tissue	LDH response	Reference
Deer mouse (*Peromyscus maniculatus*)	Gastrocnemius, diaphragm	-	(Lui et al., 2015; Nikel et al., 2018)
Mouse (*Mus musculus*)	Hindlimb muscles	28% ↓	(le Moine et al., 2011)
	Brain, liver	-	(Cáceda et al., 2001; Dukhande et al., 2011)
Rat (*Rattus norvegicus*)	Soleus	-	(Daneshrad et al., 2000)
	Gastrocnemius, heart, gastrocnemius and liver mitochondria	25-54% ↑	(Daneshrad et al., 2000; Dutta et al., 2009; Pastoris et al., 1995)
Northern Shrimp (*Pandalus borealis*)	White muscle	45-88% ↓	(Pillet et al., 2016)
Greenland halibut (*Reinhardtius hippoglossoides*)	White muscle	58% ↓	(Pillet et al., 2016)
Common carp (*Cyprinus carpio*)	White muscle	-	(Zhou et al., 2000)
	Liver	~60% ↑	(Zhou et al., 2000)
Nile tilapia (*Oreochromis niloticus*)	Liver, white muscle	80-176% ↑	(Mahfouz et al., 2015)
Gulf killifish (*Fundulus grandis*)	White muscle	30% ↓	(Martínez et al., 2006)
	Liver	30% ↑	(Martínez et al., 2006)
	Heart, brain	-	(Martínez et al., 2006)
Goldfish (*Carassius auratus*)	White and red muscle, liver,	-	(van den Thillart and Smit, 1984)
Tench (*Tinca tinca*)	White and red muscle	-	(Johnston and Bernard, 1982)
	Liver	116% ↑	(Johnston and Bernard, 1982)
Chinese shrimp (*Fenneropenaeus chinensis*)	hepatopancreas, pleopod, abdominal	26-33% ↓	(Li et al., 2018)

1.3.3. TCA cycle

The TCA cycle is an aerobic pathway generating NADH and $FADH_2$ that feed into the mitochondria to yield high amounts of ATP. Reliance on this pathway becomes difficult when O_2 availability is reduced. Most animals respond to chronic hypoxia by downregulating CS in various tissues (Table 1.6). The only study showing CS activation is for the heart in sablefish (Gerber et al., 2019). Accelerating the TCA cycle in the heart of these species may be a strategy to increase cardiac output and maintain adequate oxygen supply to other organs in hypoxia. Overall, however, flux capacity through the TCA cycle is lowered in animals exposed to chronic hypoxia. The general decrease in CS activity also indicates a reduction in mitochondrial density across tissues (DiMauro and Moraes, 1993).

Table 1.6. Effects of chronic hypoxia (minimum 1 week) on the maximal activity of citrate synthase (CS) in various animals.

Species	Tissue	CS response	Reference
Deer mouse (*Peromyscus maniculatus*)	Liver, gastrocnemius, diaphragm	-	(Lau et al., 2017; Lui et al., 2015; Nikel et al., 2018)
Mouse (*Mus musculus*)	Liver mitochondria	34% ↓	(Dutta et al., 2009)
	Hindlimb muscles, heart	-	(le Moine et al., 2011; Templeman et al., 2010)
	Gastrocnemius mitochondria	-	(Dutta et al., 2009)
	Brain, liver	-	(Cáceda et al., 2001; Dukhande et al., 2011)
Rat (*Rattus norvegicus*)	Gastrocnemius	34-39% ↓	(Pastoris et al., 1995)
	Gastrocnemius, heart, liver	-	(Daneshrad et al., 2000; Galbes et al., 2008; Kennedy et al., 2001)
Common carp (*Cyprinus carpio*)	White muscle	~25% ↓	(Zhou et al., 2000)
	Liver	-	(Zhou et al., 2000)
Northern shrimp (*Pandalus borealis*)	White muscle	40% ↓	(Pillet et al., 2016)
Greenland halibut (*Reinhardtius hippoglossoides*)	White muscle	33% ↓	(Pillet et al., 2016)
Chinese shrimp (*Fenneropenaeus chinensis*)	pancreas, pleopod, abdominal	31-70% ↓	(Li et al., 2018)
Sablefish (*Anoplopoma fimbria*)	Heart	20% ↑	(Gerber et al., 2019)

1.3.4. β-oxidation

β-oxidation is a mitochondrial pathway that breaks down fatty acids to acetyl-CoA and fuel the TCA cycle. The transmembrane enzyme CPT exerts the strongest control on flux through β-oxidation (Drynan et al., 1996), and can therefore be modulated by changes in membrane composition. Chronic hypoxia causes a general decrease in CPT (Table 1.7) and HOAD activity (another enzyme that regulates β-oxidation; Table 1.8). The only exception to this pattern is CPT activation in tench liver and red muscle (Johnston and Bernard, 1982). Otherwise, general downregulation of β-oxidation appears to be a common way to adjust ATP supply to the lower ATP demand afforded by hypometabolism.

Table 1.7. Effects of chronic hypoxia (minimum 1 week) on the maximal activity of carnitine palmitoyl transferase (CPT) in various animals.

Species	Tissue	CPT response	Reference
Rat (*Rattus norvegicus*)	Muscle, heart	16-34% ↓	(Galbes et al., 2008; Kennedy et al., 2001)
	Liver, gastrocnemius mitochondria	-	(Dutta et al., 2009; Kennedy et al., 2001)
Mouse (*Mus musculus*)	Skeletal muscle	65% ↓	(Morash et al., 2013)
	Heart	-	(Morash et al., 2013)
Tench (*Tinca tinca*)	Red muscle, liver	162-236% ↑	(Johnston and Bernard, 1982)
	White muscle	-	(Johnston and Bernard, 1982)

Table 1.8. Effects of chronic hypoxia (minimum 1 week) on the maximal activity of 3-hydroxyacyl-CoA dehydrogenase (HOAD) in various animals.

Species	Tissue	HOAD response	Reference
Deer mouse (*Peromyscus maniculatus*)	Gastrocnemius, liver	-	(Lau et al., 2017)
Mouse (*Mus musculus*)	Left ventricle	36% ↓	(Templeman et al., 2010)
Rat (*Rattus norvegicus*)	Heart, skeletal, liver and liver mitochondria	20-71% ↓	(Daneshrad et al., 2000; Dutta et al., 2009; Galbes et al., 2008; Kennedy et al., 2001)
	Soleus, gastrocnemius mitochondria	-	(Daneshrad et al., 2000; Dutta et al., 2009)
Mouse (*Mus musculus*)	Heart, skeletal	-	(Morash et al., 2013)

1.4. Effects of chronic hypoxia on mitochondria

Mitochondria are major O_2 consumers that produce ATP through oxidative phosphorylation: a process that couples the electron transport chain (ETC = enzyme complexes I to IV) with ATP synthase (complex V). The ETC pumps protons across the inner mitochondrial membrane to establish an electrochemical gradient that is used to phosphorylate ADP (McElroy and Chandel, 2017). Oxygen is consumed at complex IV (cytochrome c oxidase, COX): the final electron acceptor that reduces O_2 to water and contributes to generating the proton gradient (Schmidt-Rohr, 2020). All these protein complexes are transmembrane enzymes whose activities are modulated by changes in the phospholipid composition of the bilayer. Mitochondria also produce significant amounts of reactive oxygen species (ROS), particularly at complexes I and III (Quinlan

et al., 2013). These organelles are strategically placed to sense any changes in O_2 and initiate organism-specific responses to hypoxia. Oxygen sensing can be done through a ROS-induced response that may cause rapid accumulation of Ca^{2+} and/or activation of hypoxia inducible factor (HIF) (McElroy and Chandel, 2017). ROS can cause the formation of disulfide bonds, which may change the structure and function of proteins such as phosphatases, transcription factors and those involved in epigenetic modifications (Pamenter, 2014). Severe hypoxia causes the depolarization of mitochondria that leads complex V to switch from ATP production to ATP consumption (St-Pierre et al., 2000a). This exacerbates the existing ATP shortfall already induced by hypoxia and can eventually result in tissue failure. This section deals with the effects of hypoxia on the functional capacity of mitochondria by examining specific responses for the different respiration states and ETC complexes.

1.4.1. Endotherms

The effects of chronic hypoxia on the mitochondria of endotherms have only been investigated in rats and deer mice. After acclimation to hypoxia, rats decrease respiration capacity through ETC complexes I, II and IV in the heart (Heather et al., 2012) as well as state 3 (OXPHOS in the presence of substrates and ADP) and 4 (LEAK after ADP depletion) in the brain (Chávez et al., 1995). However, this response is not always consistent because another study shows no change in rat liver and heart (Costa et al., 1988). Hypoxia-tolerant species like deer mice have different mitochondrial responses than rats to low O_2. They increase mitochondrial respiration (CI, CII and CIV) in the diaphragm (Dawson et al., 2018), but maintain it in the gastrocnemius. In addition, mitochondrial respiration capacity is elevated in high-altitude

vs lowland deer mice (Mahalingam et al., 2017). While not the focus of this review, acute hypoxia causes a decrease in mitochondrial respiration of naked mole-rat (NMR) brain (Pamenter et al., 2018) and human pulmonary arterial endothelial cells (Chan et al., 2009). It is not surprising to find differences between tissues and between species. For endotherms, tissue differences are related to local O_2 demand and species responses depend on the environmental O_2 availability of the whole organism: normoxia (rat), life-long hypoxia (high-altitude deer mouse), intermittent hypoxia (NMR).

1.4.2. Ectotherms

Exposing ectotherms to prolonged hypoxia results in a wide-range of mitochondrial responses that do not follow a general trend. For instance, mitochondrial respiration for various states and tissues is lowered in frogs (St-Pierre et al., 2000b) and eastern oysters (Sokolova, 2018), but remains unchanged in killifish liver (Du et al., 2016) and snapper heart (Cook et al., 2013) after acclimation to hypoxia. Similarly, acute hypoxia causes a wide range of responses in shark mitochondria (Hickey et al., 2012), pacific oysters and hard-shell clams (Sokolova, 2018). However, turtles exposed to anoxia lower mitochondrial respiration in several states and tissues (Bundgaard et al., 2019; Gomez and Richards, 2018; Pamenter et al., 2016). Overall, it is impossible to predict how ectotherm mitochondria respond to chronic hypoxia because some animals maintain respiration capacity while many others prefer to: (i) regulate specific respiration states that impact ATP turnover, (ii) change mitochondrial efficiency, (iii) change mitochondrial abundance, or (iv) use a combination of the above.

1.5. Overview of molecular mechanisms involved in metabolic suppression

Much of the previously detailed responses to hypoxia are mostly controlled by post-transcriptional and post-translational mechanisms via reversible phosphorylation of proteins, DNA methylation as well as changes in relative mRNA and/or microRNA (miRNA) expression. Reversible protein phosphorylation is a post-translational mechanism that is catalyzed by kinases and phosphatases to regulate ATP-demanding processes when animals enter a hypometabolic state (Storey, 2015). This is demonstrated by the phosphorylation-mediated downregulation of ATP-producing catabolic pathways such as glycolysis (Storey and Storey, 2007) and ATP-consuming processes such as protein synthesis when entering a hypometabolic state (Storey and Storey, 2004). DNA methylation is a post-translational mechanism that allows animals to suppress their metabolic rate by repressing transcription (Storey, 2015). Most of the hypoxia-induced molecular responses are controlled by HIF. This transcription factor is composed of an O_2-sensitive α subunit and an O_2-stable β subunit, each consisting of several different forms. HIF can be expressed in many different cells and is responsible for the hypoxic regulation of various genes (Nikinmaa and Rees, 2005) and miRNAs such as miR-210 (Hadj-Moussa and Storey, 2020). MicroRNAs are short, noncoding RNA molecules that are produced canonically (He and Hannon, 2004). miRNA biogenesis begins in the nucleus where primary miRNA genes are transcribed by polymerase II. Primary miRNAs are then processed by DROSHA-dgcr8 complex to yield precursor miRNA that are transported to the cytoplasm by exportin 5. The precursor miRNAs are then cleaved by the Dicer RNAase III endonuclease in the cytoplasm to produce mature 21-23 nucleotide miRNA (Han et al., 2006). Argonaute 2 then mediates

the binding of mature miRNA to the 3'UTR of mRNA as part of the RNA-induced silencing complex. This is done through complementary base-pairing interactions between nucleotides 2 and 8 of the miRNA at the 5' end (Bartel, 2009). Because miRNAs reduce protein output from existing transcripts, they serve as perfect controllers of hypoxia-mediated HIF expression (Nikinmaa and Rees, 2005).

1.6. Thesis objectives

The effects of several environmental stressors on membrane lipid composition are well-documented. Additionally, there is plenty of evidence supporting a link between membrane lipids, maximal enzymatic activity and metabolic rate. The main goal of this thesis is to establish a new mechanism for achieving metabolic suppression during chronic hypoxia that involves altering membrane lipid composition. To test my hypothesis, I will examine the effects of chronic hypoxia on membrane lipids and ATP consuming and producing processes in the goldfish and the naked mole-rat. These champions are known for their exceptional tolerance to chronic hypoxia, which is crucial for performing the required prolonged low O_2 acclimation. This thesis is divided into 4 data chapters, of which the first three are published, and a conclusion chapter.

(1) Surprisingly, no prior studies have been done to examine the effects of chronic hypoxia on membrane lipids. In my first data chapter, I investigate the effects of chronic hypoxia on the lipid composition of goldfish membranes and on metabolic rate at two temperatures. Two different temperatures are chosen because of (i) the known association between high temperature and O_2 solubility and (ii) the known impact of temperature changes on membrane lipids. I hypothesize that goldfish remodel their membrane lipids in ways that promote metabolic suppression.

(2) After finding that goldfish remodel their membrane lipid composition in chronic hypoxia, I sought out to determine if this response is specific to ectotherms or common to other hypoxia-tolerant champions. Therefore, I collaborate with Dr. Matthew Pamenter to study the effects of chronic hypoxia on the naked mole-rat (NMR) for my second data chapter. In this chapter, I examine the effects of chronic hypoxia on membrane lipid composition, metabolic rate and maximal enzymatic activity in the NMR. I hypothesize that NMRs would remodel their membranes in ways that are similar to goldfish and downregulate maximal enzymatic activities while suppressing their metabolic rate.

(3) For my third data chapter, I aimed to quantify the effects of chronic hypoxia on goldfish enzymes involved in ATP supply and demand. Moreover, I sought to investigate the effects of long-term acclimation to hypoxia on goldfish mitochondria because they are (i) excellent oxygen sensors, (ii) major producers of cellular ATP and (iii) known to impact metabolic rate. I hypothesize that goldfish downregulate the activities of key enzymes and lower mitochondrial respiration following hypoxia acclimation.

(4) Because plenty of research confirms a role of molecular mechanisms in controlling all the endpoints I study in my first 3 data chapters, I aimed to investigate how this happens in hypoxic goldfish. In a collaboration with Dr. Jan Mennigen, I rely on the recently published goldfish genome to examine the effects of chronic hypoxia on (i) hypoxia sensing, (ii) post-transcriptional and post-translational as well as epigenetic processes (DNA methylation, miRNA biogenesis) and (iii) lipid transcripts (cholesterol

biosynthesis and β-oxidation). I hypothesize that hypoxic goldfish suppress transcription and translation to support metabolic suppression.

(5) In my conclusion chapter, I revisit the results of my four data chapters and discuss how they promote metabolic suppression. I conclude by addressing the main question of this thesis: Do membrane lipids contribute to achieving metabolic suppression in chronic hypoxia?

Chapter 2

Hypoxia-induced remodelling of goldfish membranes

Based on a manuscript by the same title

Written by

Elie Farhat, Eric D. Turenne, Kevin Choi and Jean-Michel Weber

And published in

Comparative Biochemistry and Physiology Part B: Biochemistry and Molecular Biology

https://doi.org/10.1016/j.cbpb.2019.110326

Statement of contribution: This work was performed alongside Eric Turenne and Kevin Choi.
Kevin acclimated the goldfish at 13°C and measured fatty acid composition of membrane phospholipids in brain. Eric measured cholesterol abundance in all tissues at 13°C. I measured the fatty acid composition of goldfish membranes at 13°C (liver, white muscle and gill) and 20°C (all tissues). Moreover, I measured cholesterol abundance of all tissues at 20°C, performed the metabolic rate measurements of all animals (at both 13°C and 20°C) and measured whole-body ethanol. Finally, I wrote the paper as first author and edited it with Dr. Weber.

2.1. Introduction

Hypoxia commonly occurs in aquatic environments through eutrophication and thermal stratification, but the widespread use of fertilizers and global warming are exacerbating the problem (Diaz and Rosenberg, 2008). Species particularly tolerant to hypoxia use metabolic suppression as their key strategy to cope with a lack of oxygen that normally kills most animals (Bickler and Buck, 2007; Richards, 2011; Seibel, 2011). Among teleosts, goldfish are renowned for their outstanding capacity to endure prolonged hypoxia (Nilsson, 2010). They can survive low O_2 stress for months (Richards, 2011), but their ability for metabolic suppression (a 42 to 56 % decrease in metabolic rate) has only been investigated for the first few hours of hypoxia (van Ginneken et al., 2004; Van Waversveld et al., 1989). It is unclear whether longer exposure lasting several weeks would cause further suppression. Known mechanisms to slow metabolism include downregulating ion pumps such as Na^+/K^+-ATPase (Hochachka, 1986), reducing flux through anabolic pathways such as protein synthesis, and inhibiting key enzymes of energy metabolism (Richards, 2009; Storey and Storey, 2004). Cold-acclimated goldfish can also tolerate very long periods of complete anoxia by producing ethanol (Shoubridge and Hochachka, 1980; Weber, 2016).

Ectotherms modulate the lipid composition of membranes to deal with changes in temperature (Hazel, 1995) or when they are exposed to membrane-fluidizing pollutants (Gonzalez et al., 2013). These homeoviscous responses mitigate the changes in membrane fluidity caused by environmental stress that would otherwise jeopardize normal membrane function (Hazel, 1995). Fluidity and permeability are modulated by changing both the fatty acid (FA) composition of phospholipids (PL) and the relative

abundance of cholesterol (Bell et al., 1986). Hypoxia has also been shown to alter the FA composition of membranes, but only in isolated mammalian cells (Block et al., 1989; Ježková et al., 2002). In fish, van Raaij et al (van Raaij et al., 1994) have shown that low oxygen affects the FA composition of total tissue lipids, but their study does not provide specific information about membrane lipids. Therefore, it is unclear whether chronic hypoxia could cause the restructuring of fish membranes.

The activity of key integral proteins like ion pumps is modulated by changes in the lipid composition of membranes (Harayama and Riezman, 2018). These proteins include Na^+/K^+-ATPase and Ca^{2+}-ATPase that can account for a large fraction of resting metabolic rate (Rolfe and Brown, 1997). Their activity depends on bulk properties like membrane order and permeability, or on direct interactions with specific FAs or with cholesterol (Bastiaanse et al., 1997; Calhoon et al., 2015; Yeagle, 2012). In particular, docosahexanoic acid (n-3 22:6) is a well characterized activator of Na^+/K^+-ATPase (Calhoon et al., 2015; Turner et al., 2005), and cholesterol is an inhibitor of both Ca^{2+}-ATPase (Li et al., 2004) and Na^+/K^+-ATPase (Crockett and Hazel, 1997; Kimelberg and Papahadjopoulos, 1974). Diverse approaches have been used to demonstrate the stimulating effect of 22:6 on Na^+/K^+-ATPase. They include the manipulation of 22:6 abundance in artificial membranes (Calhoon et al., 2015), feeding experiments with dietary 22:6 supplementation (Kumosani and Moselhy, 2010), and membrane crossover experiments involving phospholipid exchange between toads (low %22:6) and rats (high %22:6)(Wu et al., 2001). Limiting ion pump activity during hypoxia would significantly reduce ATP turnover, but it is currently unknown whether the remodelling of membrane lipids could be used as a mechanism to suppress metabolism. The goal of this study

was to characterize a potential link between membrane remodelling and metabolic suppression in goldfish exposed to prolonged hypoxia. I have measured the effects of 4 weeks of hypoxia at 10% air saturation (~2.1 kPa) on metabolic rate and membrane lipid composition. This hypoxic stress was selected because it induces significant suppression of goldfish aerobic metabolism, but without initiating any ATP contribution from anaerobic ethanol production (Regan et al., 2017). Because temperature-driven homeoviscous adjustments could impact the response to hypoxia, measurements were carried out in animals acclimated to two temperatures. This experimental design was selected because hypoxic remodelling could be incompatible with the homeoviscous remodelling necessary for acclimation to some temperatures. The aim was to test the hypothesis that goldfish restructure membrane lipids while suppressing metabolism to cope with prolonged hypoxia.

2.2. Methods

2.2.1. Animals

Adult common goldfish (*Carassius auratus,* Linnaeus 1758; N=88) were purchased from AQUAlity Tropical Fish Wholesale (Mississauga, Ontario, Canada) and held in a 1200 L flow-through holding tank in dechloraminated, well-oxygenated water, under a 12h:12h light:dark photoperiod, and were fed 3 mm floating fish pellets (Profishent; Martin Mills; Elmira, Ontario, Canada) once a day. They were randomly allocated to respirometry experiments (N=16, body mass 26.2 ± 1.4 g), membrane composition experiments (N=58, body mass 33.1 ± 1.4 g, liver mass 0.8 ± 0.04 g; hepatosomatic index 2.0 ± 0.1) or ethanol experiments (N=14, body mass 17.9 ± 1.6 g). All measurements were performed at 13ºC (mean 13.12 ± 0.03ºC; range 12.9-13.2ºC

(hypoxia); mean 13.17 ± 0.04°C; range 12.8-13.3°C (normoxia)) and 20°C (20.2 ± 0.01°C; range 19.6-20.5°C (hypoxia); 20.17 ± 0.02°C; range 19.4-20.6°C (normoxia)). The fish were acclimated to these temperatures for at least 2 weeks in the 1200 L holding tank before starting experiments. All procedures were approved by the Animal Care Committee of the University of Ottawa and adhered to the guidelines established by the Canadian Council on Animal Care for the use of animals in research.

2.2.2. Hypoxia acclimation and respirometry experiments

Each temperature group (13 and 20°C; N=8 per group) was placed in a normoxic 40L flow-through tank before the transition to hypoxia, and the tanks were covered by plexiglass lids to prevent air-water gas exchange. Water was then made progressively hypoxic over 7 days by bubbling increasing amounts of N_2 through a column filled with glass beads. Water PO_2 was measured using galvanic oxygen probes (Loligo Systems, Tjele, Denmark). The probes were calibrated before each measurement using air-saturated water (20.9% O_2). Oxygen availability went from 100% air saturation on day 1 to 50, 40, 30, 20, 15, and finally 10% (or 2.1 kPa) on day 7. PO_2 was maintained at that low level for a period of 4 weeks. The effects of hypoxia on MO_2 were measured in a Loligo Systems respirometer (DAQ-PAC-G1 instrument controlled with AutoResp software version 2). The same temperature ranges (given in the “Animals” section above) apply to respirometer water. Preliminary measurements of MO_2 were carried out continuously for 24 hours on animals that had been fasted for 24 h (N=5) to determine how much time they needed to reach resting metabolic rate. Their MO_2 only decreased during the first hour (as they were settling down from transfer stress), but subsequently stayed constant for the following 23 h. For the different treatment groups, 24 h-fasted

individuals were transferred from their holding tank to a 2 L respirometry chamber: (1) at the start of the experiment (normoxia), and (2) after 30 days in hypoxia. Each fish was used as its own normoxic control. Individuals were identified by unique fin morphologies, pigment patterns, fork length and/or body mass. After 1 h habituation to the respirometry chamber, each fish was measured for 3 periods of 1 h and the most reliable value among them was used in calculations (the 1 h period having a decline in pO_2 with the highest r^2). Oxygen partial pressure decreased from 20.9 to 13.8 kPa for normoxic trials and from 2.3 to 1.2 kPa for hypoxic trials. Control 24 h-measurements of MO_2 in the empty respirometer showed that bacterial respiration was negligible.

2.2.3. Membrane composition experiments

Experiments were designed as a 2x2 matrix simultaneously testing the effects of temperature (13 vs. 20°C) and chronic hypoxia (normoxic controls vs. hypoxia). Fish were randomly assigned to one of four groups: normoxia at 13°C (N=14), hypoxia at 13°C (N=13), normoxia at 20°C (N=15) and hypoxia at 20°C (N=16). A plexiglass lid was used to prevent surface access. Hypoxic conditions were progressively achieved as in the respirometry experiments. The fish were maintained in normoxia or hypoxia (10% air saturation) for 4 weeks. This duration was selected to leave enough time for membrane restructuring, knowing that homeoviscous changes to temperature take 2-3 weeks (Cossins et al., 1977; Sellner and Hazel, 1982; Smith and Kemp, 1971). To ensure that there was no effect of diet on membrane composition, the hypoxic group was fed first to satiation before providing the same amount of food to the normoxic group. At the end of the experiments, the goldfish were euthanized by cervical

dislocation. The brain, gills, white muscle and liver were sampled and stored at -20°C until analyses.

2.2.4. Lipid analyses

Total lipids were extracted from ~30 mg of each tissue as described previously (Maillet and Weber, 2006). Total lipids dissolved in chloroform were loaded on solid-phase extraction columns (Supelclean 3 mL 500 mg LC-NH2; Sigma-Aldrich; St. Louis, MO, USA). Neutral lipids, non-esterified FAs and PLs were separated by sequential elution using solvents of increasing polarity: chloroform:isopropanol (3:2 v/v), isopropyl ether:acetic acid (98:2 v/v), and methanol (Maillet and Weber, 2006). Total PL concentration was determined by gas chromatography as a measure of tissue membrane abundance by adding a PL internal standard before solid-phase column separation (40 mg/100 mL phosphatidyl choline 17:0/17:0; Avanti Polar Lipids; Alabaster, AL, USA). Total PL concentration was calculated as total fatty acids in the PL fraction divided by 2. The FA composition of membrane PL was measured after acid transesterification in acetyl chloride and methanol (90°C for 2 h). FA methyl esters were analyzed on an Agilent Technologies 6890N gas chromatograph (Mississauga, Ontario, Canada) equipped with a flame-ionization detector and a fused silica capillary column (Supelco DB-23, 60m, 0.25 mm i.d., 0.25 µm film thickness; Sigma-Aldrich) using hydrogen as carrier gas (Magnoni and Weber, 2007). Individual FAs were identified by determining exact retention times with pure standards (Supelco, Bellefonte, PA, USA). Only the FAs accounting for >1% of total FAs in PLs are reported. The following FAs were measured as more than 1% of total membrane FAs: 16:0, 16:1, 18:0, 18:1, 18:2, 18:3, 20:0, 20:2, 20:4, 20:5, 22:0, 22:3, 22:5, 22:6, and 24:0 (although not all of them

were detected in all tissues). Membrane cholesterol was measured as non-esterified (free) cholesterol in ~30 mg of tissue. Each tissue was homogenized in chloroform:methanol (2:1 v/v). Separation of aqueous and organic phases was achieved by adding 2 M KCl / 5 mM EDTA before centrifugation (10 min at 3000 g). The organic phase was dried under N_2, resuspended in 2-methoxyethanol, and cholesterol was measured by fluorometry (SpectraMax Gemini XS, Molecular Devices, Sunnyvale, California, USA) using a commercial assay kit (Cayman Chemical, Ann Arbor, Michigan, USA). This kit was selected because it allows the measurement of membrane (free, non-esterified) cholesterol separately from cholesterol esters that are only found outside membranes.

2.2.5. Ethanol analysis

Whole-body ethanol and water analyses were performed to confirm that no anaerobic metabolism was occurring at 10% air saturation. Goldfish were randomly allocated to either normoxia (N=7) or hypoxia (N=7) and kept for 4 weeks at normoxia (20.9 kPa) or at 10% air saturation (~2.1 kPa) at 13ºC. The experiment was terminated by rapid euthanasia (cervical dislocation). The fish were cut into pieces and frozen in liquid nitrogen. Four water samples were taken at 4 different time points to measure whether ethanol was released through the gills. All parts from each fish were then homogenized using a commercial blender (Magic bullet express blender, Homeland Housewares, CA, USA). Whole-body and water ethanol was measured as described in (Regan et al., 2017), using a commercial assay kit (Diagnostic Chemical Ltd., PEI, Canada).

2.2.6. Calculation and statistics

Metabolic rate was calculated as follows: $MO_2 = ([O_2]_{t0} - [O_2]_{t1}) . \frac{v}{t} . \frac{1}{M_b}$ where

MO_2 = rate of oxygen consumption (in mg O_2 kg^{-1} h^{-1})

$[O_2]_{t0}$ and $[O_2]_{t1}$ = oxygen concentration at times t_o and t_1 (in mg O_2 L^{-1})

v = respirometer volume – animal volume (in L)

$t = t_1 – t_0$ (in h), and M_b = body mass of the animal (in kg).

The double bond index (DBI) of membranes was calculated as the average number of double bonds in PL divided by the fraction of saturated FAs. Absolute concentration of membrane cholesterol in a tissue (expressed in µmol g^{-1}) is not a good indicator of the relative abundance of cholesterol in membranes if the amount of membranes per gram tissue varies with treatment. To address this problem, relative cholesterol concentration was calculated as moles of cholesterol per mole of PL and expressed as a unitless ratio. Statistical analyses were performed using SigmaPlot 12.5 (Systat, San Jose, CA, USA). Data were analyzed using two-way repeated measure ANOVA for the respirometry analysis, a two-way ANOVA for membrane lipid analyses with temperature and oxygen as main factors followed by the Holm-Sidak post-hoc test and a one-way ANOVA for the ethanol analysis. Normality was assessed using the Shapiro-Wilk test. When the assumptions of normality or equality of variances were not met, the data were normalized by log_{10} transformation. If transformation was unsuccessful, non-parametric two-way ANOVA on ranks was performed. All percentages were transformed to the arcsine of their square root before analyses. To account for multiple testing, the false discovery rate test was used to compute an adjusted level of significance of 0.042 (Benjamini and Hochberg, 1995). All values presented are means ± s.e.m.

2.3. Results

2.3.1. Respirometry

Metabolic rate was higher at 20°C than at 13°C for both, normoxic controls (P<0.05) and hypoxia-acclimated fish (P<0.001) (Fig. 2.1). At 20°C, prolonged hypoxia caused a decrease in MO_2 from 106.2 to 39.8 μmol O_2 kg^{-1} min^{-1} (P<0.01) (Fig. 2.1). At 13°C, MO_2 was suppressed from 45.8 to 11.8 μmol O_2 kg^{-1} min^{-1} (P<0.01) (Fig. 2.1). There was no interaction between oxygen availability and temperature (P>0.05). No ethanol could be detected in any fish from the control and the hypoxic group (0 μmol ethanol g^{-1}, N=7 for each treatment group), or in their tank water (0 μmol ethanol mL^{-1}, N=4 for each group).

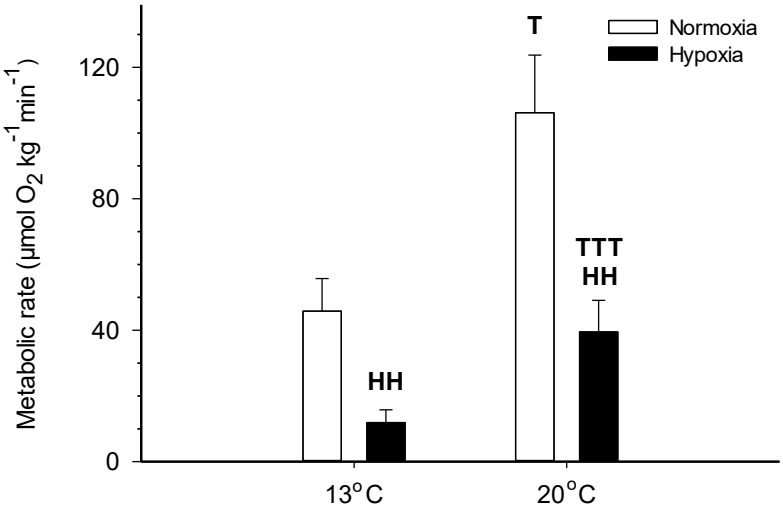

Figure 2.1. Metabolic rates of normoxic controls and hypoxia-acclimated goldfish at 13°C or 20°C. Values are means ± s.e.m. (N=8 per temperature). The effects of hypoxia within each temperature group are indicated as HH ($P < 0.01$). The effects of temperature within the normoxic or hypoxic treatments are indicated as T ($P < 0.05$) and TTT ($P < .001$).

2.3.2. Membrane cholesterol

At 13°C (Fig. 2.2A), hypoxia affected relative membrane cholesterol (expressed as a unitless ratio of μmoles of cholesterol per μmoles of membrane PL) in all tissues except the brain. It increased in gills (P=0.032) and muscle (P=0.001), but decreased in liver (P<0.042). At 20°C (Fig. 2.2B), hypoxia caused no change in relative membrane cholesterol (P>0.05). Relative cholesterol levels were higher at 20°C than 13°C in gill and liver, but lower in hypoxic muscle (P<0.001; Fig. 2.2B). There was an antagonistic interaction between oxygen availability and temperature for cholesterol content in gills (P=0.009), as well as in muscle and liver (P=0.003). Changes in absolute cholesterol levels (in μmol/g tissue) mirror the results described above for relative cholesterol

because no significant effects of hypoxia were detected on total membrane PL concentration (P>0.05).

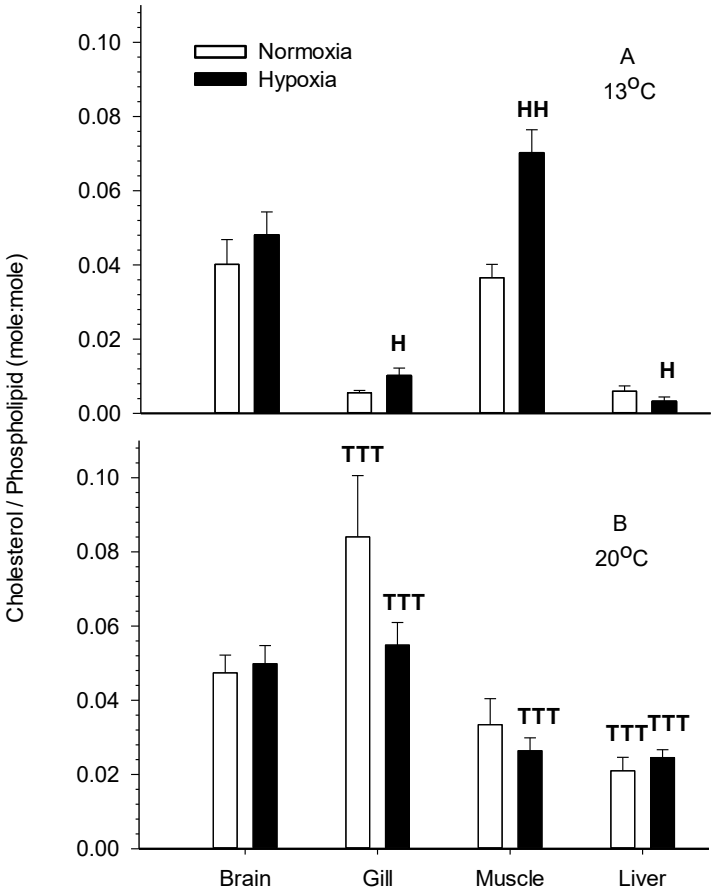

Figure 2.2. Relative membrane cholesterol levels in the tissues of normoxic controls and hypoxia-acclimated goldfish at 13°C (A) or 20°C (B). Values are means ± s.e.m. (N=13 to 16 per treatment). The effects of hypoxia within each temperature group are indicated as H ($P < 0.042$) and HH ($P < 0.01$). The effects of temperature within the normoxic or hypoxic treatments are indicated in the bottom panel as TTT ($P < 0.001$).

2.3.3. Double bond index and fatty acid chain length

At 13°C (Fig. 2.3A), hypoxia caused a decrease in DBI in the gill (P=0.009) and liver (P<0.042). At 20°C (Fig. 2.3B), hypoxia had no effect on the membrane DBI of any tissue (P>0.042). DBI was lower at 20°C than at 13°C in all tissues except the liver (P<0.042; Fig. 2.3B). There were no interactions between oxygen and temperature (P>0.042). At 13°C (Fig. 2.4A), hypoxia caused a decrease in average chain length in gill and liver (P<0.01), but had no impact in brain and muscle. At 20°C (Fig. 2.4B), hypoxia had no effect on chain length for any tissue (P>0.042). Average chain length was higher at 20°C than at 13°C in all tissues except the brain (P<0.01; Fig. 2.4B). There was an interaction between oxygen and temperature for gills (antagonistic) (P=0.007) and liver (synergistic) (P=0.035).

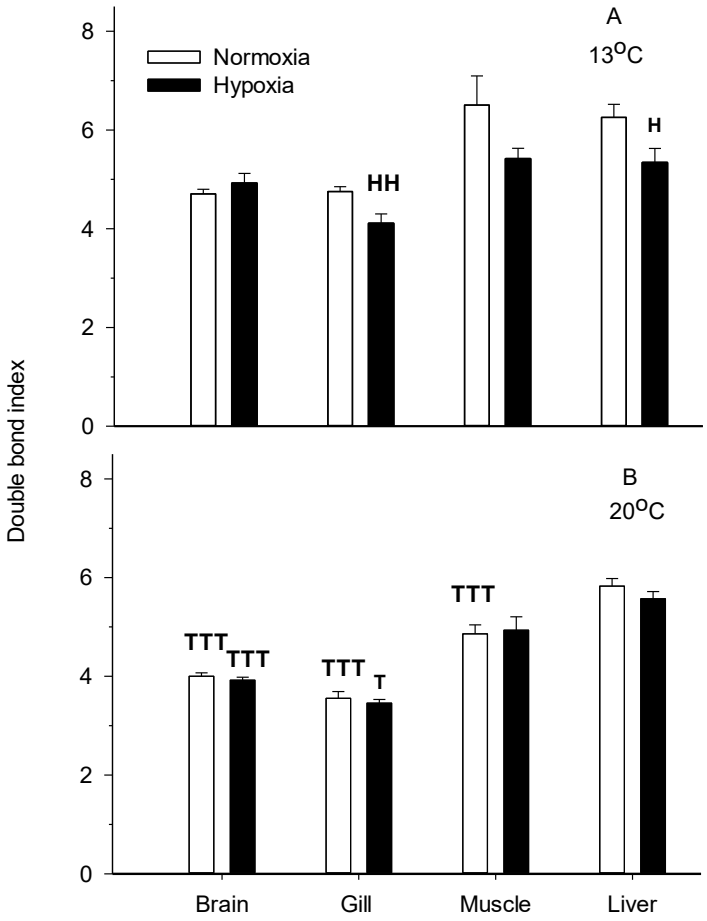

Figure 2.3. Membrane double bond index in the tissues of normoxic controls and hypoxia-acclimated goldfish at 13ºC (A) or 20ºC (B). Values are means ± s.e.m. (N=13 to 16 per treatment). The effects of hypoxia within each temperature group are indicated as H ($P < 0.042$) and HH ($P < 0.01$). The effects of temperature within the normoxic or hypoxic treatments are indicated in the bottom panel as T ($P < 0.042$) and TTT ($P < 0.001$).

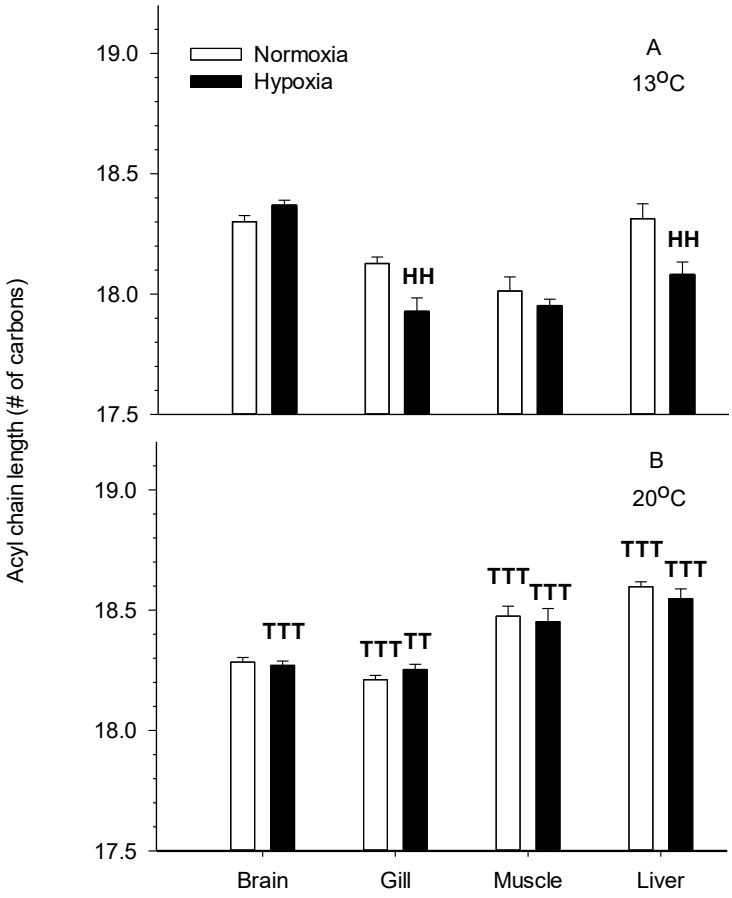

Figure 2.4. Mean fatty acid chain length in the membrane phospholipids for the tissues of normoxic controls and hypoxia-acclimated goldfish at 13°C (A) or 20°C (B). Values are means ± s.e.m. (N=13 to 16 per treatment). The effects of hypoxia within each temperature group are indicated as HH ($P < 0.01$). The effects of temperature within the normoxic or hypoxic treatments are indicated in the bottom panel as TT ($P < 0.01$) and TTT ($P < 0.001$).

2.3.4. Membrane fatty acids

Hypoxia only caused changes in PL composition at 13°C in gills, where % saturated fatty acids (SFA) was increased ($P<0.042$), and % polyunsaturated fatty acids

(PUFA) was decreased (P<0.01) (Table 2.1). At 20^{o}C, hypoxia had no effect on any tissue (P>0.042). Higher %SFA (P<0.01), but lower % monounsaturated fatty acids (MUFA) (P<0.042) and %PUFA (P<0.001) were observed at 20^{o}C than at 13^{o}C for most tissues (Table 2.1). There was a synergistic interaction between oxygen and temperature for %PUFA in gills only (P=0.023). Figure 2.5 shows changes in the relative abundance of individual FAs in gill and liver membranes at 13^{o}C. They were selected because hypoxia only caused changes in these two tissues and at this temperature. In gill (Fig. 2.5A), hypoxia caused decreases in %eicosapentaenoate (20:5; P<0.01), %docosapentaenoate (22:5; P=0.022) and %docosahexaenoate (22:6; P<0.01). In liver (Fig. 2.5B), hypoxia caused an increase in %linoleate (18:2; P=0.015), but decreases in %arachidonate (20:4; P<0.01) and %docosahexaenoate (22:6; P=0.024).

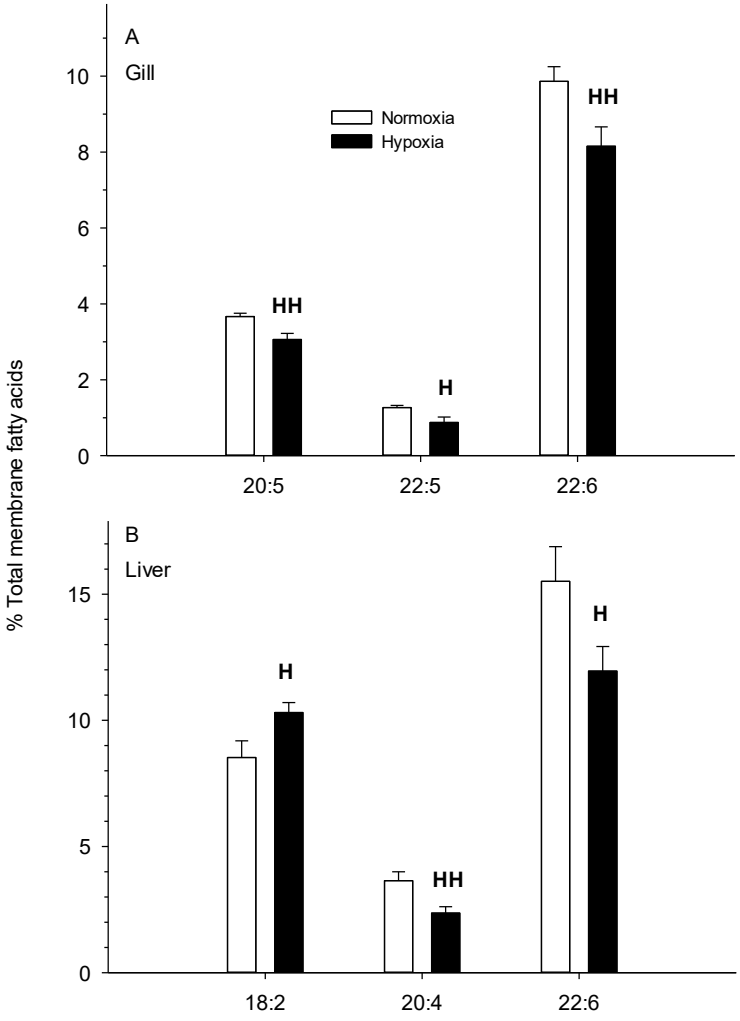

Figure 2.5. Hypoxia-mediated changes in the relative abundance of individual membrane fatty acids in goldfish gill (A) and liver (B) at 13°C. They were selected because hypoxia only caused significant changes in these two tissues and at this temperature. Values are means ± s.e.m. (N=14 for normoxia and N=13 for hypoxia). The effects of hypoxia are indicated as H ($P < 0.042$) and HH ($P < 0.01$).

Table 2.1. Fatty acid composition of membrane phospholipids in tissues of goldfish acclimated to normoxia or hypoxia at two temperatures. Values are mean percentages of total membrane fatty acids ± s.e.m. (N=13-16). Saturated fatty acids (SFA), monounsaturated fatty acids (MUFA) and polyunsaturated fatty acids (PUFA) are indicated separately. Significant effects of hypoxia and temperature are indicated in bold; $P < 0.042$ (H, T), $P < 0.01$ (HH, TT), $P < 0.001$ (TTT).

		13°C		20°C	
		Normoxia	Hypoxia	Normoxia	Hypoxia
Brain	SFA	37.15 ± 0.29	37.08 ± 0.81	**40.94 ± 0.36** ^{TTT}	**40.45 ± 0.61** ^{TTT}
	MUFA	35.81 ± 0.79	35.30 ± 0.87	35.15 ± 1.02	36.18 ± 0.63
	PUFA	27.04 ± 0.74	27.62 ± 0.39	**23.91 ± 0.77** ^{TTT}	**23.36 ± 0.64** ^{TTT}
Gills	SFA	33.90 ± 0.45	**35.89 ± 0.75** ^{H}	**42.95 ± 0.91** ^{TTT}	**43.09 ± 0.77** ^{TTT}
	MUFA	32.62 ± 0.53	33.65 ± 0.43	**31.22 ± 0.83** ^{T}	31.58 ± 0.77
	PUFA	33.48 ± 0.52	**30.46 ± 0.85** ^{HH}	**25.83 ± 0.42** ^{TTT}	**25.83 ± 0.34** ^{TTT}
Muscle	SFA	27.21 ± 0.90	29.74 ± 0.67	**41.47 ± 0.71** ^{TTT}	**40.89 ± 1.23** ^{TTT}
	MUFA	35.55 ± 1.12	35.38 ± 0.96	**21.34 ± 0.77** ^{TTT}	**22.48 ± 0.78** ^{TTT}
	PUFA	37.23 ± 1.74	34.88 ± 0.89	37.19 ± 1.13	36.63 ± 0.96
Liver	SFA	30.42 ± 0.99	31.83 ± 1.01	**35.79 ± 0.93** ^{TTT}	**35.85 ± 0.91** ^{TT}
	MUFA	33.47 ± 1.86	34.72 ± 1.22	28.93 ± 1.38	30.77 ± 1.82
	PUFA	36.10 ± 1.17	33.45 ± 1.15	35.28 ± 0.69	33.38 ± 1.07

2.4. Discussion

Goldfish exposed to several weeks of severe hypoxia suppress metabolic rate by 74% (at 13^{o}C) and 63% (at 20^{o}C) (Fig. 2.1). This study is the first to show that prolonged *in vivo* exposure to low oxygen can cause membrane remodelling. At low temperature, chronic hypoxia triggers extensive restructuring of membrane lipids in all tissues measured except the brain. These membrane responses involve changes in cholesterol and fatty acid composition. The observed hypoxia-driven increases in cholesterol (in white muscle and gills) and increases in fatty acid saturation (in gills and liver, mainly due to lower %22:6) are consistent with well characterized inhibition mechanisms of key ATPases. By contrast, hypoxia does not affect the lipid composition of membranes in warm-acclimated animals.

2.4.1. Membrane cholesterol responds to hypoxia at low temperature

At 13^{o}C, hypoxia causes large tissue-specific changes in membrane cholesterol that increases in white muscle (+92%) and in the gills (+81%) (Fig. 2.2A). These responses are intriguing because boosting relative membrane cholesterol generally inhibits integral proteins. The activities of [Ca^{2+}, Mg^{2+}]-ATPase (Ortega and Mas-Oliva, 1984), Ca^{2+}-ATPase (Li et al., 2004; Madden et al., 1981) and Na^{+}/K^{+}-ATPase (Crockett and Hazel, 1997; Kimelberg and Papahadjopoulos, 1974; Yeagle, 1983) are all downregulated by incorporating more cholesterol in the membrane. Adding cholesterol may inhibit ATPases by modifying bulk membrane properties and/or through direct molecular interaction with the proteins. For example, it could decrease overall membrane fluidity, thereby hindering the conformational changes necessary for ion pumping (Li et al., 2004; Madden et al., 1981; Mas-Oliva and Santiago-Garcia, 1990).

Cholesterol could also interact directly with the hydrophobic domains of ATPases to lower their activity (Bastiaanse et al., 1997; Madden et al., 1981). The exact mechanism of cholesterol action is presently unknown, but any inhibition of ion pumps reduces overall energy expenditure and could therefore contribute to metabolic suppression. It is also possible that some hypoxia-induced increases in cholesterol abundance observed here are associated with the formation of lipid rafts (Dietrich et al., 2001; Simons and Sampaio, 2011). Lipid rafts can include proteins such as glycosylphosphatidylinositol-anchored proteins, palmitoylated transmembrane proteins (Brown and London, 1998) as well as Ca^{2+}-ATPase (Sepúlveda et al., 2006), but not Na^{+}/K^{+}-ATPase (Eckert et al., 2003; Martens et al., 2000). Raft proteins could be bound to cholesterol which might impact protein conformation and function (Simons and Sampaio, 2011). This could possibly cause a decrease in protein activity and, subsequently, a reduction in MO_2. It has also been shown that increasing cholesterol decreases membrane permeability to oxygen in some mammalian cells (Dotson et al., 2017; Subczynski et al., 1991). If goldfish membranes were to behave similarly, the cholesterol increase seen in muscle and gill could potentially assist metabolic suppression.

Unlike muscle and gill, the liver shows a decrease in membrane cholesterol during hypoxia (-46%) that could activate some hepatic ATPases (Bastiaanse et al., 1997). However, it is also conceivable that this tissue uses a different strategy to suppress metabolism in hypoxia. Protein synthesis is another energy-costly process (Rolfe and Brown, 1997) that is downregulated in the liver of hypoxic goldfish by stimulating AMP- activated protein kinase (AMPK) (Jibb and Richards, 2008). This stimulation of AMPK is associated with the phosphorylation and, thus, inactivation of

eukaryotic elongation factor-2 that inhibits protein synthesis. In goldfish, this AMPK response is only observed in the liver (not in muscle, brain or gill), and it suppresses other ATP-consuming processes such as cholesterol synthesis (Hardie et al., 2003). Therefore, AMPK modulation could explain why cholesterol abundance is decreased in the hepatic membranes of hypoxic goldfish (Fig. 2.2A). It should also be noted here that the effects of cholesterol are rather complex and that, in some cases, optimal levels of the sterol can yield maximal Na^+/K^+-ATPase activity. However, this was mostly observed in artificial lipid bilayers that may not reflect the behavior of real biological membranes. In such reconstituted systems, increasing or decreasing cholesterol from the optimum can cause inhibition of Na^+/K^+-ATPase (Cornelius, 1995; Garcia et al., 2019).

Finally, membrane cholesterol did not respond to chronic hypoxia in goldfish brain. This could be because membrane lipids do not generally seem to respond as strongly to a variety of stresses in the brain as in other tissues. Seasonal changes did not have any effect on membrane cholesterol and phospholipid composition in frog brains (Reynolds et al., 2014). Furthermore, (Buda et al., 1994) tested several fish species and showed that brain phospholipids do not respond to temperature. (Hulbert and Else, 1999) also suggested that slowing membrane processes down in the brain via changes in membrane lipids could be disadvantageous as it might decrease overall behavioural responsiveness. This could be important for goldfish because they stay active during hypoxia rather than becoming comatose like turtles.

2.4.2. Membrane fatty acids respond to hypoxia at low temperature

At 13^{o}C, prolonged hypoxia increases membrane saturation (decreases DBI) and mean acyl chain length in gill and liver (Figs. 2.3 and 2.4). The changes in DBI should affect membrane fluidity (Hazel, 1995; Raynard and Cossins, 1991) and may reduce the activity of membrane proteins (Harayama and Riezman, 2018). This decrease in DBI, coupled with the increase in cholesterol, also strengthens the possibility of lipid raft formation in the gills (Dietrich et al., 2001; Simons and Ikonen, 1997). More specifically, results show that gill membranes alter their bulk properties through decreases in several PUFAs: 20:5 (-16.5%), 22:5 (-31%) and 22:6 (-17%) (Fig. 2.5A). Liver membranes achieve the same overall decrease in DBI through large reductions in 20:4 (-35%) and 22:6 (-23%) that overturn the smaller effect of an increase in 18:2 (+21%) (Fig. 2.5B). The observed reductions in gill and liver 22:6 are particularly interesting because this acid is a known activator of Na^{+}/K^{+}-ATPase, even though its exact mechanism of action is presently unclear (Calhoon et al., 2015; Turner et al., 2005). The hypoxia-induced decrease in liver 22:6 (Fig. 2.5B) could inhibit Na^{+}/K^{+}-ATPase particularly strongly because: (1) this mechanism is amplified in membranes that lack cholesterol (Cornelius, 2008), and (2) liver membranes have a particularly low intrinsic cholesterol abundance that is further reduced by hypoxia (Fig. 2.2A). Prolonged hypoxia also decreases mean fatty acid chain length in gill and liver (Fig. 2.4A). Such a change can affect protein activity by altering membrane thickness, thereby altering how well the width of the lipid bilayer matches the size of integral proteins (Lee, 2004; Lee, 2011). For instance, the activity of sarcoplasmic reticulum calcium-ATPase (SERCA) can be modulated by manipulating the length of acyl carbon chains in artificial membranes (Gustavsson et al.,

2011). Therefore, the decrease in chain length observed here in hypoxia could inhibit ATPases and further reduce energy use.

2.4.3. Homeoviscous responses of membrane lipids to temperature

Thermal acclimation is known to elicit a homeoviscous response (Crockett, 1998; Hazel, 1995) and differences between the 2 temperature groups reported here are generally consistent with the maintenance of normal membrane fluidity. The exact remodelling mechanism is tissue specific and involves changes in fatty acid composition, cholesterol abundance, or both. Overall, the transition from 13^{o}C to 20^{o}C causes changes in cholesterol (Fig. 2.2), a decrease in DBI (Fig. 2.3), and an increase in mean acyl chain length (Fig. 2.4). Cholesterol stabilizes membranes by protecting them from sudden phase transitions (Zehmer and Hazel, 2004) and it plays an important role in preserving lipid raft integrity (Zehmer and Hazel, 2005). This is why the effects of changes in cholesterol on fluidity are difficult to predict because they depend on temperature and on the intrinsic abundance of the sterol in each tissue. This may explain why acclimation to higher temperature causes a cholesterol increase in gill and liver, but a decrease in muscle. The restructuring of membrane PL observed here in goldfish causes a decrease in fluidity to counteract the fluidizing effects of high temperature as previously reported for a variety of ectotherms (Harayama and Riezman, 2018). As expected, goldfish decrease DBI (in brain, gill and muscle; Fig. 2.3) and increase mean acyl chain length (in gill, muscle and liver; Fig. 2.4) during warm acclimation.

2.4.4. Lowering metabolic rate to save energy

Metabolic suppression occurs in response to low environmental oxygen (Boutilier and St-Pierre, 2000; Buck et al., 1993), low temperature (Campbell et al., 2008) and fasting (Young and Landsberg, 1977). This important strategy to cope with hypoxia is therefore routinely used by animals such as goldfish (Van Waversveld et al., 1989), turtles (Buck et al., 1993), pelagic crabs (Seibel et al., 2017), naked mole-rats (Pamenter et al., 2015) and squids (Seibel et al., 2014). I show that acclimation to hypoxia elicits deep metabolic suppression in the goldfish (Fig. 2.1). Four weeks of severe hypoxia reduce metabolic rate by 63% in 20^{o}C animals and 74% in 13^{o}C fish. These results are consistent with the decreases previously reported for short term hypoxic stress (53 to 59% at 20^{o}C) (van Ginneken et al., 2004; Van Waversveld et al., 1989).

In these experiments, normoxic fish ate the same amount as the hypoxic fish fed ad libitum. Because caloric requirements of the normoxic fish were higher (no metabolic suppression), it could be argued that they were underfed, leading to lower metabolic rates due to food restriction. If this was the case, measured metabolic suppression of 63% (20^{o}C) and 74% (13^{o}C) may be underestimates of true values. This study reveals that goldfish undergo the strongest metabolic suppression at low temperature and after prolonged hypoxia, when they decrease MO_2 by 94% compared to normoxic fish acclimated to the higher temperature (Fig. 2.1). It could be argued that this extremely low metabolic rate can only be achieved through the combined effects of multiple mechanisms that may include ATPase inhibition through membrane remodelling. Interestingly, membrane lipids only respond to hypoxia at 13^{o}C, but only show little

change at 20°C. This could be explained if the homeoviscous adjustments needed to survive at 20°C were to make the membrane response to hypoxia difficult or impossible. Such a scenario appears unlikely because I could not identify any specific cholesterol or FA responses where temperature and hypoxia acclimation would interfere with each other.

2.5. Conclusions

When exposed to prolonged hypoxia, goldfish have the capacity for deep metabolic suppression (Fig. 2.1). This study shows that cold-acclimated animals undergo extensive, tissue-specific restructuring of membrane lipids (Figs. 2.2-2.5) as they reach minimal metabolic rates. The experiments carried out here only provide general information on total membrane composition of each tissue. The evidence found about the effects of chronic hypoxia averaged over all membranes suggests that more detailed analyses of individual membrane types within each tissue and of specific membrane regions like lipid rafts will be productive avenues for future work. Hypoxia-driven membrane remodelling involves changes in cholesterol abundance and fatty acid composition of phospholipids as classically observed during homeoviscous adjustments to temperature. By contrast, hypoxia fails to modify the membranes of warm-acclimated fish, and this could make survival more challenging in a warmer future. At low temperature, the most prominent changes caused by chronic hypoxia are increases in cholesterol (an inhibitor of ATPases) and decreases in 22:6 (a well characterized activator of ATPases). Because ion pumping by membrane-bound ATPases accounts for a large fraction of total energy use in resting tissues, I propose that the membrane

responses reported here in cold-acclimated animals could be a novel mechanism to promote metabolic suppression.

Chapter 3

Naked mole-rats suppress energy metabolism and modulate membrane cholesterol in chronic hypoxia

Based on a manuscript by the same title

Written by

Elie Farhat, Maiah Devereaux, Matthew Pamenter and Jean-Michel Weber

And published in

American Journal of Physiology-Regulatory, Integrative and Comparative Physiology
https://doi.org/10.1152/ajpregu.00057.2020

Statement of contribution: This work was performed alongside Maiah Devereaux. Maiah acclimated the naked mole-rats to their conditions and measured their metabolic rate, while I performed all the other measurements. These measurements include maximal enzymatic activities (PK, LDH, CS, CPT, HOAD and Na^+/K^+-ATPase) and the membrane lipid composition (cholesterol abundance and fatty acid composition of phospholipids). I also wrote the paper as first author and edited it with Dr. Weber.

3.1. Introduction

Hypoxia-tolerant organisms use metabolic suppression as a key strategy to cope with reduced oxygen levels, which are otherwise deleterious to most animals (Bickler and Buck, 2007; Richards, 2011; Seibel, 2011). The primary physiological mechanisms that promote suppression include downregulating energy metabolism [tricarboxylic acid (TCA) cycle, glycolysis, β-oxidation (Martínez et al., 2006; Solaini et al., 2010; Storey, 1997)] as well as major cellular consumers of ATP such as ion pumps (Hochachka, 1986). It has recently been suggested that membrane remodelling may play a role in the overall inhibition of energy metabolism in hypoxic goldfish (Chapter 2). The lipid composition of membranes affects the activity of integral proteins and could therefore play a role in mediating metabolic suppression. For example, changes in cholesterol (a modulator of Na^+/K^+-ATPase) and %docosahexaenoic acid (22:6 or DHA; an activator of Na^+/K^+-ATPase) could be involved in reducing metabolic rate (Bastiaanse et al., 1997; Harayama and Riezman, 2018). It has been recently shown that chronic hypoxia causes extensive changes in the membrane lipid composition of goldfish (Chapter 2): a hypoxia-tolerant vertebrate that utilizes significant metabolic rate depression to tolerate severe hypoxia and anoxia (Regan et al., 2017). However, the plasticity of membrane lipids in response to hypoxia has never been investigated in mammals.

Naked mole-rats (NMRs; *Heterocephalus glaber*, Linnaeus 1758), are fossorial and hypoxia-tolerant mammals that live in poorly ventilated underground burrows where temperatures are high (25-49^{o}C) and oxygen levels are putatively hypoxic (Holtze et al., 2018; Park et al., 2017). In laboratory conditions, acute exposure to a few hours of 3% O_2 causes an 85% decrease in metabolic rate (Pamenter et al., 2018): the strongest

suppression of metabolism among hypoxia-tolerant mole-rat species (Ivy et al., 2019). However, it is unclear how NMRs cope with more chronic hypoxia.

Whereas the impact of hypoxia on membrane lipid composition is largely unexplored in mammals, the effects of hypoxia acclimation on the activities of key enzymes of energy metabolism have received more attention. For example, in rats, mice, and high-altitude deer mice, hypoxia generally stimulates glycolysis (Daneshrad et al., 2000; Dutta et al., 2009; Malthankar-Phatak et al., 2008; Pastoris et al., 1995), and, apart from deer mice, downregulates β-oxidation (Cheviron et al., 2014; Dutta et al., 2009; Galbes et al., 2008). Most investigations of TCA cycle enzymes suggest that their activity is not modified by low oxygen (Cáceda et al., 2001; Cheviron et al., 2012; Daneshrad et al., 2000; Galbes et al., 2008), although inhibition was observed in one study (Solaini et al., 2010). Several reports also show that Na^+/K^+-ATPase activity is decreased in the lungs of hypoxic rats (Carpenter et al., 2003; Mairbäurl et al., 1997; Wodopia et al., 2000). However, none of these enzymes have been explored in the hypoxia-tolerant NMR. Therefore, the goals of this study were to test the hypotheses that during chronic hypoxia, NMRs: (i) downregulate key enzymes of TCA cycle, glycolysis, and β-oxidation, (ii) inhibit Na^+/K^+-ATPase, and (iii) alter the composition of membrane lipids concomitantly with metabolic suppression.

3.2. Methods

3.2.1. Animals

Adult NMRs (n = 37, body mass 45 ± 3.1 g; 2-5 years old) were group-housed in interconnected multi-cage systems (30°C; 70% humidity; 12L:12D light cycle) and were fed fresh tubers, vegetables, fruit and Pronutro cereal supplement *ad libitum*. All

experimental procedures were approved by the University of Ottawa's Animal Care Committee (protocol # 2535) in accordance with the Animals for Research Act and the Canadian Council on Animal Care.

3.2.2. Experimental design

Subordinate animals were randomly allocated to respirometry experiments or enzyme/membrane experiments. For each set of experiments, the animals were randomly divided into normoxic controls and a hypoxic treatment group. Both groups were placed in separate chambers with controlled, continuous air flow either normoxic (21% O_2; 0.04% CO_2; balance N_2) or hypoxic (11% O_2; 0.04% CO_2; balance N_2) and were kept under these conditions for 4-6 weeks. This duration was selected to provide enough time for potential membrane restructuring, given that homeoviscous adjustments to changes in environmental temperature can take 3 weeks in ectotherms (Sellner and Hazel, 1982).

3.2.3. Whole-body respirometry

After normoxic or hypoxic acclimation, animals were individually placed unrestrained into a 450 mL plexiglass respirometer, which was held inside a larger environmental chamber held at 30°C. Animals were provided a thin layer of corn cob bedding. The respirometer was continuously ventilated with gas mixtures set to the desired fractional gas composition by calibrated rotameters (Krohne, Duisburg, Germany). Inflowing gas was set at a flow rate of 100 mL min^{-1}, determined using a calibrated mass flow meter (Alicat Scientific, Tuscon, AZ, USA). The excurrent gas was passed through a desiccant (Drierite, W.A. Hammond Drierite Co. Ltd., Xenia, OH)

before entering the cells of the CO_2 and O_2 analyzers (FC-10 O_2 and CA-10 CO_2 Analyzers, Sable Systems), which were used to determine the gas concentrations of inspired and expired air. Before each trial the CO_2 and O_2 analyzers were calibrated using 100% N_2, compressed air (20.95% O_2), and a span gas (1.5% CO_2; balance N_2). The animals were placed in the respirometer for 1 h before measurements to familiarize them with their new surroundings. Oxygen consumption ($\dot{V}O_2$) and carbon dioxide production ($\dot{V}CO_2$) were then recorded for the next hour. $\dot{V}O_2$ and $\dot{V}CO_2$ measured during the last 30 min (three 10-min intervals) of the recording period were averaged to determine baseline values for each animal. For 5 min at the end of the recording period, incurrent gas concentrations were measured by bypassing the experimental chamber and diverting air flow directly to the CO_2 and O_2 analyzers. Body temperature was recorded non-invasively every 10 min using an RFID microchip reader (Allflex USA Inc., Dallas, TX) to scan previously implanted RFID microchips (Destron Fearing, Langeskov, Denmark). Normoxic controls (33.1 ± 0.13^{o}C) and hypoxic animals (33 ± 0.12^{o}C) had the same body temperature. Chamber temperature was recorded every 2 seconds using a custom designed thermocouple (range 29.8^{o}C-30.2^{o}C).

3.2.4. Enzyme assays

At the end of the experiments, NMRs were quickly euthanized by cervical dislocation. Because different tissues do not always respond similarly to physiological stresses, the brain, heart, liver, skeletal (temporalis) muscle and kidney were sampled in < 2 min, immediately frozen in liquid N_2 and stored at -80^{o}C until analysis. All enzyme activities were measured using a Spectra Max Plus384 Absorbance Microplate Reader (Molecular Devices, Sunnyvale, CA). To measure the activities of key enzymes involved

in (i) glycolysis (pyruvate kinase (PK) and lactate dehydrogenase (LDH)), (ii) the tricarboxylic acid cycle (citrate synthase (CS)) and (iii) β-oxidation (carnitine palmitoyl transferase (CPT) and 3-hydroxyacyl CoA dehydrogenase (HOAD)), 50 mg of each frozen tissue was weighed and homogenized on ice in 19 volumes of extraction medium (25 mM Tris/HCl + 1 mM EDTA as well as 5 mM dithiothreitol (DTT), 0.05% (volume/volume) Triton X-100 that were added on the day of the experiment to complete the enzyme extraction). Homogenates were then centrifuged at 4^{o}C at 2400g for 5 min and the resulting supernatant was stored at -80^{o}C until analysis. All assay conditions were first optimized to give maximal rates with the skeletal muscle and, thus, may not yield the maximal rate in all tissues. All homogenates were subjected to a freeze/thaw cycle. Preliminary experiments were carried out to ensure that all substrate and cofactor concentrations were saturating but not inhibitory. Control reactions (containing no substrate) were run simultaneously for each enzyme to measure background activity if present. All assays were run in triplicate at 32^{o}C.

Assay conditions were as follows: PK: (A_{340}; pH 7.35; (Zammit et al., 1978)): 0.17 mM NADH, 5 mM ADP, 80 mM KCl, 10 mM $MgCl_2$, 5 mM phospho(enol)pyruvate (PEP) (omitted from the control), excess coupling enzyme (LDH) in 160 mM triethanolamine/HCl. LDH: (A_{340}; pH 7.3; (Zammit and Newsholme, 1976)): 0.17 mM NADH, 1 mM KCN, 2 mM pyruvate (omitted from the control) in 50 mM Tris/HCl. CS: (A_{412}; pH 8.1; (Alp et al., 1976)): 0.2 mM 5,5'-dithiobis-(2-nitrobenzoic acid) (DTNB), 0.1 mM acetyl-CoA, and 0.5 mM oxaloacetate (omitted from the control) in 50 mM Tris-HCl. CPT: (A_{412}; pH 8; (Guglielmo et al., 2002)): 0.15 mM DTNB, 0.035 mM palmitoyl CoA, carnitine (omitted from the control) in 50 mM Tris. HOAD: (A_{340}; pH 7.4; (Guglielmo et

al., 2002)): 0.2 mM NADH, 0.1 mM acetoacetyl-CoA (omitted from the control) in 50 mM Imidazole + 1 mM EDTA. The measurements of CPT activity here most likely reflect the behaviour of CPT2 because CPT1 is inactivated by freezing (McClelland et al., 2005).

The activity of Na^+/K^+-ATPase (A_{340}) was measured by using a modified protocol from (McCormick, 1993). Frozen tissue was weighed (~100 mg) and homogenized on ice with a sonicator (Fisher Scientific Sonic Dismembrator model 100, San Diego, CA) in a 4:1 SEI:SEID buffer (SEI: 250 mM sucrose, 10 mM EDTA, 42 mM imidazole, pH 7.3; SEID: 100 mL SEI + 0.5 g sodium deoxycholate). Homogenates were then centrifuged at 10,000g for 5 min at 4°C and the resulting supernatant was directly used in the assay. The assay was performed in quadruplicate (2 replicates contained 10 µL of homogenate + 200 µL of assay solution A (50 mM imidazole, 2.8 mM PEP, 0.7 mM ATP, 0.22 mM NADH, 5 mM PK and 4 mM LDH, pH 7.5) and 2 replicates contained 10 µL of homogenate + 200 µL of assay solution B (Solution A + 0.5 mM ouabain). Ouabain was added to block Na^+/K^+-ATPase and measure any detectable ATP use not associated with this enzyme. All enzyme measurements performed in this study provide information on capacity for flux in different key pathways. Because enzyme V_{max} was measured under optimal *in vitro* conditions, the observed changes may not necessarily reflect the effects of chronic hypoxia on *in vivo* fluxes.

3.2.5. Membrane lipid analyses

Total lipids were extracted from ~30 mg of each frozen tissue sample as described previously (Maillet and Weber, 2006). Briefly, tissues were homogenized with a Polytron (Kinematica AG, Luzern, Switzerland) and total lipids were extracted twice in chloroform-methanol (2:1 v/v). After filtration, 0.25% KCl was added and the

mixture centrifuged to separate aqueous and organic phases. The aqueous phase was discarded and the organic phase containing the lipids was dried on a rotating evaporator (Büchi Rotavapor, Flawil,Switzerland). Following extraction and drying, total lipids were resuspended in chloroform before being loaded on solid-phase extraction columns (Supelclean 3 mL 500 mg LC-NH2; Sigma-Aldrich; St. Louis, MO, USA). Neutral lipids, non-esterified fatty acids (FAs) and phospholipids (PLs) were separated by sequential elution using solvents of increasing polarity: chloroform:isopropanol (3:2 v/v), isopropyl ether:acetic acid (98:2 v/v), and methanol (Maillet and Weber, 2006). Total PL concentration was determined by gas chromatography as a measure of tissue membrane abundance by adding a PL internal standard before solid-phase column separation (40 mg/100 mL phosphatidyl choline 17:0/17:0; Avanti Polar Lipids; Alabaster, AL, USA). The PL fraction was then used for analysis of its FA composition, which was measured after acid transesterification in acetyl chloride and methanol (90°C for 2 h). FA methyl esters were analyzed on an Agilent Technologies 6890N gas chromatograph (Mississauga, Ontario, Canada) equipped with a flame-ionization detector and a fused silica capillary column (Supelco DB-23, 60m, 0.25 mm i.d., 0.25 µm film thickness; Sigma Aldrich), using hydrogen as carrier gas. The following conditions were used during analysis: (i) oven temperature was programmed for 1 min at 130°C and raised up to 170°C at a rate of 6.5°C min^{-1}, then up to 215°C at 2.75°C min^{-1}, and maintained at 215°C for 12 min, then up to 230°C at 40°C min^{-1}, and maintained at 230°C for 3 min, (ii) injector temperature was 270°C using a 50:1 split ratio, and (iii) detector temperature was 280°C. Individual FAs were

identified by determining exact retention times with pure standards (Supelco, Bellefonte, PA, USA). Only the FAs accounting for >1% of total FAs in total PLs are reported.

Membrane cholesterol was measured as non-esterified (free) cholesterol in ~30 mg of tissue. Each tissue was homogenized in chloroform:methanol (2:1 v/v). Separation of aqueous and organic phases was achieved by adding 2 M KCl / 5 mM EDTA before centrifugation (10 min at 3,000g). The organic phase was dried under N_2, resuspended in 2-methoxyethanol, and cholesterol was measured by fluorometry (SpectraMax Gemini XS, Molecular Devices, Sunnyvale, California, USA) using a commercial assay kit (Cayman Chemical, Ann Arbor, Michigan, USA). This kit was selected because it allows the measurement of membrane (free, non-esterified) cholesterol separately from cholesterol esters that are only found outside membranes.

3.2.6. Calculations and statistics

Respirometry data were collected using LabChart software and analyzed in PowerLab (AD Instruments, Colorado Springs, CO). Using these measurements, $\dot{V}O_2$ was then calculated using equation 10.6 in (Lighton, 2018): $\dot{V}O_2 = FRi\ [(FiO_2 – FeO_2) – FeO_2\ (FeCO_2 – FiCO_2)]/(1 – FeO_2)$. Also, $\dot{V}CO_2$ was calculated using equation 10.7 in (Lighton, 2018): $\dot{V}CO_2 = FRi\ [(FeCO_2 – FiCO_2) – FeO_2\ (FiO_2 – FeO_2)]/(1 – FeCO_2)$. In both equations FRi is the incurrent flow rate (mL min^{-1}), FiO_2 and $FiCO_2$ are the fractional concentrations of incurrent O_2 and CO_2 of dry gas, and FeO_2 and $FeCO_2$ are the fractional concentrations of excurrent O_2 and CO_2 from the experimental chamber. Total PL concentration was calculated as follows: [PL] = [Σ ((area under the curve of individual FA) * (PL 17:0/17:0 internal standard concentration)) / (individual FA molar weight)] / 2. The double bond index (DBI) of membranes was calculated as the average

number of double bonds in PLs divided by percent saturated fatty acids. Absolute concentration of membrane cholesterol in a tissue (expressed in μmol g^{-1}) is not indicative of the relative amount of cholesterol in membranes if treatment causes changes in membrane abundance. To address this problem, relative cholesterol concentration was calculated as moles of cholesterol per mole of PL and expressed as a unitless ratio (Yeagle et al., 1988). Statistical analyses were performed using SigmaPlot 12.5 (Systat, San Jose, CA, USA). Normoxic and hypoxic animals were compared using a two-tailed t-test. Normality was assessed using the Shapiro-Wilk test and homoscedasticity by the Levene test. When the assumptions of normality or equality of variances were not met, the data were normalized by $\log_{10}$ or square root transformation. If transformation was unsuccessful, non-parametric Mann-Whitney U test was performed. Values presented are means ± SE, and a level of significance of $P<0.05$ was used in all tests.

3.3. Results

3.3.1. Metabolic rate

Chronic hypoxia decreased $\dot{V}O_2$ by 34% and $\dot{V}CO_2$ by 33% ($P<0.01$) (Fig. 3.1).

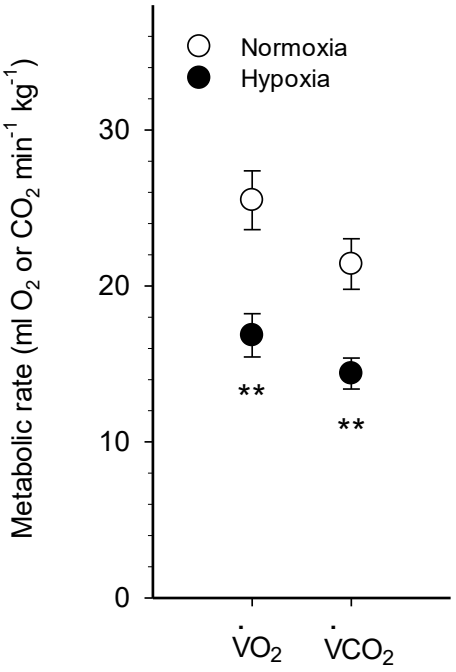

Figure 3.1. Metabolic rates of normoxic controls and hypoxia-acclimated naked mole-rats. Oxygen consumption ($\dot{V}O_2$) and carbon dioxide production ($\dot{V}CO_2$) are presented. Values are means ± SE (N=9 in normoxia and N=7 in hypoxia). Significant effects of hypoxia are indicated as ** (*P*<0.01).

3.3.2. Enzyme activities

Glycolysis

Observed changes in PK and LDH activities suggest that glycolytic capacity was reduced by hypoxia (Figs. 3.2A and 3.2B). PK activity was strongly downregulated by chronic hypoxia and this response was observed in all tissues (Fig. 3.2A; *P*<0.01). LDH activity decreased in liver and muscle (*P*<0.001), increased in kidney (*P*<0.01), and was unchanged in brain and heart (*P*>0.05) (Fig. 3.2B). Overall, enzyme activities calculated

per gram tissue or per gram protein were affected very similarly and lead to the same conclusions apart from LDH in brain and kidney (see Table 3.1).

TCA cycle

CS activity was decreased in brain ($P<0.01$), liver ($P<0.01$) and muscle ($P<0.001$). It was almost doubled in heart ($P<0.001$), but remained unchanged in kidney ($P>0.05$) (Fig. 3.2C). Results were relatively similar when correcting per gram protein except for a decrease in kidney CS activity per gram protein (Table 3.1).

Beta oxidation

β-oxidation capacity was reduced in liver and muscle where the activities of CPT (Fig 3.2D) and HOAD (Fig. 3.2E) were downregulated by hypoxia ($P<0.01$ or $P<0.001$). These same enzymes were not affected in brain, heart and kidney ($P>0.05$). Standardizations per g tissue and per g protein showed the same effects of hypoxia on CPT and HOAD (Table 3.1).

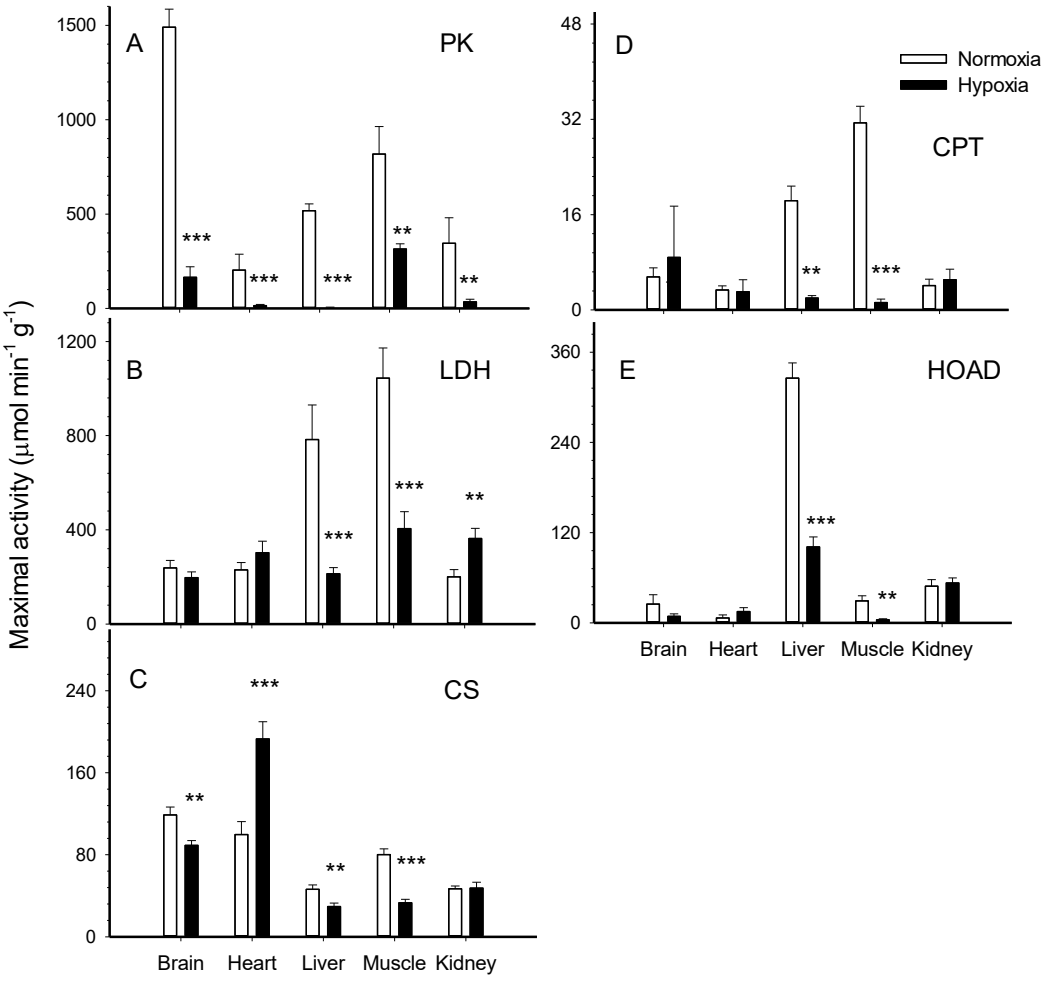

Figure 3.2. Maximal enzymatic activity per gram tissue of (A) pyruvate kinase (PK), (B) lactate dehydrogenase (LDH), (C) citrate synthase (CS), (D) carnitine palmitoyl transferase (CPT) and (E) 3-hydroxyacyl CoA dehydrogenase (HOAD) in the tissues of normoxic controls and hypoxia-acclimated naked mole-rats. Values are means ± SE (N=12 in normoxia and N=9 in hypoxia). Significant effects of hypoxia are indicated as ** (P<0.01) and *** (P<0.001).

Table 3.1. Effects of chronic hypoxia on the activities of key enzymes of energy metabolism (standardized either per gram tissue or per gram protein) in various tissues of naked mole-rats (N=12 in normoxia and N=9 in hypoxia). Significant effects of hypoxia are indicated as * (P<0.05), ** (P<0.01) and *** (P<0.001), and presented as percent differences between treatments. No effect of hypoxia is indicated by NS (P>0.05).

	PK		LDH		CS		CPT		HOAD	
	/g_{tissue}	/$\mu g_{protein}$	/g_{tissue}	/$\mu g_{protein}$	/g_{tissue}	/$\mu g_{protein}$	/g_{tissue}	/$\mu g_{protein}$	/g_{tissue}	/$\mu g_{protein}$
Brain	-89%***	-97%***	NS	-73%***	-25%**	-76%***	NS	NS	NS	NS
Heart	-93%***	-90%***	NS	NS	+94%***	+115%***	NS	NS	NS	NS
Liver	-99%***	-99%***	-73%***	-82%***	-36%**	-57%**	-89%**	-98%**	-69%***	-80%***
Muscle	-61%**	-79%**	-62%***	-80%***	-59%***	-78%***	-96%***	-98%**	-86%**	-93%***
Kidney	-90%**	-96%**	+81%**	NS	NS	-56%***	NS	NS	NS	NS

Na⁺/K⁺-ATPase

Hypoxia downregulated Na^+/K^+-ATPase in the brain, but upregulated it in liver (P<0.05) without affecting muscle and heart (P>0.05) (Fig. 3.3).

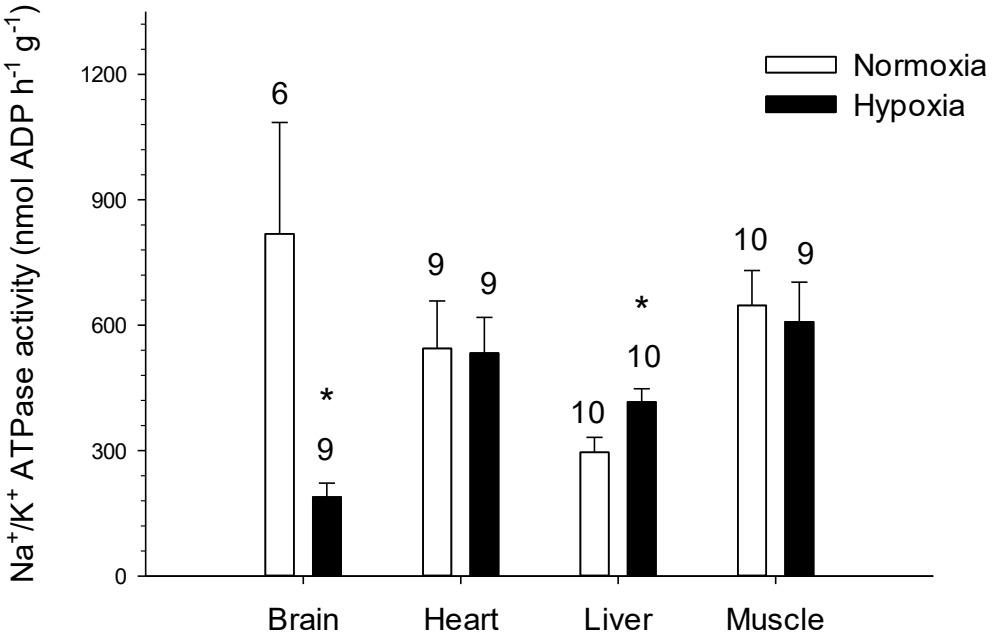

Figure 3.3. Na^+/K^+-ATPase activity per gram tissue in the tissues of normoxic controls and hypoxia-acclimated naked mole-rats. Values are means ± SE Sample sizes are indicated on the figure. Significant effects of hypoxia are indicated as * (P<0.05).

3.3.3. Membrane lipids

Hypoxia caused large changes in cholesterol abundance in all tissues. Relative cholesterol increased in heart, muscle (P<0.05) and kidney (P<0.01), it decreased in brain (P<0.05) and liver (P<0.001) (Fig. 3.4). The effects of hypoxia acclimation on the total PL content per gram tissue (an index of membrane abundance in [PL]/g), the DBI,

and the absolute concentration of saturated (SFA), monounsaturated (MUFA), and polyunsaturated fatty acids (PUFA) of NMR membranes are shown in Table 3.2. Hypoxia elicited a decrease in DBI in liver, but an increase in muscle without affecting the other tissues. There was an increase in [PL] in brain and liver, but a decrease in muscle. Chronic hypoxia had no effect on the PL concentration of heart and kidney. %SFA increased in liver, decreased in muscle, but did not change in the other tissues. %MUFA did not change in all tissues except liver where it decreased. %PUFA decreased in liver and kidney, increased in muscle, but did not change in the other tissues (Table 3.2). Surprisingly, NMR membranes of all tissues only contained trace amounts of 22:6 in both normoxic and hypoxic animals (see Figs. 1-5 in appendix B).

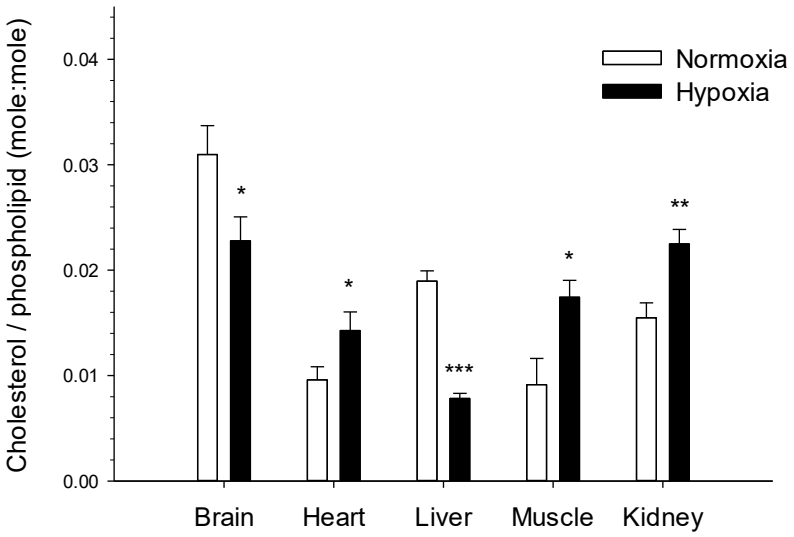

Figure 3.4. Relative membrane cholesterol levels in the tissues of normoxic controls and hypoxia-acclimated naked mole-rats. Values are means ± SE (N=12 in normoxia and N=9 in hypoxia). Significant effects of hypoxia are indicated as * (P<0.05), ** (P<0.01) and *** (P<0.001).

Table 3.2. Relative effects of chronic hypoxia on the membrane phospholipids of naked mole-rat tissues. Double bond index (DBI), phospholipid/g_{tissue} (PL/g), saturated fatty acids (SFA), monounsaturated fatty acids (MUFA) and polyunsaturated fatty acids (PUFA) are indicated separately. Absolute concentrations of PL and FAs in moles per gram tissue (see Table 1 in appendix B) were used to calculate the percent changes presented. Values are means ± SE (N=12 in normoxia and N=9 in hypoxia). Significant effects of hypoxia are indicated as * (P<0.05), ** (P<0.01) and *** (P<0.001). No effect of hypoxia is indicated by NS (P>0.05).

	DBI	PL/g	SFA	MUFA	PUFA
Brain	NS	+18%**	NS	NS	NS
Heart	NS	NS	NS	NS	NS
Liver	-23%*	+50%**	+24%*	-43%***	-12%*
Muscle	+22%*	-28%***	-27%*	NS	+11%*
Kidney	NS	NS	NS	NS	-5%*

3.4. Discussion

Several weeks of hypoxia cause a 34% decrease in the metabolic rate of NMRs (Fig. 3.1). I show that this suppression occurs simultaneously with a major decrease in the capacity for energy metabolism, the downregulation of brain Na^+/K^+-ATPase, and widespread changes in membrane lipids. Chronic hypoxia decreases the activities of key enzymes in glycolysis, the TCA cycle and the β-oxidation pathway, but also induces important changes in the relative abundance of membrane cholesterol in all tissues. Together, these changes in protein activities and membrane composition may reflect a coordinated physiological response to hypoxia, although a clear functional link between membrane changes and enzyme downregulation could not be established in this study.

Nevertheless, this is the first demonstration that hypometabolic NMRs alter the lipid composition of their membranes in response to chronic *in vivo* exposure to hypoxia.

3.4.1. Metabolic suppression in hypoxia

The degree of metabolic rate suppression observed after 4 weeks at 11% O_2 is consistent with the only previous report of NMR metabolic rate measured during chronic hypoxia (25-33% reduction after 10 days at 8% O_2) (Chung et al., 2016). More information is available for acute exposure of a few hours only. NMRs rapidly exposed to progressive hypoxia from 9 to 3% O_2 experience a stepwise decrease in metabolic rate, with the strongest suppression occurring at the lowest oxygen level (55% decrease in MO_2 at 9% O_2, but a more than 80% decline at 3% O_2) (Pamenter et al., 2019). In addition to tolerating extremely low oxygen, NMRs have the capacity to survive in complete anoxia for up to 18 min (Park et al., 2017). However, the goal of this study was not to examine the effects of anoxia (when reliance on anaerobic glycolysis becomes essential for survival), but to characterize those of chronic hypoxia on aerobic metabolism.

3.4.2. Downregulation of glycolysis

Chronic hypoxia causes large tissue-specific changes in the activities of the glycolytic enzymes PK and LDH (Table 3.1; Figs. 3.2A and 3.2B). The general downregulation of PK suggests that glycolytic capacity is reduced, but this enzyme shares flux control with phosphofructokinase and hexokinase that were not measured here. If PK behaviour is indicative of overall changes in pathway capacity, NMRs respond very differently than hypoxic rats (Daneshrad et al., 2000; Dutta et al., 2009;

Malthankar-Phatak et al., 2008; Pastoris et al., 1995), mice (Cáceda et al., 2001) and deer mice (Cheviron et al., 2012; Lau et al., 2017), who either activate or do not modulate glycolysis in hypoxia. Conversely, NMRs respond by downregulating the glycolytic supply of pyruvate to the TCA cycle. In NMRs, the strong downregulation of PK observed in all tissues (61-99% decrease in activity; Fig. 3.2A) would concomitantly slow the aerobic production of ATP. The 62-73% downregulation of LDH observed in liver and muscle also shows that NMRs do not rely on anaerobic metabolism at this level of hypoxia (Fig. 3.2B). This is perhaps not surprising because the anaerobic use of total carbohydrate reserves could only last minutes to hours, not several weeks. A recent study reported that NMRs store more cardiac glycogen than mice (Faulkes et al., 2019), and this observation was interpreted as an indication that cardiac glycolysis is activated in hypoxia. The results presented here do not support this idea because heart PK activity is strongly decreased (Fig. 3.2A), suggesting that glycolysis is downregulated rather than upregulated, at least in chronic hypoxia. Hypoxic NMRs can afford to slow down glycolysis because they rely on the suppression of aerobic metabolism that likely spares small carbohydrate stores and minimizes the accumulation of anaerobic end-products.

3.4.3. Effects of chronic hypoxia on citrate synthase

In concert with the downregulation of glycolysis, the activity of CS is decreased in NMR brain, liver and muscle (25-59%) (Fig. 3.2C). These responses were not observed in chronically hypoxic rats (Daneshrad et al., 2000; Galbes et al., 2008), mice (Cáceda et al., 2001) or deer mice (Cheviron et al., 2012; Lau et al., 2017), which instead maintain normoxic CS activity. Sustaining aerobic ATP supply from the TCA cycle

becomes problematic when oxygen is scarce, and NMRs can afford to downregulate this pathway because ATP demand is lowered by metabolic suppression. Tissue CS activity can be modulated by changing mitochondrial density to adjust enzyme abundance (DiMauro and Moraes, 1993). This is supported here because acute hypoxia has no effect on CS activity in NMR brains (Pamenter et al., 2018), whereas chronic hypoxia downregulates the enzyme (this study; Fig. 3.2C); and a few hours of acute hypoxia does not provide sufficient time to alter mitochondrial density.

In contrast to other tissues, activity is upregulated by chronic hypoxia in NMR heart (94%; Fig. 3.2C), indicating that the TCA cycle is stimulated in this organ. The utility of this response is not intuitively obvious; however, similar responses have been observed in the hearts of other animals such as high-altitude Andean mice (Schippers et al., 2012) and sablefish (Gerber et al., 2019). It is possible that activating the TCA cycle in this key organ is necessary because cardiac output must be increased to compensate for the decreased arterial O_2 saturation caused by hypoxia. However, such a scenario is not consistent with lower heart rate during acute hypoxia (Pamenter et al., 2019), although it is unclear whether more chronic hypoxia could have the opposite effect on heart rate. Taken together, CS upregulation and PK downregulation suggest that the chronically hypoxic NMR heart switches to using more lipids and less carbohydrates, thus increasing its reliance on acetyl-CoA from β-oxidation rather than glycolysis. Such a change in fuel selection precludes NMR hearts from taking advantage of the 10-25% higher ATP yield per mole O_2 provided by carbohydrates over lipids (Hochachka et al., 1991; Hutter et al., 1985; McClelland et al., 1998) and it has also been reported for various cardiac pathologies (Kolwicz and Tian, 2011). Here, this

response is consistent with the idea that the higher cardiac glycogen reserves of NMR (Faulkes et al., 2019) are used for acute and severe hypoxia, rather than for coping with chronic low oxygen stress. These observations suggest that metabolically-suppressed NMRs can survive at 11% O_2 without harnessing all the oxygen-saving mechanisms available to them.

3.4.4. Tissue-specific downregulation of β-oxidation

Chronic hypoxia causes the downregulation of the β-oxidation enzymes CPT (Fig. 3.2D) and HOAD (Fig. 3.2E) in most tissues except the heart and kidney. These findings agree with previous studies in rats (Daneshrad et al., 2000; Dutta et al., 2009; Galbes et al., 2008) and mice (Morash et al., 2013), but not high altitude deer mice in which either increased (Cheviron et al., 2012; Cheviron et al., 2014) or sustained HOAD activity has been reported (Lau et al., 2017). Reducing flux through β-oxidation logically follows the downregulation of: (i) the other main pathways of energy metabolism (glycolysis and TCA cycle), and (ii) multiple ATP-utilizing processes (overall metabolic suppression) observed in most NMR tissues. The absence of a change in the β-oxidation pathway in brain, kidney and heart may be related to the potentially higher energy demands of these critical organs. More research will be needed to examine the underlying physiological reasons why some tissues maintain β-oxidation and others do not.

3.4.5. Na^+/K^+-ATPase activity is downregulated in NMR brains

Chronic hypoxia reduces Na^+/K^+-ATPase activity in NMR brain (77%), but not in muscle, liver or heart (Fig. 3.3). This localized response may be a conserved adaptation

shared by hypoxia-tolerant organisms because similar changes also occur in anoxic turtle brain (Hylland et al., 1997), but not in chronically hypoxic mice (Cáceda et al., 2001). The brain is highly metabolically active (accounting for ~20% of whole-body metabolic rate in NMRs (Gesser et al., 1977)), and uses ~60% of its total ATP supply for pumping ions to ensure normal electric activity. The brain relies on Na^+/K^+-ATPase to maintain Na^+ and K^+ gradients and, indirectly, to regulate the transport of Ca^{2+} and neurotransmitters (Erecińska and Silver, 1994). Any failure of this pump in hypoxia-sensitive neurons leads to a spike in intracellular calcium concentration that can eventually cause cell death (Hochachka, 1986). The robust reduction of Na^+/K^+-ATPase activity observed here in NMR brains must occur together with a decrease in ion channel leak, so that ATP supply and demand can remain in balance (Bickler and Buck, 1998; Boutilier and St-Pierre, 2000). However, the potential inhibition of ion channels in the hypoxic NMR brain has not been explored.

3.4.6. Changes in membrane composition caused by chronic hypoxia

This study is the first to demonstrate that *in vivo* exposure to chronic hypoxia can alter the composition of membrane lipids in mammals. It is unclear whether such changes only occur in hypoxia-tolerant species or if it is a general mammalian response. In NMRs, chronic hypoxia caused widespread changes in the membrane cholesterol abundance of all tissues. This result is intriguing because studies on artificial membranes (Garcia et al., 2019; Yeagle et al., 1988) and on manipulated fish membranes (Crockett and Hazel, 1997) show that changes in intrinsic, baseline cholesterol generally downregulates Na^+/K^+-ATPase: possibly contributing to metabolic suppression. NMR brains may use this mechanism because a large decrease in

membrane cholesterol (Fig. 3.4) occurs together with the strong downregulation of Na^+/K^+-ATPase (Fig. 3.3). However, results from other NMR tissues do not support this idea because membrane cholesterol is modified without downregulating Na^+/K^+-ATPase activity.

In contrast to previous findings on goldfish (Chapter 2), chronic hypoxia does not cause major changes in the fatty acid composition of NMR membranes (Table 3.2). Because 22:6 is a known activator of ion pumps (Calhoon et al., 2015; Turner et al., 2005), decreasing its relative abundance could be used to suppress metabolism (Chapter 2). However, this study shows that NMRs cannot rely on this mechanism because they have no room to reduce membrane 22:6 from an intrinsically low level of < 2% in non-hypometabolic animals (Figures 1-5 in appendix B). Interestingly, 22:6 is much more abundant in mouse PLs (11-26%), and the very low levels of this peroxidation-prone polyunsaturated fatty acid found in NMRs may explain their longer lifespan and lower metabolic rate (Hulbert et al., 2006).

3.5. Perspectives and significance

This study shows that the downregulation of energy metabolism and brain Na^+/K^+-ATPase, as well as the widespread restructuring of membranes are coordinated physiological responses that accompany metabolic suppression in NMRs. Instead of activating anaerobic metabolism, chronic hypoxia downregulates the aerobic supply of acetyl-CoA from glycolysis and β-oxidation to the TCA cycle in brain, muscle and liver. By contrast, the NMR heart maintains aerobic metabolism, possibly to keep adequate oxygen supply to the other organs. These tissue-specific responses suggest that local metabolic requirements vary greatly. Therefore, characterizing the effects of chronic

hypoxia on the metabolic capacity and fuel preference of isolated mitochondria from different tissues may be a productive avenue for future research. Hypoxia-induced changes in membrane lipids occur in NMRs (Fig. 3.4) and goldfish (Chapter 2), but the physiological significance of this response is still unclear. Do the observed changes in NMR membrane cholesterol play a role in promoting metabolic suppression? A common membrane signal regulating the joint inhibition of ion pumps and ion channels could be an exquisite way to preserve the balance between ATP supply and demand in the hypometabolic state, and it could serve as a neuroprotective mechanism in NMR brain. To determine whether membrane restructuring and metabolic suppression are physiologically linked, it may be useful to mimic the membrane changes observed *in vivo* on artificial membranes to characterize how ion pumps and channels are affected.

Chapter 4

Goldfish response to chronic hypoxia: Mitochondrial respiration, fuel preference and energy metabolism

Based on a manuscript by the same title

Written by

Elie Farhat, Hang Cheng, Caroline Romestaing, Matthew Pamenter and Jean-Michel Weber

And published in

Metabolites

https://doi.org/10.3390/metabo11030187

Statement of contribution: This work was performed alongside Hang Cheng and Dr. Caroline Romestaing. I acclimated the fish and measured all enzymatic activities. Moreover, I isolated the red muscle fibres and measured mitochondrial respiration rates in all tissues alongside both Hang and Dr. Romestaing. Finally, I wrote the paper as first author and edited it along with Dr. Jean-Michel Weber.

4.1. Introduction

Hypoxia is a state of oxygen limitation commonly found in many environments. It presents a dangerous challenge requiring animals to enter a hypometabolic state for survival (Bickler and Buck, 2007). Under normoxic conditions, adenosine triphosphate (ATP) is mainly produced by oxidative phosphorylation (OXPHOS) in the mitochondria through the electron transport chain (ETC) (Semenza, 2007; Solaini et al., 2010). In hypoxia-sensitive species, this critical pathway of energy metabolism is inhibited when O_2 is scarce, causing an imbalance between the now lower supply of ATP and normal energetic demand (Boutilier, 2001). By contrast, hypoxia-tolerant animals can maintain this balance by regulating the activity of key enzymes of energy metabolism (e.g., slowing the tricarboxylic acid (TCA) cycle and stimulating glycolysis) (Martínez et al., 2006; Solaini et al., 2010), and by downregulating ion pumps such as Na^+/K^+-ATPase (Hochachka, 1986). Mitochondria are thought to play a key role in coordinating these responses because of their ability to detect changes in O_2 (Pamenter, 2014). Mitochondrial respiration can be affected by hypoxia acclimation differently, depending on metabolic fuel, species, and tissue. For instance, respiration capacity is decreased in the tissues of shovelnose ray sharks (Hickey et al., 2012), oysters (Sokolova, 2018), and frogs (St-Pierre et al., 2000b), but maintained in epaulette sharks (Hickey et al., 2012), killifish (Du et al., 2016), and snappers (Cook et al., 2013). Goldfish are among the champions of hypoxia tolerance (Bickler and Buck, 2007), particularly at low water temperatures, but how their mitochondria respond to prolonged hypoxia is presently unknown.

Goldfish can suppress metabolic rate by 42–74% to cope with a lack of O_2 (Chapter 2) (van Ginneken et al., 2004; Van Waversveld et al., 1989) and they have larger glycogen stores than hypoxia-sensitive species (Richards, 2009). This indicates a potentially higher capacity for glycolysis and increased reliance on carbohydrates during prolonged hypoxia (Jibb and Richards, 2008). It would be useful to establish whether hypoxic goldfish favor carbohydrates over lipids by quantifying the activities of key enzymes involved in glycolysis and β-oxidation, and by testing the metabolic fuel preference of individual tissues. Therefore, the main goal of this study was to determine how prolonged hypoxia affects the respiration capacity and fuel selection of mitochondria in different goldfish tissues. To complement this investigation of fuel preference and to help identify potential mechanisms of metabolic suppression, I have also measured key enzymes of energy metabolism involved in glycolysis, β-oxidation and the TCA cycle, as well as Na^+/K^+-ATPase in brain, liver, and white muscle. I hypothesized that hypoxia-acclimated goldfish will (i) favor carbohydrates over lipids, and (ii) decrease overall flux capacity for energy metabolism to promote metabolic suppression. I anticipated that changes both in mitochondrial respiration and in enzyme activities would reflect these responses, but more strongly so in a critical tissue like the brain.

4.2. Methods

4.2.1. Animals

Adult common goldfish (*Carassius auratus* (Linnaeus 1758)) (*N* = 43, body mass 20.9 ± 0.2 g) were purchased from AQUAlity Tropical Fish Wholesale (Mississauga, Ontario, Canada) and held in a 1200 L flow-through holding tank in dechloraminated,

well-oxygenated water, under a 12 h:12 h light:dark photoperiod, and were fed 3 mm floating fish pellets (Profishent; Martin Mills; Elmira, Ontario, Canada) once a day. They were randomly allocated to normoxia or hypoxia. All measurements were performed at 13°C, and the fish were acclimated to this temperature for at least 2 weeks in the holding tank before starting experiments. Water was then made progressively hypoxic over 7 days by bubbling increasing amounts of N_2 through a column filled with glass beads. Water PO_2 was measured using galvanic oxygen probes (Loligo Systems, Tjele, Denmark). The probes were calibrated before each measurement using air-saturated water (20.9% O_2). Oxygen availability went from 100% saturation on day 1 to 50, 40, 30, 20, 15, and finally 10% (or 2.1 kPa) on day 7. PO_2 was maintained at that low level for a period of at least 4 weeks. This level of hypoxia was selected because it induces significant suppression of goldfish aerobic metabolism, but without causing any ATP synthesis from anaerobic ethanol production (Chapter 2). All procedures were approved by the Animal Care Committee of the University of Ottawa (protocol BL-1625) and adhered to the guidelines established by the Canadian Council on Animal Care for the use of animals in research.

4.2.2. Mitochondrial respiration

After at least 4 weeks of acclimation to either normoxia or hypoxia, goldfish were quickly euthanized by cervical dislocation and brain, liver, white muscle, heart, and red muscle were carefully dissected. At least 150 mg of freshly collected brain, liver, and white muscle were quickly frozen in liquid N_2 and stored at −80°C for enzyme analyses. Approximately 30–50 mg of fresh brain, liver, white muscle, heart, and red muscle were placed in ice-cold BIOPS buffer (10 mM Ca-ethylene glycol-bis(β-aminoethyl ether)-

N,N,N′,N′-tetraacetic acid (EGTA) buffer, 0.1 µM free calcium, 20 mM imidazole, 20 mM taurine, 50 mM 2-(N-Morpholino) ethanesulfonic acid potassium salt (K-MES), 0.5 mM 1,4-dithiothreitol (DTT), 6.56 mM $MgCl_2$, 5.77 mM ATP, and 15 mM phosphocreatine, pH 7.1) for mitochondrial respiratory capacity measurements.

Tissues were prepared for mitochondrial respiration in two different ways. Brain, liver, and white muscle were prepared by relying on a shredding technique adapted from (Kuznetsov et al., 2002; Kuznetsov et al., 2008; Larsen et al., 2014; Salin et al., 2016; Velasco et al., 2012). Briefly, tissues were cut in ice-cold MiR05 (0.5 mM EGTA, 3 mM $MgCl_2.6\ H_2O$, 60 mM lactobionic acid, 20 mM taurine, 10 mM KH_2PO_4, 20 mM 4-(2-Hydroxyethyl)piperazine-1-ethanesulfonic acid (HEPES), 110 mM D-sucrose, and 1 g L^{-1} fatty acid-free bovine serum albumin (BSA), pH 7.3) respirometry buffer using microdissecting scissors to obtain a small particulate solution (liver/white muscle) or by using a pestle for brain. The homogenization was completed by pipetting several times to obtain very small tissue pieces (tested by pipetting through a 1 mL tip for white muscle or 0.2 mL tip for brain and liver). The shredded homogenates were then diluted in MiR05 to obtain the desired final concentration (100 mg mL^{-1} for the liver, 60 mg mL^{-1} for the white muscle, and 5 mg mL^{-1} for brain). The entire procedure was carried out at 4°C and completed within 20 min of the fish being euthanized. Red muscle and heart were used to prepare permeabilized muscle fiber bundles as previously described (Bourguignon et al., 2017; Pesta and Gnaiger, 2012). Briefly, a small piece of red muscle immersed in BIOPS was dissected to separate muscle fibers. Fiber bundles were transferred to BIOPS solution supplemented with saponin (50 µg mL^{-1}) and mixed gently at 4°C for 30 min. The permeabilized fibers were then gently washed once by

mixing for 10 min at 4°C in the Mir05 solution. Muscle fibers were then weighed, and their respiration was monitored with an Oroboros oxymeter at 13°C in a hyperoxygenated respiratory buffer Mir05.

Mitochondrial respiration of all samples was measured at 13°C using two Oxygraph-2k high-resolution respirometers (Oroboros Instruments, Innsbruck, Austria) running in parallel, each with a specific substrate protocol (carbohydrates or lipids). Oxygen concentration (pmol mL^{-1}) was recorded using DatLab software (Oroboros Instruments). A two-point calibration of the oxygen electrodes was done daily: air saturation with the addition of oxygen and zero oxygen saturation with the addition of sodium dithionite. For the shredded preparation, homogenates were placed into the calibrated chamber with saponin (50 µg mL^{-1}) for 15 min before starting any measurement. To avoid any limitation of oxygen diffusion to the cell, measurements were run under hyperoxygenated conditions (350–450 µmol L^{-1}). Oxygen was added to the respirometry chambers at the beginning of the protocol. Mass-specific O_2 consumption was expressed as pmol O_2 s^{-1} mg^{-1} wet tissue. Two sequential substrate–uncoupler–inhibitor–titration (SUIT) protocols were run simultaneously for each tissue as follows:

For the carbohydrate protocol, substrates were added in the following order: 5 mM/2.5 mM pyruvate/malate (PM) to ensure electron entry to complex I of the ETC (nonphosphorylating/LEAK), followed by saturating concentrations of ADP (1 mM for brain and 0.5 mM for liver/white muscle) to obtain the phosphorylating respiration rate/to activate ATP synthesis (OXPHOS), 10 mM glutamate to estimate amino acid utilization, 10 mM succinate to fully activate the ETC and obtain the real OXPHOS state by

supporting electron entry to complex I + II, and 10 μM cytochrome C to test for the integrity of the outer mitochondrial membrane (rate below 15% was considered acceptable) (Kuznetsov et al., 2002). A titration of 2 μM carbonyl cyanide m-chlorophenyl hydrazone (CCCP) was used to obtain the CCCP-uncoupled respiration rate, 2.5 μM antimycin A to inhibit complex III and obtain a residual oxygen consumption that is not linked to mitochondria. Finally, 2.5 μM ascorbate and a titration of N,N,N′,N′-tetramethyl-p-phenylenediamine (TMPD; final concentration = 2–2.5 mM TMPD) to measure complex IV state 3 respiration and obtain the maximal activity of cytochrome c oxidase (COX) as an estimate of mitochondrial density (Larsen et al., 2012).

For the lipid protocol, substrates were added in the following order: 0.04 mM/2.5 mM palmitoylcarnitine/malate (PCM) to measure complex I + II respiration (nonphosphorylating/LEAK). At this concentration of malate, note that the exact contribution of complex II to the respiration rates measured is unclear. This is followed by the addition of a saturating concentration of ADP (as in the carbohydrate protocol), 10 μM cytochrome C, 2–4 μM CCCP, 2.5 μM antimycin A, 2.5 μM ascorbate, and finally, a titration of TMPD (final concentration = 2–2.5 mM; brain, liver, and white muscle only). Note that “carbohydrate protocol” and “lipid protocol” are so named to express what starting substrate is used in each procedure. COX activity was measured in both protocols in the presence of multiple substrates at the time antimycin A was added to the respirometer chamber.

4.2.3. Enzyme assays

All enzyme activities were measured using a Spectra Max Plus384 Absorbance Microplate Reader (Molecular Devices, Sunnyvale, CA). To measure the activities of

key enzymes involved in (i) glycolysis (hexokinase (HK), pyruvate kinase (PK), and lactate dehydrogenase (LDH)), (ii) β-oxidation (carnitine palmitoyl transferase (CPT) and 3-hydroxyacyl CoA dehydrogenase (HOAD)), and (iii) the tricarboxylic acid cycle (citrate synthase (CS)), ~50 mg of each frozen tissue was weighed and homogenized on ice in 19 volumes of extraction medium (25 mM Tris/HCl + 1 mM EDTA as well as 5 mM dithiothreitol and 0.05% (vol/vol) Triton X-100 that were added on the day of the experiment to complete the enzyme extraction). Homogenates were then centrifuged at 4°C at 2400× *g* for 5 min, and the resulting supernatant was stored at −80°C until analyses. All homogenates were subjected to one freeze/thaw cycle. Preliminary experiments were carried out to ensure that all substrate and cofactor concentrations were saturating but not inhibitory. Control reactions (containing no substrate) were run simultaneously for each enzyme to measure background activity, if present. All assays were run in triplicate.

Assay conditions were as follows: HK (A340; EC 2.7.1.1; (Best et al., 2014)): 1 mM glucose, 5 mM $MgCl_2$, 0.24 mM NADH, 2 mM phosphoenolpyruvate (PEP), 5 U/mL PK, 20 U/mL LDH, and 4 mM ATP (omitted from the control). PK: (A340; EC 2.7.1.40; (Zammit et al., 1978)): 0.17 mM NADH, 5 mM ADP, 80 mM KCl, 10 mM $MgCl_2$, 5 mM PEP (omitted from the control), and excess coupling enzyme (LDH) in 160 mM triethanolamine/HCl. LDH: (A340; EC; 1.1.1.27; (Zammit and Newsholme, 1976)): 0.17 mM NADH, 1 mM KCN, and 2 mM pyruvate (omitted from the control) in 50 mM Tris/HCl. CS: (A412; EC 2.3.3.1; (Alp et al., 1976)): 0.2 mM 5,5′dithiobis(2-nitrobenzoic acid) (DTNB), 0.1 mM acetyl-CoA, and 0.5 mM oxaloacetate (omitted from the control) in 50 mM Tris-HCl. CPT: (A412; EC 2.3.1.21; (Guglielmo et al., 2002)): 0.15 mM DTNB,

0.035 mM palmitoyl CoA, carnitine (omitted from the control) in 50 mM Tris. HOAD: (A340; EC 1.1.1.35; (Guglielmo et al., 2002)): 0.2 mM NADH, and 0.1 mM acetoacetyl-CoA (omitted from the control) in 50 mM Imidazole + 1 mM EDTA.

The activity of Na^+/K^+-ATPase (A340) was measured by using a modified protocol from (McCormick, 1993). Frozen tissue was weighed (~100 mg) and homogenized on ice with a sonicator (Fisher Scientific Sonic Dismembrator model 100, San Diego, CA) in a 4:1 SEI:SEID buffer (SEI: 250 mM sucrose, 10 mM EDTA, and 42 mM imidazole; SEID: 100 mL SEI + 0.5 g sodium deoxycholate). Homogenates were then centrifuged at 10,000× *g* for 5 min at 4°C, and the resulting supernatant was directly used in the assay. The assay was performed as previously described (McCormick, 1993) in quadruplicate (2 replicates contained 10 µL of homogenate + 200 µL of assay solution A (50 mM imidazole, 2.8 mM PEP, 0.7 mM ATP, 0.22 mM NADH, 5 mM PK, and 4 mM LDH) and 2 replicates contained 10 µL of homogenate + 200 µL of assay solution B (Solution A + 0.5 mM ouabain)). Ouabain was added to block Na^+/K^+-ATPase and measure any detectable ATP use not associated with this enzyme.

4.2.4. Calculations and statistics

Antimycin A values were subtracted from PM/PCM, ADP, glutamate, succinate, and CCCP values to obtain all desired states (LEAK, OXPHOS, and CCCP-uncoupled). Ascorbate values were subtracted from TMPD values to calculate COX activity. Mitochondrial respiratory control ratio (RCR), an indicator of mitochondrial coupling, was calculated as a ratio between OXPHOS and LEAK (OXPHOS/LEAK). All respiratory states were normalized to COX activity to avoid any intrinsic variation in mitochondrial density/content. Statistical analyses were performed using SigmaPlot 12.5 (Systat, San

Jose, CA, USA). Data were analyzed using a repeated-measures two-way analysis of variance (RM-ANOVA) for the mitochondrial respiration experiments to test for significant interactions between the two independent variables: (i) oxygen level (normoxia vs. hypoxia) and (ii) type of fuel (lipids vs. carbohydrates), followed by the Holm–Sidak post hoc test. A two-tailed t-test was used to analyze the effects of hypoxia on all enzyme activities. Normality was assessed using the Shapiro–Wilk test, and homoscedasticity by the Levene's test. When the assumptions of normality or equality of variances were not met, the data were normalized by log10. If transformation was unsuccessful, nonparametric Mann–Whitney U test was performed. All values presented are means ± standard error of the mean (s.e.m), and a level of significance of $p < 0.05$ was used in all tests.

4.3. Results

4.3.1. Mitochondrial Respiration

4.3.1.1. LEAK

Nonphosphorylating respiration (LEAK) represents mitochondrial respiration in the presence of pyruvate/malate for the carbohydrate protocol and palmitoylcarnitine/malate for the lipid protocol. There was no effect of either O_2 or fuel type on the heart or red muscle ($p > 0.05$) (Figure 4.1). In normoxia, the liver consumed less O_2 when using carbohydrates rather than lipids ($p < 0.05$). White muscle had higher O_2 consumption when using carbohydrates than when using lipids for both normoxia ($p < 0.001$) and hypoxia ($p < 0.05$). Acclimation to hypoxia caused an increase in LEAK respiration of brain when using lipids and of liver when using carbohydrates ($p < 0.05$).

Moreover, there was a significant interaction between the type of fuel used and chronic hypoxia acclimation in the brain ($p < 0.05$).

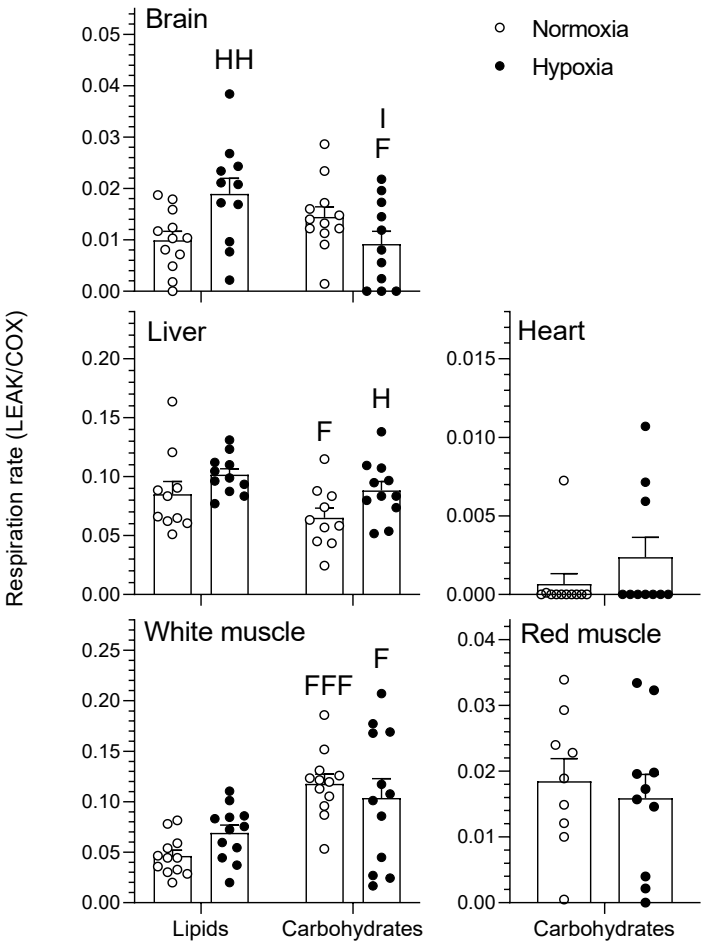

Figure 4.1. Mitochondrial oxidative fuel preference during nonphosphorylating respiration (LEAK) (pmol O_2 sec^{-1} mg^{-1}) normalized to cytochrome c oxidase (COX) respiration in the tissues of normoxic controls (N = 12) and hypoxia-acclimated goldfish (N = 11). LEAK represents mitochondrial respiration in the presence of pyruvate/malate for the carbohydrate protocol and palmitoylcarnitine/malate for the lipid protocol. Values are means ± standard error of the mean (s.e.m). Dots represent individual data points. Differences between fuels are indicated as F ($p < 0.05$) and FFF ($p < 0.001$). Differences between oxygen levels are indicated as H ($p < 0.05$) and HH ($p < 0.01$). Significant interaction between type of fuel and oxygen is indicated as I ($p < 0.05$).

4.3.1.2. OXPHOS

OXPHOS represents mitochondrial respiration following the addition of saturating concentrations of ADP in the presence of pyruvate/malate for the carbohydrate protocol and palmitoylcarnitine/malate for the lipid protocol. The type of fuel used had a significant effect on the OXPHOS respiration rates of goldfish mitochondria in various tissues (Fig 4.2). Specifically, respiration rates of normoxic brain as well as normoxic and hypoxic white muscle mitochondria were higher when using carbohydrates rather than lipids ($p < 0.01$). However, mitochondrial respiration rate of hypoxic liver was lower when using carbohydrates rather than lipids ($p < 0.05$). Neither heart nor red muscle OXPHOS respiration rates differed between oxygen levels ($p > 0.05$). Chronic hypoxia acclimation caused an increase in brain respiration rate when using lipids ($p < 0.01$) without affecting other tissues ($p > 0.05$). Additionally, there was an interaction between the two factors in both brain and white muscle that was only observed when normalizing to COX activity ($p < 0.05$). Mitochondrial respiratory control ratio (RCR), an index of mitochondrial coupling that was calculated as a ratio between OXPHOS and LEAK respiration, was higher in normoxic liver as well as hypoxic white muscle when using carbohydrates rather than lipids ($p < 0.01$). Chronic hypoxia caused a decrease in liver RCR when using carbohydrates ($p < 0.05$) without affecting other tissues ($p > 0.05$) (Figure 4.3). There was also a significant interaction between type of fuel and oxygen in liver and white muscle ($p < 0.05$). Finally, neither type of fuel nor hypoxia acclimation influenced brain or red muscle RCR ($p > 0.05$). OXPHOS respiration ranked in this order for lipids (heart > red muscle = brain > liver > white muscle) and this slightly different order for carbohydrates (heart > red muscle = brain > white muscle > liver) ($p <$

0.001) when not normalizing by COX (data not shown). For OXPHOS respiration normalized with COX (Figure 4.2), rates ranked in this order for lipids (brain > liver = white muscle) and for carbohydrates (heart = brain = white muscle > red muscle = liver) ($p < 0.05$).

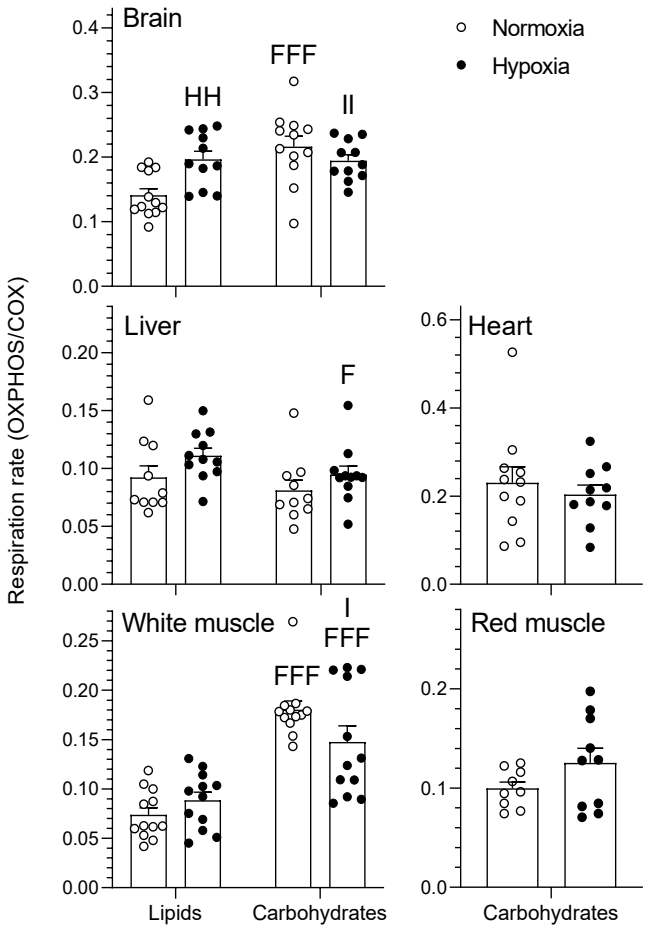

Figure 4.2. Mitochondrial oxidative fuel preference during oxidative phosphorylation (OXPHOS) respiration (pmol O_2 sec^{-1} mg^{-1}) normalized to COX respiration in the tissues of normoxic controls (N = 12) and hypoxia-acclimated goldfish (N = 11). OXPHOS represents mitochondrial respiration following the addition of saturating concentrations of ADP in the presence of pyruvate/malate for the carbohydrate protocol and palmitoylcarnitine/malate for the lipid protocol. Values are means ± s.e.m. Dots represent individual data points. Differences between fuels are indicated as F ($p < 0.05$) and FFF ($p < 0.001$). Difference between oxygen levels is indicated as HH ($p < 0.01$). Significant interactions between type of fuel and oxygen are indicated as I ($p < 0.05$) and II ($p < 0.01$).

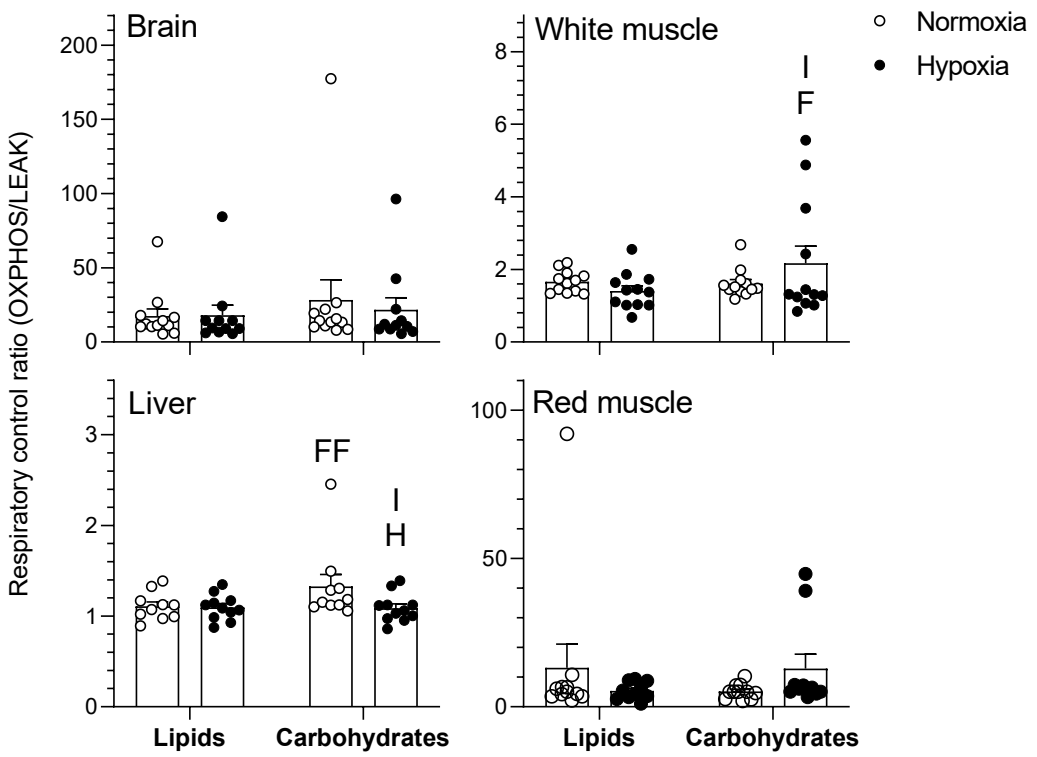

Figure 4.3. Respiratory control ratio (RCR) in the tissues of normoxic controls (*N* = 12) and hypoxia-acclimated goldfish (*N* = 11). RCR was calculated as the ratio between OXPHOS respiration and LEAK respiration (OXPHOS/LEAK). Values are means ± s.e.m. Dots represent individual data points. Differences between fuels are indicated as F ($p < 0.05$) and FF ($p < 0.01$). Difference between oxygen levels is indicated as H ($p < 0.05$). Significant interaction between type of fuel and oxygen is indicated as I ($p < 0.05$).

4.3.1.3. CCCP-uncoupled state

The carbonyl cyanide m-chlorophenyl hydrazone (CCCP)-uncoupled state represents mitochondrial respiration following titration of carbonyl cyanide m-chlorophenyl hydrazone (CCCP) in the presence of pyruvate/malate + ADP + glutamate + succinate + cytochrome C for the carbohydrate protocol and palmitoylcarnitine/malate

+ ADP + cytochrome C for the lipid protocol. Respiration rate was higher when using carbohydrates rather than lipids in normoxic brain as well as in normoxic and hypoxic liver and white muscle ($p < 0.05$). Chronic acclimation to hypoxia caused a decrease in CCCP-uncoupled respiration rates of brain and white muscle, but an increase in heart, when using carbohydrates ($p < 0.05$) (Fig 4.4). Finally, CCCP-uncoupled red muscle mitochondria were not affected by O_2 ($p > 0.05$).

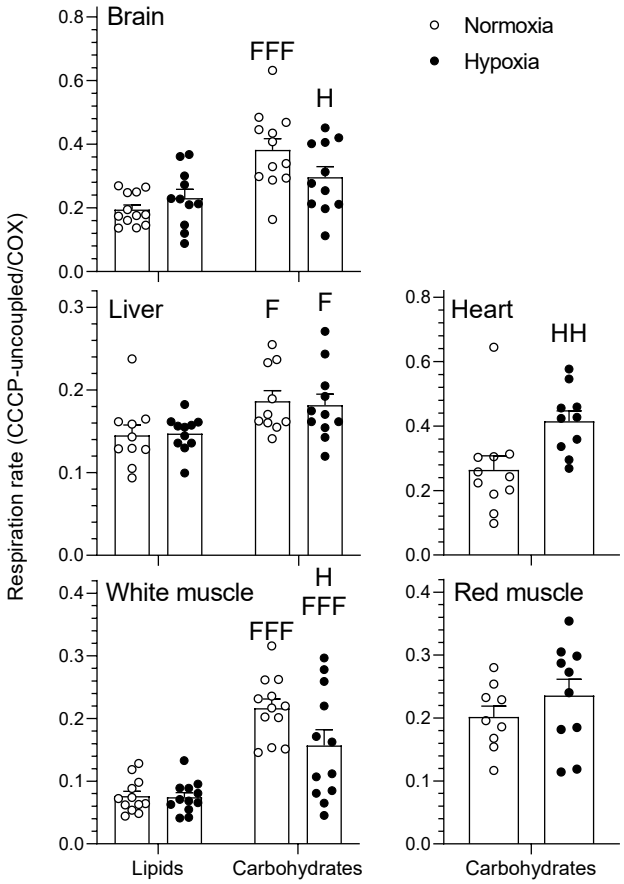

Figure 4.4. Mitochondrial oxidative fuel preference during the CCCP-uncoupled state (pmol O_2 sec^{-1} mg^{-1}) normalized to COX respiration in the tissues of normoxic controls (*N* = 12) and hypoxia-acclimated goldfish (*N* = 11). The CCCP-uncoupled state represents mitochondrial respiration following titration of carbonyl cyanide m-chlorophenyl hydrazone (CCCP) in the presence of pyruvate/malate + ADP + glutamate + succinate + cytochrome C for the carbohydrate protocol and palmitoylcarnitine/malate + ADP + cytochrome C for the lipid protocol. Values are means ± s.e.m. Dots represent individual data points. Differences between fuels are indicated as F ($p < 0.05$) and FFF ($p < 0.001$). Differences between oxygen levels are indicated as H ($p < 0.05$) and HH ($p < 0.01$).

4.3.1.4. Cytochrome oxidase

Cytochrome *c* oxidase (COX) represents mitochondrial respiration following addition of ascorbate and a titration of N,N,N′,N′-tetramethyl-p-phenylenediamine (TMPD) in the presence of pyruvate/malate + ADP + glutamate + succinate + cytochrome c + CCCP + antimycin A for the carbohydrate protocol and palmitoylcarnitine/malate + ADP + cytochrome c + CCCP + antimycin A for the lipid protocol. Both the type of fuel and O_2 affected maximal COX respiration in goldfish brain and white muscle, but only O_2 impacted the liver (Figure 4.5). Chronic hypoxia caused a decrease in COX respiration rate when using lipids in brain, liver, and white muscle ($p < 0.05$) as well as in red muscle ($p < 0.05$) when using carbohydrates, without affecting heart ($p > 0.05$). Moreover, COX respiration decreased in normoxic and hypoxic brain ($p < 0.001$) as well as normoxic white muscle ($p < 0.01$) when using carbohydrates rather than lipids (Figure 4.5). There were interactions between type of fuel and O_2 in brain and white muscle COX.

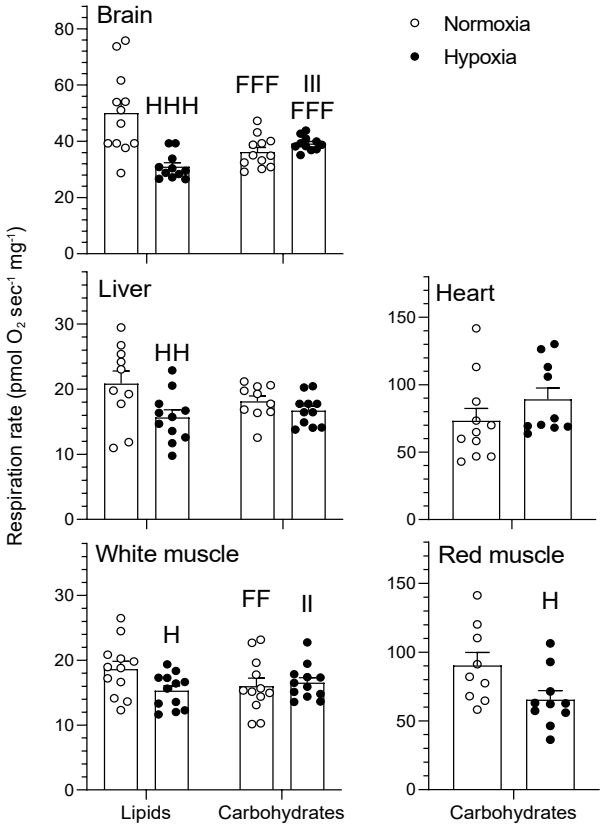

Figure 4.5. Mitochondrial oxidative fuel preference of COX in brain, liver, and white muscle of normoxic controls (*N* = 12) and hypoxia-acclimated goldfish (*N* = 11). COX respiration represents mitochondrial respiration following addition of ascorbate and a titration of N,N,N′,N′-tetramethyl-p-phenylenediamine (TMPD) in the presence of pyruvate/malate + ADP + glutamate + succinate + cytochrome c + CCCP + antimycin A for the carbohydrate protocol and palmitoylcarnitine/malate + ADP + cytochrome c + CCCP + antimycin A for the lipid protocol. Values are means ± s.e.m. Dots represent individual data points. Differences between fuels are indicated as FF ($p < 0.01$) and FFF ($p < 0.001$). Differences between oxygen levels are indicated as H ($p < 0.05$), HH ($p < 0.01$), and HHH ($p < 0.001$). Significant interactions between type of fuel and oxygen are indicated as II ($p < 0.01$) and III ($p < 0.001$).

4.3.2. Energy metabolism enzymes

The activity of hexokinase (HK) increased in white muscle (82%; $p < 0.01$), decreased in brain (12%; $p < 0.05$), and was maintained in liver ($p > 0.05$). Moreover, chronic hypoxia caused a 47% decrease in liver pyruvate kinase (PK) activity ($p < 0.05$) as well as an 18% decrease in carnitine palmitoyl transferase (CPT) and 70% increase in 3-hydroxyacyl CoA dehydrogenase (HOAD) activity of brain ($p < 0.05$). Chronic hypoxia did not change the activities of lactate dehydrogenase (LDH) and citrate synthase (CS) in any measured tissue ($p > 0.05$) (Table 4.1).

Table 4.1. Effects of chronic hypoxia on the activities of key enzymes of glycolysis, β-oxidation and tricarboxylic acid (TCA) cycle in goldfish brain, liver, and white muscle (N = 10 for each treatment group). All values are given in μmol g^{-1} min^{-1} and presented as means ± s.e.m. Differences between oxygen levels are indicated as * ($p < 0.05$) and ** ($p < 0.01$). Values in color show how hypoxia affects enzyme activity: green for activation and red for inhibition.

	Hexokinase		**Pyruvate Kinase**		**Lactate Dehydrogenase**		**Carnitine Palmitoyl Transferase**		**3-Hydroxyacyl CoA Dehydrogenase**		**Citrate Synthase**	
	Normoxia	**Hypoxia**	**Normoxia**	**Hypoxia**	**Normoxia**	**Hypoxia**	**Normoxia**	**Hypoxia**	**Normoxia**	**Hypoxia**	**Normoxia**	**Hypoxia**
Brain	16.64 ± 0.68	14.58 * ± 0.37	39.42 ± 3.06	37.75 ± 3.65	212.5 ± 13.23	204.12 ± 14.15	0.17 ± 0.01	0.14 * ± 0.04	0.1 ± 0.01	0.17 * ± 0.03	0.81 ± 0.24	0.57 ± 0.35
Liver	2.19 ± 0.23	1.89 ± 0.17	124.03 ± 20.95	65.15 * ± 14.38	344.89 ± 45.04	388.96 ± 43.38	10.34 ± 1.05	10.35 ± 1.04	0.29 ± 0.029	0.3 ± 0.03	2.09 ± 0.19	2.83 ± 0.42
White muscle	1.48 ± 0.11	2.69 ** ± 0.29	109.53 ± 5.2	96.63 ± 6.58	96.86 ± 13.51	118.53 ± 20.51	14.31 ± 1.67	11.73 ± 1.39	0.29 ± 0.05	0.46 ± 0.13	5.06 ± 0.31	4.71 ± 0.34

4.3.3. Na^+/K^+-ATPase

Chronic hypoxia caused a 40% decrease in the activity of Na^+/K^+-ATPase in goldfish brains ($p < 0.001$) but did not affect liver or white muscle ($p > 0.05$) (Figure 4.6).

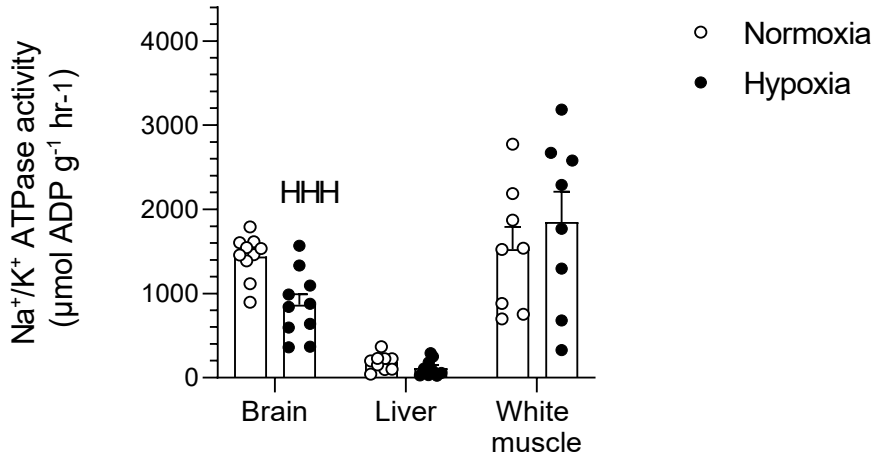

Figure 4.6. Effects of chronic hypoxia on Na^+/K^+-ATPase activity in the brain, liver, and white muscle of normoxic controls ($N = 10$) and hypoxia-acclimated goldfish ($N = 10$). Values are means ± s.e.m. Dots represent individual data points. Significant effect of hypoxia is indicated as HHH ($p < 0.001$).

4.4. Discussion

This study is the first to investigate the effects of hypoxia acclimation on mitochondrial metabolism and Na^+/K^+-ATPase activity of the goldfish. It shows that the capacity for mitochondrial respiration of these champions of hypoxia tolerance depends on prevalent oxygen availability in the environment and on the type of metabolic fuel oxidized in a tissue-specific manner. OXPHOS respiration is higher for carbohydrates in brain and white muscle, whereas liver mitochondria reach higher maximal rates with lipids. Respiration rates are higher in brain when using lipids (LEAK and OXPHOS) and in liver when using carbohydrates (LEAK). Hypoxia acclimation causes significant

tissue-specific changes in respiration rates of most tissues that differ with type of fuel and/or respiration state of mitochondria. COX respiration is lowered by chronic hypoxia acclimation in most tissues. In brain, hypoxia increases LEAK and OXPHOS respiration when using lipids, but decreases CCCP-uncoupled respiration when using carbohydrates. Therefore, hypoxia does not cause a consistent decrease in mitochondrial respiration capacity. Results also reveal that chronic hypoxia has widespread, tissue-specific effects on maximal flux capacity for glycolysis and β-oxidation, and causes strong downregulation of Na^+/K^+-ATPase in the brain. Hypoxia does not lead to universal tissue preference for carbohydrates over lipids. Instead, fuel selection strategies of individual tissues vary greatly. Overall, this study shows that hypoxia-acclimated goldfish mainly promote metabolic suppression by modulating glycolytic capacity and Na^+/K^+-ATPase, rather than by consistently downregulating mitochondrial respiration in all tissues.

4.4.1. Effects of hypoxia on mitochondrial respiration

Hypoxia has virtually no effects on LEAK, OXPHOS, and CCCP-uncoupled respiration when no normalization to COX is performed (results not shown). However, some significant changes in mitochondrial respiration capacity caused by acclimation to hypoxia become apparent when these respiration states are standardized per COX respiration (Figures 4.1–4.4). This means that mitochondrial density is probably decreased by hypoxia in most tissues (see further discussion of COX respiration below). The effects of hypoxia acclimation differ depending on fuel type and mitochondrial respiration state. For example, brain respiration rates are increased by hypoxia during LEAK (substrates without ADP; complex I only; Figure 4.1) and OXPHOS (substrates

with ADP; complexes I+II; Figure 4.2) (lipids; 39–91%) (Figures 4.1, 4.2), but lowered in the CCCP-uncoupled state (carbohydrates; 23%). Moreover, low O_2 causes an increase in respiration rates of liver (carbohydrates; LEAK; 36%) and heart (carbohydrates; CCCP-uncoupled; 57%), but a decrease in liver (carbohydrates; RCR; 18%) and white muscle (carbohydrates; CCCP-uncoupled; 28%). RCR values of liver and white muscle were still low even after careful optimization of the homogenates of both tissues, indicating that preparation quality was lower. Reasons why this was the case are unknown, but respiration rates for these two tissues should be interpreted with caution. The decrease in liver RCR could mean that the mitochondria of this tissue are more uncoupled and less efficient because of the increase in LEAK and the lack of change in OXPHOS respiration. Results in muscle (white and red) and heart LEAK and OXPHOS are consistent with two previous studies on mitochondria from killifish liver (Du et al., 2016) and snapper heart (Cook et al., 2013) that also maintain respiration capacity after acclimation. However, most ectotherms normally show a clear downregulation of mitochondrial performance when exposed to chronic hypoxia. They include shovelnose ray sharks (Hickey et al., 2012), some mollusks (Sokolova, 2018), and frogs (St-Pierre et al., 2000b). The absence of a clear downregulatory response of goldfish mitochondrial respiration in this study is unexpected because goldfish suppress whole-animal metabolic rate by 74% after 4 weeks at 10% air saturation (Chapter 2). General across-tissue changes in mitochondrial respiration capacity are unlikely to be involved in supporting such a deep hypometabolic state. It could be argued that selective pressure for mitochondrial plasticity to support hypoxia tolerance is lacking because the goldfish has evolved the capacity to survive in complete anoxia (Weber, 2016). However, this

reasoning can only be invoked at low temperatures because anoxic survival remains limited to less than a day at 20^{o}C and above (Van den Thillart et al., 1983). As primary generator of cell power, mitochondria pump protons through their inner membrane via several enzyme complexes to establish an electrochemical gradient that eventually leads to the production of ATP at complex V (McElroy and Chandel, 2017). Severe hypoxia depolarizes mitochondria, making complex V switch from producing ATP to consuming ATP (St-Pierre et al., 2000a). This causes a mismatch between ATP supply and demand that affects tissue function. Complex IV (cytochrome c oxidase, COX) is a major contributor to the proton gradient as it uses O_2, the final electron acceptor that is eventually reduced to water (Schmidt-Rohr, 2020). It is interesting to note that COX activity is reduced by hypoxia in most tissues. This enzyme complex is downregulated in brain, liver, white muscle, and red muscle following acclimation (Figure 4.5). It could indicate a possible regulation of the proton gradient in ways that decrease complex V activity, as observed in anoxic turtles that are also known for their extreme tolerance to hypoxia (in brain; (Pamenter et al., 2016), in heart, and liver; (Gomez and Richards, 2018)). Reduced COX respiration could also mean that mitochondrial density is decreased by hypoxia acclimation in all these tissues (although the lack of change in CS activity does not support this notion; see Table 4.1). It is therefore possible that a reduction in COX activity could help metabolic suppression. This study does not address the potential contribution of reactive oxygen species (ROS) to the hypoxia acclimation response. Investigating this contribution could be productive because the mitochondrion is a major producer of ROS, with the vast majority coming from complexes I and III (Quinlan et al., 2013). This organelle is well positioned to sense any

changes in O_2 levels and initiate organism-specific adaptations. This sensing can be done acutely or chronically through an ROS-induced response that may cause rapid accumulation of Ca^{2+} and/or activation of hypoxia inducible factor (HIF) (McElroy and Chandel, 2017). ROS can cause the formation of disulfide bonds, which may change the structure and function of proteins such as phosphatases, transcription factors, and those involved in epigenetic modifications (Pamenter, 2014). Overall, the present results demonstrate that goldfish mitochondria respond in a tissue-specific manner to chronic hypoxia. Their response can differ between respiration states and is dependent on the type of fuel oxidized. Because goldfish mitochondria show no consistent decrease in respiration capacity, they appear to mainly support metabolic suppression by decreasing their number.

4.4.2. Tissue-specific fuel preference of goldfish mitochondria

Metabolic fuel preference of different goldfish tissues has not been investigated previously. Even for more thoroughly studied fish species like rainbow trout, quantitative information about substrate preference is scarce. Nevertheless, it is known that white muscle is mostly geared to use carbohydrates, whereas red muscle favors lipid oxidation (Weber and Haman, 2004). Major indices of mitochondrial respiration (LEAK, OXPHOS, CCCP-uncoupled state, and RCR) are mostly dependent on the type of metabolic fuel oxidized. Furthermore, substrate preference shows great tissue specificity (Figures 4.1–4.4). Respiration capacity is higher for carbohydrates than for lipids in the brain (normoxia; OXPHOS; 53%) and white muscle (normoxia and hypoxia; LEAK and OXPHOS; 39–154%), whereas it is the opposite in the brain (hypoxia; LEAK; 51%), and liver (normoxia and hypoxia; LEAK and OXPHOS; 12–36%; Figures 4.1 and

4.2). Heart and red muscle of normoxic and hypoxic goldfish do not show preference for a particular fuel as they oxidize carbohydrates and lipids equally well. Overall results show interesting inter-tissue differences in fuel selection that are not affected by chronic hypoxia.

In the CCCP-uncoupled state, mitochondrial respiration capacity is also higher in brain (normoxia and hypoxia; 28–96%), white muscle (normoxia and hypoxia; 111–184%), and liver (normoxia and hypoxia; 23–29%) when using carbohydrates rather than lipids (Figure 4.4). In normoxia and hypoxia, it is intriguing to see that the liver shows opposite fuel selection strategies between the CCCP-uncoupled state (Figure 4.4; carbohydrates > lipids) and LEAK and OXPHOS respiration (Figure 4.1 and 4.2; lipids > carbohydrates). CCCP-uncoupled respiration only reflects substrate oxidation, independent of complex V, whereas OXPHOS is further constrained by ATP turnover (Bundgaard et al., 2019). The contrasting fuel preferences between CCCP-uncoupled and OXPHOS respiration of the liver indicate that mitochondrial capacity for carbohydrate oxidation is limited by maximal complex V activity in this tissue. The higher reliance of white muscle on carbohydrates (Figures 4.1 and 4.2) is further supported by the higher mitochondrial RCR of this tissue when oxidizing carbohydrates (Figure 4.3). Overall, mitochondria favor the use of carbohydrates in brain and white muscle, prefer lipids in liver, and rely equally on both fuels in heart and red muscle. These tissue-specific patterns of fuel selection are largely independent of environmental oxygen availability.

4.4.3. Chronic hypoxia and glycolysis

Acclimation to low oxygen downregulates liver PK and brain HK, but upregulates white muscle HK (Table 4.1). Therefore, glycolytic capacity may be decreased in liver and brain, but increased in white muscle of hypoxia-acclimated goldfish. These tissue-specific responses show that aerobic supply of pyruvate from glycolysis to the TCA cycle varies between tissues. This indicates an increased reliance of white muscle on carbohydrates during chronic hypoxia and is also supported by (i) higher mitochondrial OXPHOS respiration (Figure 4.2), and (ii) higher glycogen stores in white muscle (but not liver) of goldfish acclimated to hypoxia (van den Thillart et al., 1980). The lack of change in LDH activity in hypoxia-acclimated goldfish suggests that anaerobic supply of ATP is not enhanced. This makes sense because goldfish do not rely on anaerobic ATP production at this level of hypoxia that does not cause the conversion of lactate to ethanol (Chapter 2) (Regan et al., 2017).

The variable glycolytic responses observed in different goldfish tissues do not allow to characterize a consistent pattern and echo the wide range of effects previously reported for ectotherms. For example, chronic hypoxia downregulates HK in tench white muscle (Johnston and Bernard, 1982), upregulates it in killifish brain (Martínez et al., 2006), but maintains it in goldfish white muscle (van den Thillart and Smit, 1984). Variable responses have also been reported for liver PK, which is upregulated in Nile tilapia (Mahfouz et al., 2015), but maintained in killifish (Martínez et al., 2006) and in goldfish (van den Thillart and Smit, 1984). These different responses may be associated with various experimental conditions (e.g., temperature and diet) used in specific experiments on these different fish species. Under standardized conditions, it would be

useful to explore whether glycolysis responds differently in hypoxia-tolerant vs. hypoxia-sensitive species, but no comparable data can be obtained for sensitive species because they cannot survive equivalent levels of hypoxia. Unfortunately, a common glycolytic response of hypoxia-tolerant ectotherms cannot be inferred from the current information. Like other species examined to date, the goldfish regulates the aerobic supply of ATP through glycolysis in a tissue-specific manner to cope with chronic hypoxia.

4.4.4. β-oxidation and TCA cycle

Acclimation to low O_2 causes no major changes in the capacity for β-oxidation and TCA cycle of goldfish tissues (Table 4.1). Aerobic supply of acetyl-CoA through these pathways is maintained during chronic hypoxia, even though demand is lowered by metabolic suppression (Chapter 2). This contrasts with previous studies on ectotherms that either downregulate (Li et al., 2018; Pillet et al., 2016; Zhou et al., 2000) or upregulate (Gerber et al., 2019; Johnston and Bernard, 1982) lipid catabolism and the TCA cycle. The only effects of chronic hypoxia on goldfish β-oxidation detected here were the downregulation of CPT and upregulation of HOAD in the brain (Table 4.1). The physiological implications of this contrasting brain response remain unclear, but results from brain mitochondria OXPHOS respiration (Figure 4.2) suggest an overall increase in β-oxidation capacity in this tissue during chronic hypoxia.

4.4.5. Downregulation of Na^+/K^+-ATPase in goldfish brain

The most striking physiological response to chronic hypoxia characterized here is a drastic downregulation of Na^+/K^+-ATPase in goldfish brain. The activity of this

essential ion pump is decreased by 40% in the central nervous system, but remains unaffected in white muscle and liver (Figure 4.6). The same brain-specific response was previously reported in hypoxic naked mole-rats (Chapter 3) and anoxic pond slider turtles (Hylland et al., 1997). However, it cannot be concluded that this physiological strategy is a required feature of the champions of hypoxia tolerance because crucian carp exposed to complete anoxia do not use it (Hylland et al., 1997). Most of the ATP consumed by the brain is used to maintain electrical activity by pumping ions (Soengas and Aldegunde, 2002). Na^+/K^+-ATPase is arguably responsible for the majority of the brain ATP consumption and it is essential to maintain Na^+ and K^+ gradients, as well as to regulate Ca^{2+} and neurotransmitter transport (Erecińska and Silver, 1994). Downregulating this pump will inevitably result in a decrease in O_2 consumption. However, reducing Na^+/K^+-ATPase must occur concomitantly with a decrease in ion channel leak to maintain membrane gradients (Bickler and Buck, 1998; Boutilier and St-Pierre, 2000) and to protect against intracellular Ca^{2+} buildup that can lead to neuronal death (Hochachka, 1986). A previous study shows that the anoxic goldfish brain downregulates Ca^{2+} channel activity together with Na^+/K^+-ATPase (Wilkie et al., 2008). This suggests that channel arrest occurs when oxygen is absent, and determining whether it is also the case in chronic hypoxia will be a productive avenue for future research.

4.5. Conclusions

This study shows that acclimation to hypoxia causes significant changes in mitochondrial respiration of all goldfish tissues. However, these mitochondrial responses vary greatly between tissues and often depend on the substrate being

oxidized. All the respiration parameters measured here are stimulated or reduced by hypoxia, at least for one of the metabolic fuels tested: LEAK (brain and liver), OXPHOS (brain), RCR (liver), CCP-uncoupled (brain, white muscle and heart), and COX (all tissues except heart). Therefore, hypoxia acclimation causes a rather complex array of mitochondrial responses because no consistent across-tissue pattern could be established except for a general decrease in COX respiration. This observed change in COX activity suggests that hypoxia causes an organism-wide reduction in mitochondrial density. Downregulating COX could aid in achieving hypometabolism by indirectly inhibiting complex V via a reduction in the proton gradient. Regardless of environmental oxygen conditions, goldfish mitochondria favor the use of carbohydrates in brain and white muscle, prefer lipids in liver, and rely equally on both in heart and red muscle. Hypoxia causes the goldfish brain to switch to oxidizing lipids rather than carbohydrates with no clear preference observed in other tissues. Results also demonstrate a strong hypoxia-driven downregulation of brain Na^+/K^+-ATPase that supports whole-animal metabolic suppression and suggests concomitant channel arrest. The brain is the organ most affected by chronically low oxygen because it shows important responses in mitochondrial respiration (increase in LEAK and OXPHOS when using lipids, decrease in CCCP-uncoupled respiration when using carbohydrates, and decrease in COX when using lipids), as well as changes in the activities of key enzymes (HK, CPT, HOAD, and Na^+/K^+-ATPase). Overall, hypoxia-acclimated goldfish mainly promote metabolic suppression by regulating the glycolytic supply of pyruvate, downregulating brain Na^+/K^+-ATPase, and most likely decreasing mitochondrial abundance.

Chapter 5

Transcriptional and epigenetic repression supports metabolic suppression in chronically hypoxic goldfish

Based on a manuscript to be submitted by the same title

Written by

Elie Farhat, Giancarlo Talarico, Mélissa Gregoire, Jean-Michel Weber and Jan A. Mennigen

Statement of contribution: This work was performed alongside Mélissa Gregoire, Giancarlo Talarico and Dr. Mennigen. I (i) acclimated the fish, (ii) extracted the RNA and DNA, (iii) measured mRNA relative abundance and (iv) performed an ELISA to measure global DNA methylation. Mélissa and Giancarlo did the western blots. Dr. Mennigen and Giancarlo visualized the membranes. Dr. Mennigen helped me perform the ELISA. Finally, I wrote the paper with some input from Dr. Mennigen. We will be submitting this work for publication soon.

5.1. Introduction

Environmental hypoxia is a widely occurring environmental phenomenon that can be lethal to most animals. This state of O_2 limitation requires animals to suppress their metabolic rate to survive (Bickler and Buck, 2007). Metabolic suppression can be achieved through post-transcriptional and post-translational modifications as well as epigenetics (Storey, 2015; Storey and Storey, 1990). These mechanisms allow for the downregulation of energetically costly processes such as (i) Na^+/K^+-ATPase, (ii) the hypoxia sensing machinery (Palmer and Clegg, 2014), (iii) transcription and translation (Storey and Storey, 2004) and (iv) protein synthesis by repressing mechanisms such as the mammalian target of rapamycin (m-TOR) signaling pathway (Liu et al., 2006). I previously discussed the downregulation of Na^+/K^+-ATPase during chronic hypoxia in chapters 3 and 4. This chapter will place more emphasis on the effects of low O_2 on hypoxia sensing, transcription/translation dynamics and protein synthesis via the m-TOR pathway.

The hypoxia sensing machinery functions via enzymes, such as the Egl Nine (*egln*) Family, that immediately respond to intracellular decreases in O_2 (Ivan and Kaelin Jr, 2017; Semenza, 2001a; Semenza, 2001b). *Egln*s are prolyl hydroxylases that target hypoxia induced factors (both HIF-1 and HIF-2), key transcription factors involved in the molecular orchestration of physiological responses to hypoxia (Ivan and Kaelin Jr, 2017). Additionally, noncoding transcripts such as miRNAs have emerged as transcriptional markers of hypoxia and indeed important mediators of physiological responses to hypoxia (Chan et al., 2012; Hadj-Moussa et al., 2018; Hadj-Moussa et al., 2020; Serocki et al., 2018). As such, miRNA-210 has emerged as the master hypoxia-

miR (Chan et al., 2012; Hadj-Moussa and Storey, 2020), complementing classical HIF-mediated physiological responses to hypoxia via post-transcriptional regulation (Pocock, 2011).

Transcription and translation are molecular level energy sinks that are up or downregulated by hypoxia (Casey et al., 2002; Chee et al., 2019). Indeed, consequences of hypoxia exposure on global DNA methylation levels, as well as gene expression of DNA enzymes involved in DNA methylation dynamics/turnover [the DNA methylation *de novo* writer, methyltransferase (*dnmt*) and eraser ten-eleven translocation (*tet*)] have been well described in cancer research, where both global hyper- and hypo-methylation have been described (Wang et al., 2017). Moreover, hypoxia regulates components of the canonical microRNA biogenesis machinery (Bandara et al., 2017; Nallamshetty et al., 2013), supporting the notion that hypoxia may globally affect post-transcriptional regulation of gene expression and translation of transcripts.

Goldfish are champions of hypoxia tolerance that suppress their metabolic rate by up to 74% to cope with prolonged exposure to low O_2 (van Ginneken et al., 2004; Van Waversveld et al., 1989)(Chapter 2). This hypometabolic state occurs together with tissue-specific downregulation of Na^+/K^+-ATPase. Results from chapter 4 show that goldfish brains increase reliance on lipid oxidation during chronic hypoxia based on mitochondrial fuel selection. Moreover, hypoxia-exposed goldfish stimulate AMP-activated protein kinase and increase eukaryotic elongation factor 2 phosphorylation to support the necessary downregulation of liver protein synthesis (Jibb and Richards, 2008). Chapters 2 and 3 also show that changes in membrane lipid composition,

particularly cholesterol abundance, could promote hypometabolism in goldfish during chronic hypoxia via lipid-enzyme interactions (Chapter 2). It is currently unclear how goldfish adjust cholesterol abundance in their membranes when responding to chronic hypoxia. Thus, it is imperative to probe transcripts of protein coding genes and miRNAs involved in cholesterol biosynthesis and degradation during chronic hypoxia.

The four goals of this chapter are as follows: For the first goal, I investigate the responses of *egln* genes orchestrating the oxygen sensing machinery in goldfish exposed to chronic hypoxia. The second goal is to assess whether gene expression of epigenetic pathways and global epigenetic markers are responsive to chronic hypoxia in patterns suggesting transcriptional and post-transcriptional silencing at the genome level [DNA methylation dynamics, global DNA methylation, miRNA biogenesis pathway]. The third goal is to assess if the protein synthesis pathway is downregulated by reducing translation-dependent energy expenditure via the m-TOR pathway [phosphorylated ribosomal protein S6 (p-S6), phosphorylated eukaryotic translation initiation factor 4E binding protein 1 (p-4EBP1) and phosphorylated protein kinase B (p-AKT)]. The fourth goal is to investigate the molecular targets that regulate changes in cholesterol and lipid oxidation. I hypothesize that epigenetic regulation in the form of global DNA methylation and miRNA-dependent post-transcriptional control may reduce overall genome transcription and translation in chronically hypoxic goldfish. To test this hypothesis, I examine the effects of chronic hypoxia at two time points (1 and 4 weeks exposure) on all parameters in the goldfish.

5.2. Methods:

5.2.1. Animals

Adult common goldfish (*Carassius auratus*, Linnaeus 1758; N=36) were purchased from AQUAlity Tropical Fish Wholesale (Mississauga, Ontario, Canada) and held in a 1200 L flow-through holding tank in dechloraminated, well-oxygenated water, under a 12 h:12 h light:dark photoperiod, and were fed 3mm floating fish pellets (Profishent; Martin Mills; Elmira, Ontario, Canada) once a day. They were randomly allocated to normoxia or hypoxia. All measurements were performed at 13°C, and the fish were acclimated to this temperature for at least 2 weeks in the holding tank before starting experiments. Water was then made progressively hypoxic over 7 days by bubbling increasing amounts of N_2 through a column filled with glass beads. Water PO_2 was measured using galvanic oxygen probes (Loligo Systems, Tjele, Denmark). The probes were calibrated before each measurement using air-saturated water (20.9% O_2). Fish were randomly allocated to either normoxia, 1 week hypoxia (1H) or 4 weeks hypoxia (4H) (N = 12 per group). Oxygen availability for the hypoxic groups (1H and 4H) went from 100% saturation on day 1 to 50, 40, 30, 20, 15, and finally 10% (or 2.1 kPa) on day 7. PO_2 was maintained at that low level for a period of 1 week or 4 weeks. This level of hypoxia was selected because it induces significant suppression of goldfish aerobic metabolism, but without causing any ATP synthesis from anaerobic ethanol production (Chapter 2). All procedures were approved by the Animal Care Committee of the University of Ottawa (protocol BL-1625) and adhered to the guidelines established by the Canadian Council on Animal Care for the use of animals in research.

5.2.2. Real-time RT-PCR assays for mRNA quantification

Total RNA from brain, liver, white muscle and heart was extracted by homogenizing 50 mg of tissue in TRIzol reagent (Invitrogen, Burlington, ON, Canada) using a sonicator (Fisher Scientific Sonic Dismembrator model 100, San Diego, CA, USA). Extracted RNA was quantified using a NanoDrop 2000c UV-Vis Spectrophotometer (Thermo-Fisher Scientific, Mississauga, ON, Canada). Next, cDNA was generated using a QuantiTech Reverse Transcription Kit (Qiagen, Toronto, ON, Canada) following the manufacturer's protocol which includes a DNA wipeout step before reverse transcription occurs. Two-step relative abundance real-time RT-PCR assays were performed on a BioRad CFX96 instrument (Bio-Rad, Mississauga, ON, Canada) to quantify fold-changes in relative hepatic mRNA abundances of key transcripts involved in canonical miRNA biogenesis [argonaute-2 (*ago2a)*, *dgcr8*, *dicer*, *exportin5*], DNA methylation dynamics (*tet2*, *tet3, dnmt3*), hypoxia sensing (*egln1*, *egln3*) and lipids [hydroxymethylglutaryl-CoA synthase (*hmgcs1*), cholesterol 7alpha-hydroxylase (*cyp7a)*, liver X receptor (*lxr) and* carnitine palmitoyltransferase 1a (*cpt1a)*]. A standard curve consisting of serial dilutions of pooled cDNA and individual samples were run in duplicate for each experiment. The total volume was 20 µL, which consisted of 1 µL of diluted cDNA template, 1 µL of 10 nM specific forward and 1 µL of 10 nM specific reverse primer (Tables 5.1-5.3), 10 µL of SsoAdvanced Universal Inhibitor-Tolerant SYBR Green Supermix (Bio-Rad), and 7 µL of H_2O for each individual reaction. Real-time RT-PCR cycling parameters were a 5 min activation step at 95°C, followed by 40 cycles consisting of a 20 s denaturation step at 95°C and a 30 s annealing and extension step at a primer-specific temperature (Tables 5.1-5.3). After each run, melting

curves were produced and monitored for single peaks to confirm the specificity of the reaction and the absence of primer dimers. All amplification efficiencies calculated from serially diluted 7-point standard curves were between 86.8–110%, with R^2 values > 0.91 (Tables 5.1-5.3). Relative transcript abundance derived from standard curves was normalized using the NORMA-Gene approach as described by Heckman et al. (Heckmann et al., 2011).

Table 5.1. Real-time RT-PCR primer sequences and reaction parameters of gene targets involved in hypoxia sensing.

Gene target	Primer pair (5' to 3')	Tissue	Annealing temperature (°C)	Efficiency (%)	R^2
egln1 XM_026223343.1	F: ACAATAAACCACGCCCACTC R: GCCTCGACAACTGAACACAA	Heart	62	86.8	0.95
egln3 XM_026286524.1	F: CCGCCGAGAGGATTTATTTT R: ACGTTAGCAGCGGGTTATTC	Liver	62	114	0.98
		White muscle	62	106.2	0.91
		Heart	64	94.7	0.99
		Brain	64	107	0.99

Table 5.2. Real-time RT-PCR primer sequences and reaction parameters of gene targets involved in DNA methylation dynamics (*tet2*, *tet3* and *Dnmt3*) and miRNA biogenesis pathway (*dgcr8*, *dicer*, *exportin5* and *ago2a*).

Gene target	Primer pair (5' to 3')	Tissue	Annealing temperature (°C)	Efficiency (%)	R^2
tet2 XM_026204431.1	F: TTCCTTGACCCTGAAATTGG R: CTTTCTCTCGGGCCTTCTCT	Liver	61	89.1	0.99
		White muscle	62	94.7	0.99
		Heart	62	97.8	0.99
		Brain	62	93.6	0.99
tet3 XM_026244985.1	F: CCCACCAGCCTAATGAAAAA R: GGTGATCTCTCAGGGCAAAA	Liver	64	106	0.99
		White muscle	64	92.6	0.98
		Heart	62	105.5	0.99
		Brain	62	107.7	0.98
dnmt3 XM_026244444.1	F: CCTGTGCTTGTTGATGCTGT R: GGTGATGGTGCGAACTTTTT	Liver	62	108.5	0.97
		White muscle	62	90	0.96
		Heart	62	110	0.99
dgcr8 XM_026256969.1	F: TAAAGCACCTCCACCACCTC R: GTTTGTCCCTGTCCACTGCT	Liver	62	99.9	0.99
		White muscle	62	108.8	0.93
		Heart	62	108.3	0.94
		Brain	63	106	0.91
dicer XM_026285621.1	F: CGCTGACGAGTTCGATTACA R: TGGACTGCTTCCCAATATCC	Liver	62	106.2	0.91
		White muscle	64	102.7	0.98
		Heart	62	95.2	0.99
		Brain	64	95.6	0.99
exportin5 XM_026224889.1	F: GGCTGTGAATGTGATGATGG R: CAGGCCCATAGTGCTGTTTT	Liver	62	87.5	0.99
		White muscle	62	89.7	0.97
		Heart	62	87.7	0.98
		Brain	62	92.2	0.98
ago2a XM_026231597.1	F: CGTTGTTGGCAGTATGGATG R: TAGTAGATGATGCGCGTTGG	Liver	62	102.4	0.97
		White muscle	62	92.4	0.99
		Heart	62	92.6	0.98
		Brain	62	106.7	0.93

Table 5.3. Real-time RT-PCR primer sequences and reaction parameters of gene targets involved in cholesterol biosynthesis (*hmgcs1*, *lxr* and *cyp7a*) and β-oxidation (*cpt1a*).

Gene target	Primer pair (5' to 3')	Tissue	Annealing temperature (°C)	Efficiency (%)	R^2
hmgcs1 (non-paralogue specific) XM_026219183.1 XM_026273158.1	F: GACTTCGGCTTCATGGTGTT R: GACGCCTTGGTCTTGTTCTC	Liver	62	106.3	0.99
		White muscle	62	106.9	0.95
		Heart	64	95.8	0.98
		Brain	64	108.4	0.98
lxr XM_026215287.1	F: GGCAGTGAAGCAGACAACAA R: GAGTCCCCATGACCAACATC	Liver	64	108.4	0.99
		White muscle	62	107.3	0.99
		Heart	63	93.7	0.96
		Brain	64	99.4	0.90
cyp7a (non-paralogue specific) XM_026206536.1 XM_026198858.1	F: GAACCTGCATCAGACCTTCC R: CTCCATCCAATTCCTTTCCA	Liver	64	96.3	0.98
		Heart	62	93.5	0.97
		Brain	62	106.8	0.98
cpt1a XM_026267939.1	F: GCAGATGGAGAGGATTCTGG R: GTTCTTGCCGTGTCTGAGGT	Liver	62	107.8	0.99
		Heart	64	100.9	0.97
		Brain	62	109.5	0.99

5.2.3. Global DNA methylation

Relative levels of global DNA methylation (%) was assessed using the MethylFlash Global DNA Methylation (5-mC) ELISA Easy Kit, Colorimetric (Source: Epigentek, Cat # P-1030), according to manufacturer's instructions. This kit quantifies global DNA methylation levels by measuring levels of 5-methylcytosine (5-mC) colorimetrically in an ELISA assay using genomic DNA. Briefly, genomic DNA extracted from brain liver, white muscle and heart tissues of normoxic, 1 week hypoxic (1H) and 4 weeks hypoxic (4H) goldfish were incubated with 100 µL of binding solution in a 96-well

microplate for 60 min at 37°C. A negative control representing unmethylated polynucleotide containing 50 % of cytosine, and positive controls representing methylated polynucleotide containing 50 % 5-methylcytosine were also loaded into independent wells on the same microplate. The wells were then incubated for 60 min at room temperature with a capture antibody (1 ng mL^{-1}). Following the incubation period, the binding solution was removed and each well was washed 3 times with diluted washing buffer. Subsequently, a 50 µL aliquot of 5-mC detection complex antibody solution cocktail (1 µL of mC antibody + 1 µL of signial indicator + 1 µL of enhancer solution in 1 mL of diluted washing buffer) was added and incubated at room temperature for 50 min. This solution complex was then removed before washing each well with diluted washing buffer 5 times. Following that, 100 µL of developer solution was added to each well simultaneously and incubated at room temperature for 3 min until the developer solution turned blue. Finally, 100 µL stop solution was added to each well to halt the reaction and then absorbance values were read using a Spectra Max Plus384 Absorbance Microplate Reader (Molecular Devices, Sunnyvale, CA) at 450 nm.

5.2.4. Western blotting

Frozen liver and white muscle from the normoxic and 1H and 4H goldfish groups (N = 4 per group) were homogenized on ice with a sonicator (Fisher Scientific Sonic Dismembrator model 100, San Diego, CA) in 400 µL of buffer per 100 mg of tissue. During homogenization, samples were kept in a buffer containing 150 mmol/L NaCl, 10 mmol/L Tris, 1 mmol/L EGTA, 1 mmol/L EDTA (pH 7.4), 100 mmol/L sodium fluoride, 4 mmol/L sodium pyrophosphate, 2 mmol/L sodium orthovanadate, 1% (vol/vol) Triton X-100, 0.5% (vol/vol) NP40-IGEPAL, and a protease inhibitor cocktail (Roche, Basel,

Switzerland). Homogenates were centrifuged at 15000 g for 5 min at 4°C, and the resulting supernatants were recovered and stored at -80°C. Protein concentrations were determined using a Bio-Rad protein assay kit (Bio-Rad Laboratories, Munich, Germany) with BSA as standard. A denaturing, nonreducing SDS-PAGE was used to separate proteins. Lysates were diluted in the previously described buffer containing protease inhibitor for a total of 30 µg of total protein for liver and 50 µg of total protein for white muscle in 15 µL before 15 µL of 2x Laemmli buffer were added for a total loading volume of 30 µL. The prepared samples were denatured at 95°C for 2 min and quick chilled on ice before loading on the gel. Gels were cast as 10% resolving gel consisting of 5 mL ddH20, 2.5 mL buffer B pH 8.8 (1.5 M Tris base, 0.04% SDS at pH 8.8; both BioShop, Burlington, ON Canada) dissolved in dH_2O, 2.5 mL 40% acryl/Bis (Bio-Rad, Mississauga, ON, Canada) and polymerized with 50 µL 10% APS (Sigma-Aldrich Oakville, ON, Canada) and 20 µL TEMED (Life Technologies Burlington, ON, Canada), and a 4% stacking gel [consisting of 3.25 mL ddH_2O, 1.25 mL buffer C pH 6.8 (0.5 M Tris, 0.04% SDS dissolved (BioShop) in dH_2O], 0.5 mL 40% acryl/bis polymerized with 25 µL 10% APS, and 10 µL TEMED. Gels were immersed in 1x Tris glycine SDS (TGS) running buffer, consisting of Tris base 2.5 mM, glycine 0.192 M, and 0.1% SDS (all BioShop Canada) dissolved in dH_2O, and samples were loaded with 5 µL of Page Ruler prestained protein ladder (Thermo Fisher, Ottawa, ON, Canada).

Proteins were migrated in the gel at 100 V. After migration, they were blotted onto nitrocellulose 0.45-mm pore size membrane paper (Millipore, Etobicoke, ON, Canada) by wet transfer using the Mini TransBlot system (Bio-Rad) with blotting buffer (250 mM Tris base, 1920 mM glycine; all BioShop Canada) dissolved in dH_2O, by

applying 100 V for 2 h. Membranes were incubated with Odyssey blocking buffer (LI-COR Biosciences Lincoln, NE) for 1 h at room temperature using an orbital shaker. After the blocking step was completed, membranes were cut based on the molecular weight marker to allow separate development of post-translationally modified p-Akt (Ser473), p-S6 (Ser235/236) and p-4EBP1(Thr37/46) proteins with specific primary antibodies validated in fish (Forbes et al., 2019; Mennigen et al., 2014). Partial membranes containing the relevant molecular weight range of proteins were incubated with rabbit raised primary p-Akt (no. 9271), p-S6 (no.2211) or p-4EBP1(no.9459) antibodies (Cell Signaling Technology Ozyme, Saint Quentin Yvelines, France), respectively, at a concentration of 1:10000 on an orbital shaker at 4°C overnight. Membranes were washed four times for 5 min with PBS + 0.1% Tween 20 (Sigma-Aldrich) then incubated with an IRDye Infrared dye (680 nm coupled) secondary goat anti-rabbit IgG antibody (LI-COR Biosciences). Bands were visualized by infrared fluorescence using the Odyssey Imaging System (LI-COR Biosciences) and quantified by Odyssey Infrared imaging system software (v.3.0; LI COR Biosciences). p-Akt, p-S6 and p-4EBP1 protein intensity were normalized to rabbit β-tubulin (no. 2146; Cell Signaling Technologies) intensity and expressed as relative-fold change compared with control groups for liver and white muscle.

5.2.5. Statistics

Statistical analyses were performed using SigmaPlot 12.5 (Systat, San Jose, CA, USA). Data were analyzed using a one-way analysis of variance (ANOVA) for all experiments to test for the significant effects of hypoxia, followed by the Holm-Sidak post-hoc test for multiple comparisons. Normality was assessed using the Shapiro-Wilk

test and homoscedasticity by the Levene's test. When the assumptions of normality or equality of variances were not met, the data were normalized by log10 or square root transformation. If transformation was unsuccessful, non-parametric Kruskal-Wallis one-way ANOVA on ranks test was performed. All values presented are means ± s.e.m, and a level of significance of $P<0.05$ was used in all tests.

5.3. Results

5.3.1. Hypoxia sensing in goldfish

The expression of *egln3* was higher in the 1H and 4H groups of all tissues (vs normoxia; $P<0.001$) except in brain where it was only higher in the 1H group ($P<0.001$) (Fig. 5.1A). There were no differences between 1H and 4H in any tissue ($P>0.05$). Moreover, expression of *egln1* in the heart remained unchanged in the 1H and 4H groups ($P>0.05$) (Fig. 5.1B).

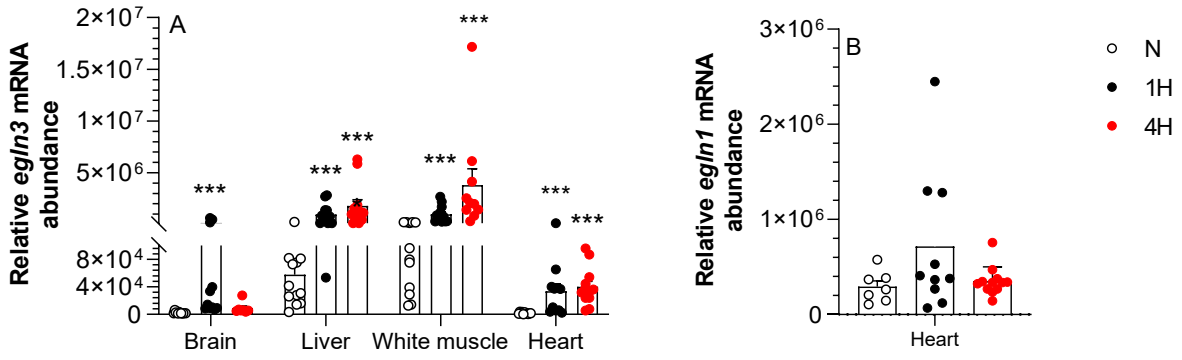

Figure 5.1. Relative abundance of mRNA targets involved in the oxygen sensing machinery in tissues of normoxic controls (N), 1 week hypoxic (1H) and 4 weeks hypoxic (4H) goldfish presented in panel A *(egln3*) and B (*egln1*). Values are means ± standard error of the mean (s.e.m); sample size = 10-12 per group. Dots represent individual data points. Differences between normoxia and hypoxia are indicated as *** ($p < 0.001$).

5.3.2. DNA methylation

The expression of *tet2* was higher in the 4H group in brain (vs normoxia and 1H; P<0.001), liver (vs normoxia; P<0.05) and heart (vs 1H; P<0.05), but lower in white muscle (vs 1H; P<0.001). Moreover, expression in the 1H group was increased in brain (P<0.05), liver (P<0.05) and white muscle (P<0.001) when compared to the normoxic group, without changing in heart (P>0.05) (Fig. 5.2A). Expression of *tet3* was higher in the 4H group in brain (vs normoxia and 1H; P<0.01), white muscle and heart (both vs normoxia; P<0.01). Expression of *tet3* was also higher in the 1H group in white muscle and heart (P<0.05) when compared to normoxia. There was no effect of either 1H or 4H on *tet3* expression in the liver (P>0.05) (Fig. 5.2B). Finally, expression of *dnmt3* was

only increased in 4H heart (vs normoxia and 1H; $P<0.001$), without changing in the other tissues ($P>0.05$) (Fig. 5.2C). Global DNA methylation was increased in the 4H group in brain (vs normoxia and 1H; $P<0.01$) and in heart (vs 1H; $P<0.05$) without changing in this group in other tissues ($P>0.05$). However, methylation was decreased in the 1H group in brain (vs normoxia; $P<0.05$), without changing in the other tissues ($P>0.05$). There were no effects of hypoxia (1H or 4H) on DNA methylation in either liver or white muscle ($P>0.05$) (Fig. 5.2D).

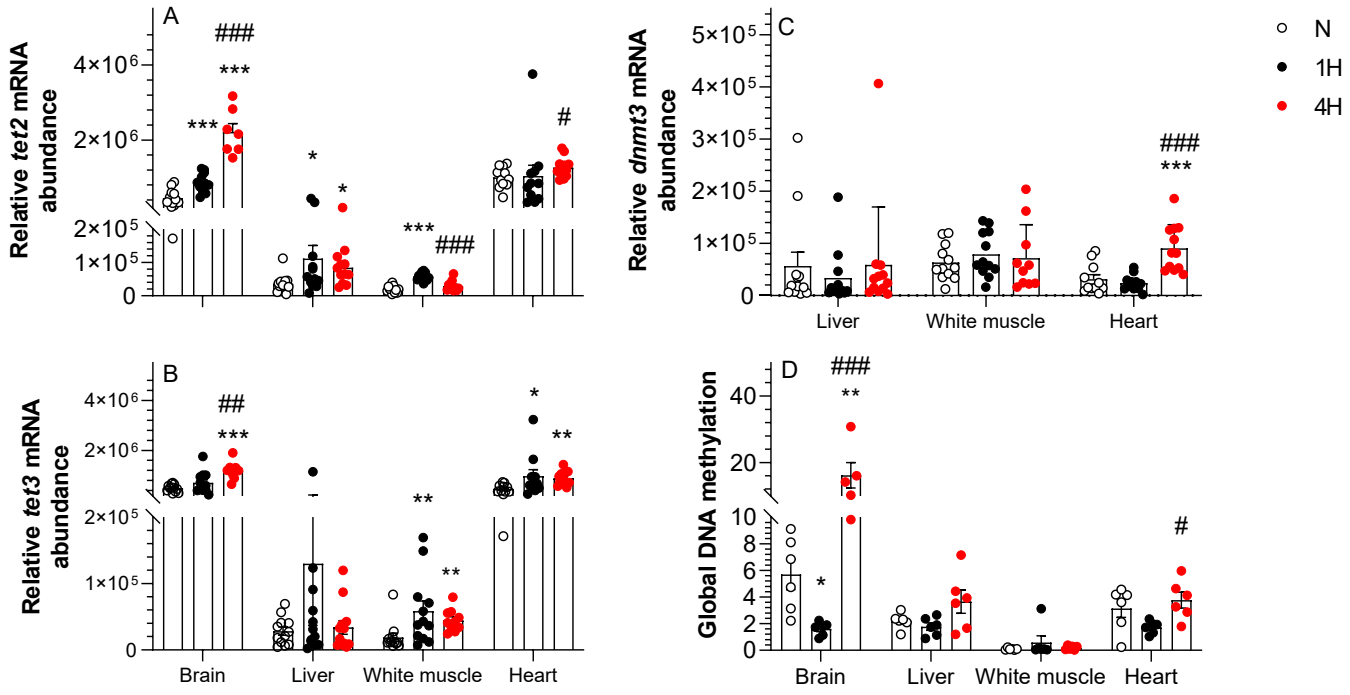

Figure 5.2. DNA methylation in tissues of normoxic controls (N), 1 week hypoxic (1H) and 4 weeks hypoxic (4H) goldfish. Expression of mRNA targets involved in DNA methylation dynamics are presented in panels A (*tet2*), B (*tet3*) and C (*dnmt3*). Global DNA methylation is presented in panel D. Values are means ± standard error of the mean (s.e.m); sample size = 10-12 per group. Dots represent individual data points. Differences between normoxia and hypoxia are indicated as * ($p < 0.05$), ** ($p < 0.01$) and *** ($p < 0.001$). Differences between 1H and 4H are indicated as # ($p < 0.05$), ## ($p < 0.01$) and ### ($p < 0.001$).

5.3.3. miRNA biogenesis pathway

The expression of *ago2a* was higher in the 4H group in brain (vs normoxia) and heart (vs normoxia and 1H) ($P<0.05$), but it remained constant in the other tissues

(P>0.05) (Fig. 5.3A). *Dicer* expression was only increased in the 4H group of white muscle (vs 1H; P<0.05), without being affected in other tissues (P>0.05) (Fig. 5.3B). Moreover, the expression of *dgcr8* was only higher in 4H brain (vs 1H; P<0.01) without changing in other tissues (P>0.05) (Fig. 5.3C). Finally, the expression of *exportin5* was increased in the 4H group of brain (vs 1H; P<0.001) and in liver (vs normoxia; P<0.05) without changing in white muscle and heart (P>0.05) (Fig. 5.3D).

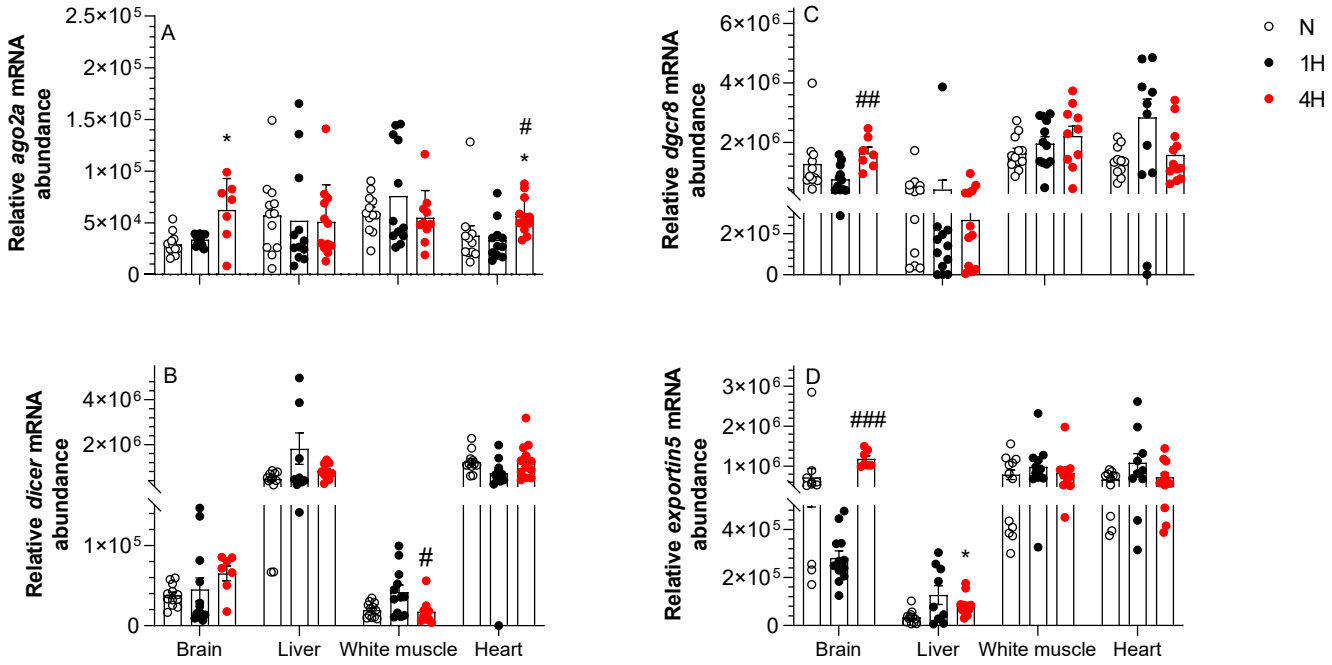

Figure 5.3. The miRNA biogenesis pathway (*ago2a*, panel A; *dicer*, panel B; *dgcr8*, panel C; *exportin5*, panel D) in tissues of normoxic controls (N), 1 week hypoxic (1H) and 4 weeks hypoxic (4H) goldfish. Values are means ± standard error of the mean (s.e.m); sample size = 10-12 per group. Dots represent individual data points. Differences between normoxia and hypoxia are indicated as * ($p < 0.05$). Differences between 1H and 4H are indicated as # ($p < 0.05$), ## ($p < 0.01$) and ### ($p < 0.001$).

5.3.4. m-TOR signalling pathway

Chronic hypoxia did not elicit any changes in the expression of the measured target proteins p-S6 (liver and white muscle), p-4EBP1 (liver and white muscle) and p-AKT (liver) ($P>0.05$) (Fig. 5.4).

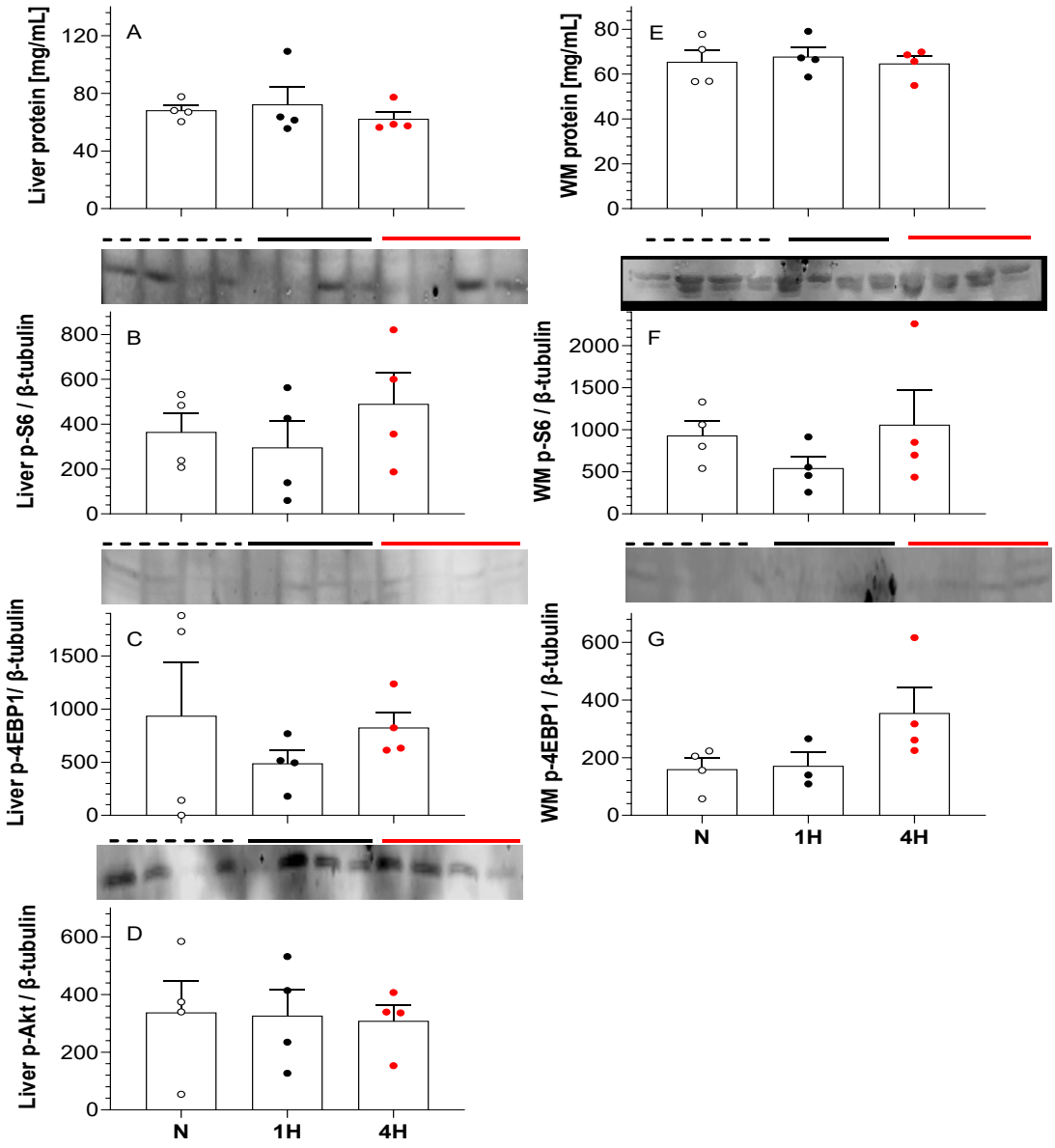

Figure 5.4. Expression of targets involved in the m-TOR signalling pathway [phosphorylated ribosomal protein S6 (p-S6; panels B and F), phosphorylated eukaryotic translation initiation factor 4E binding protein 1 (p-4EBP1; panels C and G) and phosphorylated protein kinase B (p-AKT; panel D) and total protein concentrations (panels A and E) in liver and white muscle (WM) of normoxic controls (N; open circles, dashed lines), 1 week hypoxic (1H; black circles, solid black lines) and 4 weeks hypoxic

(4H; red circles, solid red lines) goldfish. All targets are normalized to β-tubulin. Values are means ± standard error of the mean (s.e.m); sample size = 4 per group. Dots represent individual data points. Individual western blots are placed above each corresponding panel. There were no significant effects of hypoxia found ($p > 0.05$).

5.3.5. Lipid transcripts

The expression of *hmgcs1* was higher in the 4H group in brain (vs normoxia and 1H; $P<0.05$) and in white muscle (vs normoxia; $P<0.05$), but lower in the heart (vs normoxia; $P<0.05$) without changing in liver ($P>0.05$) (Fig. 5.5A). Moreover, *lxr* expression was increased in the 4H group in brain (vs normoxia and 1H; $P<0.001$), white muscle (vs 1H; $P<0.05$) and heart (vs normoxia; $P<0.001$), but expression was lower in liver (vs normoxia; $P<0.01$) and heart (vs 1H; $P<0.001$). Expression of *lxr* in the 1H group only decreased in liver (vs normoxia; $P<0.05$) without changing in the other tissues ($P>0.05$) (Fig. 5.5B). Additionally, the expression of *cyp7a* was increased in the 4H group in brain (vs 1H; $P<0.05$), lowered in both the 1H and 4H groups in liver (vs normoxia; $P<0.01$), but remained constant in heart ($P>0.05$) (Fig.5.5C).

The expression of *cpt1a* was only increased in the 4H group in brain (vs normoxia and 1H; $P<0.001$), without changing in liver and heart ($P>0.05$) (Fig. 5.6).

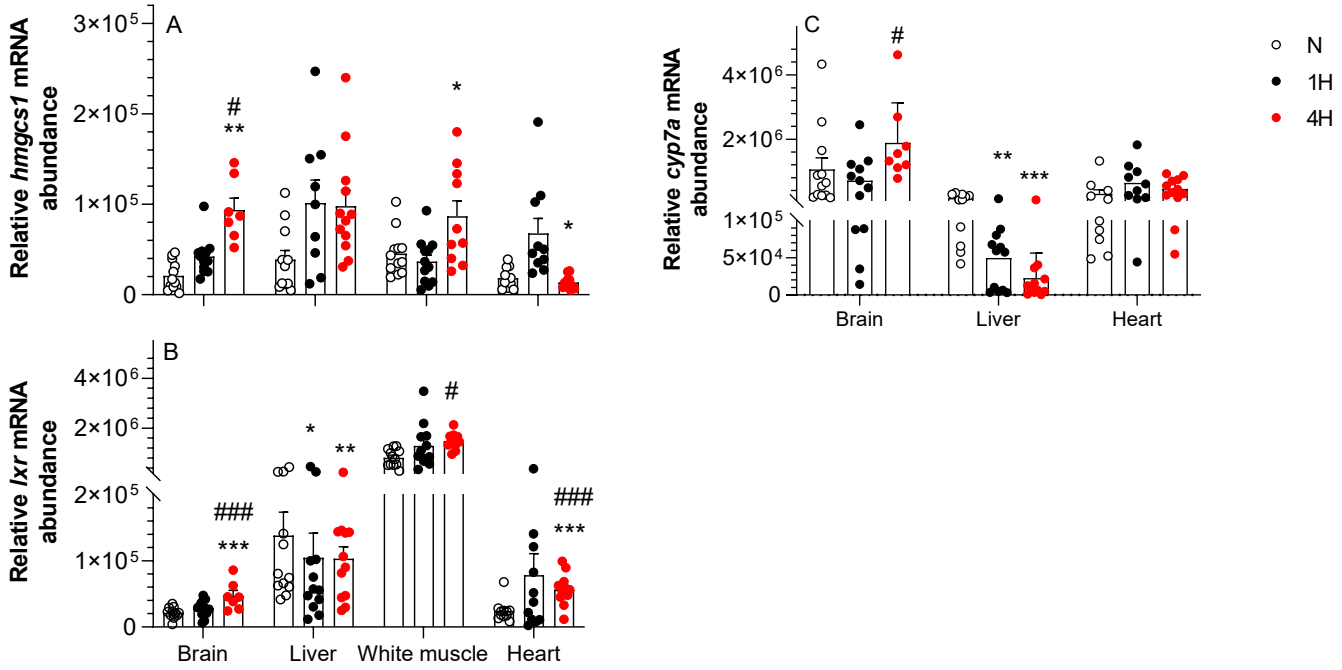

Figure 5.5. Expression of mRNA targets involved in cholesterol biosynthesis (A: *hmgcs1*; B: *lxr*; C: *cyp7a*) in tissues of normoxic controls (N), 1 week hypoxic (1H) and 4 weeks hypoxic (4H) goldfish. Values are means ± standard error of the mean (s.e.m); sample size = 10-12 per group. Dots represent individual data points. Differences between normoxia and hypoxia are indicated as * ($p < 0.05$), ** ($p < 0.01$) and *** ($p < 0.001$). Differences between 1H and 4H are indicated as # ($p < 0.05$) and ### ($p < 0.001$).

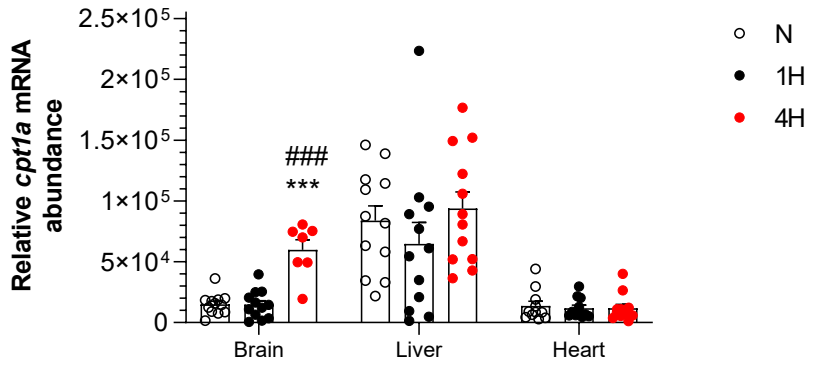

Figure 5.6. Expression of the β-oxidation mRNA, *cpt1a*, in tissues of normoxic controls (N), 1 week hypoxic (1H) and 4 weeks hypoxic (4H) goldfish. Values are means ± standard error of the mean (s.e.m); sample size = 10-12 per group. Dots represent individual data points. Differences between normoxia and hypoxia are indicated as *** ($p < 0.001$). Differences between 1H and 4H are indicated as ### ($p < 0.001$).

5.4. Discussion

This study is the first to investigate the effects of chronic hypoxia on (i) genes involved in the oxygen sensing machinery, (ii) transcription/translation via DNA methylation dynamics and miRNA biogenesis pathways, (iii) mTOR-dependent translational machinery involved in protein synthesis and (iv) changes in the expression of transcripts involved in cholesterol biosynthesis and β-oxidation in the hypoxia tolerant goldfish. It shows that components of hypoxia sensing are robustly activated across tissues irrespective of hypoxia duration. In some tissues, I also report the induction of gene expression for enzymes involved in global DNA methylation turnover and DNA hypermethylation along with the activation of the miRNA biogenesis pathway. These responses suggest a global role for epigenetic posttranscriptional repression of transcription especially in the hypoxic brain, that probably support the downregulation of

Na^+/K^+-ATPase in this critical tissue (see chapter 4). Chronic hypoxia does not suppress the m-TOR protein-signalling pathway in white muscle or liver, which suggests that these tissues do not utilize hypermethylation to lower cellular energy expenditure. Finally, molecular evidence from enzymes involved in cholesterol metabolism-related transcripts support the membrane results from chapter 2 that show an increase in membrane cholesterol of white muscle but no change in the brain. Overall, this study reveals that hypoxia-acclimated goldfish promote metabolic suppression via multiple posttranscriptional and epigenetic modifications.

5.4.1. Chronic hypoxia induces the oxygen sensing machinery across tissues

Long-term acclimation to hypoxia greatly influences the hypoxia sensing machinery in goldfish tissues (Fig. 5.1). Hypoxia sensing is highly evolutionary conserved at the molecular level (Bunn and Poyton, 1996) and relies on *egln*s to sense changes in O_2. Several *egln* isoforms exist (*egln*1-3) that allow for the extension of O_2 sensing capacity across large ranges of O_2 levels (Ivan and Kaelin Jr, 2017). Under normoxic conditions, *egln*-mediated hydroxylation of HIF promotes von Hippel Lindau factor-mediated ubiquitination resulting in protein degradation. Under hypoxic conditions, lack of substrates results in decreased hydroxylation levels in HIF, thus stabilizing the transcription factor and promoting transcriptional responses to hypoxia via hypoxia response elements (HREs) in nuclear DNA (Ivan and Kaelin Jr, 2017). While HIF activity is therefore principally regulated at the protein level, *egln1* and *egln3* have been shown to be part of a feedback loop, as their genes' promotor region exhibit HREs through which they are potently induced, possibly to compensate for reduced enzyme activity under hypoxic conditions (Ivan and Kaelin Jr, 2017). This transcriptional

regulation loop makes *egln*s good transcriptional markers of the molecular oxygen sensing machinery (Pescador et al., 2005).

Comparative investigation of hypoxia tolerant organisms such as the naked mole-rat and crucian carp has provided evidence for a role of differential regulation of the molecular hypoxia sensing machinery (Pamenter, 2014). The higher HIF expression in naked mole-rats has been linked to mutations in the HIF amino acid sequence that is believed to alter protein half-life by limiting von Lippel Lindau factor-dependent ubiquitination and proteasomal degradation (Kim et al., 2011). In hypoxia tolerant crucian carp and goldfish, these mutations are not present from genome derived amino acid sequences (data not shown), suggesting different molecular mechanisms. Interestingly, the goldfish genome has undergone a complex evolutionary history, resulting in the presence of several paralogues of the molecular oxygen sensing machinery. While the abundance of oxygen sensing machinery paralogues complicates the detailed functional analysis in fish species (Pelster and Egg, 2018), it is possible that the particular high retention of HIF-1α in the goldfish genome may be responsible for a high baseline HIF-1 abundance, although the validation of this hypothesis is difficult experimentally. Here, taking advantage of the recently published goldfish genome (Chen et al., 2019), I provide a detailed description of investigated components of the goldfish molecular hypoxia sensing repertoire using basic phylogenetic approaches. Goldfish possess 5 *egln1* (including 2 *egln1b*), 2 *egln2* and 3 *egln3* genes. As expected, promotor regions up to 2000bp upstream of the transcription start sites (TSS) of quantified transcripts of the *egln1* and *egln3* genes contain HREs, in line with

characterized HREs in mammalian *egln1* and *egln3* (Metzen et al., 2005; Pescador et al., 2005).

Transcript levels of the specific *egln1* paralogue (XP206079128.1) were only quantifiable in the heart (Fig. 5.1B), supporting tissue-specific expression patterns of goldfish *Egln* paralogues. Conversely, *egln3* paralogue (XP026142309.1) transcripts were ubiquitously expressed. Both paralogues were potently induced by both 1 week and 4 weeks hypoxia across tissues (Fig. 5.1A), confirming activation of molecular hypoxia sensing pathways across tissues. A notable exception is the transient induction observed in the 1 week hypoxic goldfish brain, as *egln3* transcript abundance in the 4 week hypoxic brain are indistinguishable from baseline *egln3* transcript levels under normoxic conditions. Interestingly, this brain-specific reduction in 4 weeks hypoxia is mirrored by DNA hypermethylation (Fig. 5.2D), raising the possibility that global hypermethylation may include a locus specific methylation in CpG elements found in the HRE promotor region of the profiled *Egln3* transcript, a regulatory mechanism described for *egln3* gene expression (D'Anna et al., 2020; Hatzimichael et al., 2010). However, promotor specific DNA methylation profiling, for example via bisulfite sequencing approaches, would be necessary to confirm this possibility.

5.4.2. A role for transcription/translation silencing in hypoxic goldfish brain

The reduction of energy demands in the form of metabolic suppression under chronic hypoxia is well documented in the goldfish (Chapter 2) (Richards, 2009; van Ginneken et al., 2004; Van Waversveld et al., 1989). While tissues have different energetic demands and thus contribute differentially to the organismal MO_2 (Chapter 4), transcription and translation are molecular level energy sinks that are responsive to

hypoxia (Casey et al., 2002). Here I hypothesized that epigenetic regulation in the form of global DNA methylation and miRNA dependent posttranscriptional control may reduce overall genome transcription and affect transcript translation.

I report a general increase in expression of the demethylases *tet2* (Fig. 5.2A) and *tet3* (Fig. 5.2B) in brain, liver and white muscle after 1 and 4 weeks hypoxia. In contrast, the DNA methyltransferase transcript *dnmt3* is only induced in the 4 weeks hypoxic heart (Fig. 5.2C). This indicates a general demethylation occurring across goldfish tissues, except for the heart that increases de novo methylation in chronic hypoxia. Demethylation via the *tet* family may not be promoting overall metabolic suppression because *tet*s require oxygen for catalytic function (Matuleviciute et al., 2021). However, results from global DNA methylation do not support the general demethylation in liver, white muscle and heart (Fig. 5.2D). Only brain is globally hypermethylated after 4 weeks hypoxia, following an initial hypomethylation occurring after 1 week exposure to hypoxia (Fig. 5.2D). The role of global DNA hypermethylation in the hypoxic goldfish brain in silencing transcription and translation is supported by induction of the epigenetic machinery expression. Indeed, the expression of several transcripts involved in the miRNA biogenesis pathway were induced in the brain (upregulation of *ago2a*, *dgcr8* and *exportin5*) following 4 weeks hypoxia (Fig. 5.3).

The highly aerobic brain is considered to be a disproportionately large contributor to organismal energy demands in mammals and fish (Soengas and Aldegunde, 2002). Indeed, larger brain size in weakly electric African fish has been linked to higher energetic demands and reduced hypoxia tolerance, underlining the important role of brain energy metabolism (Sukhum et al., 2016). Interestingly, several responses to

chronic hypoxia in the goldfish brain promote energy savings. For example, the activity of Na^+/K^+-ATPase, a major consumer of cellular ATP, is downregulated in goldfish brain but not other tissues (Chapter 4). Na^+/K^+-ATPase is crucially involved in maintaining neuronal membrane potential, and neuronal 'channel arrest' has been linked to a reduction in brain energy demands as well as hypoxia tolerance. Moreover, GABAergic signalling supresses neuronal signalling and is necessary for the suppression of neuronal excitotoxicity, a consequence of channel arrest in hypoxia (Hossein-Javaheri and Buck, 2021). The observed DNA hypermethylation and the induction of transcripts involved in miRNA biogenesis in 4 weeks hypoxic brain are indicative of transcription/translation suppression at the DNA and posttranscriptional level. This supports a pattern of lowered brain activity and, consequentially, a decrease in energy demand that supports hypometabolism. Future studies investigating differentially methylated regions at the DNA level or small RNAseq-based confirmation of general induction of miRNAs are warranted to provide more evidence for transcription/translation silencing in 4 weeks hypoxic brain. Finally, roles for an additional epigenetic factor, histone modifications in molecular hypoxia responses are emerging, as several histone-modifying enzymes possess oxygen sensitive domains. Thus, the potential role of histone modification in different hypoxia-tolerant species represents a potentially fruitful avenue, although detailed characterization of epigenetic modifications in the context of hypoxia tolerance in goldfish will suffer from the drawbacks of a complex genome.

5.4.3. Chronic hypoxia does not repress m-TOR in liver and muscle

Protein synthesis is a major consumer of ATP (Bickler and Buck, 2007; Rolfe and Brown, 1997) and downregulating it in chronic hypoxia greatly promotes metabolic suppression (Hochachka et al., 1996). Here, the effects of hypoxia on key mTOR-dependent translational machinery such as S6, 4EBP1 and AKT were examined in liver and white muscle (Fig. 5.4). There was no suppression in the active (phosphorylated) forms of S6, 4EBP1 and AKT in either liver or white muscle. This does not support the previously reported decreases in protein synthesis rates of hypoxic goldfish liver that are mediated by activation of AMPK (Jibb and Richards, 2008), an inhibitor of m-TOR (Liu et al., 2006). This different response could be due to the different hypoxia-exposure time between the two studies, which would indicate a transient response of AMPK in hypoxic goldfish. The lack of suppression in protein synthesis via the m-TOR pathway suggests that the translation machinery via this pathway is not involved in reducing ATP demand in chronically hypoxic goldfish liver and white muscle.

5.4.4. Molecular regulation of cholesterol biosynthesis in hypoxia

Chronic hypoxia influences the lipid composition of goldfish membranes in ways that support metabolic suppression (Chapter 2). Here, I examine the effects of chronic hypoxia on the expression of *hmgcs1* (Fig. 5.5A), *lxr* (Fig. 5.5B) and *cyp7a* (Fig. 5.5C). *Hmgcs1* encodes the first of 2 rate-limiting enzymes in the cholesterol biosynthesis pathway by catalyzing the condensation of acetyl-CoA with acetoacetyl-CoA towards 3-hydroxy-3-methylglutaryl (HMG)-CoA (Vock et al., 2008). Inversely, *lxr* plays a critical role in cholesterol efflux by regulating the expression of several genes and it activates a negative feedback mechanism that limits cholesterol uptake (Lee and Tontonoz, 2015).

Likewise, *cyp7a* is an indicator of cholesterol efflux because it is the first and rate-limiting enzyme in synthesizing bile acids from cholesterol (Chiang and Ferrell, 2020). All the transcripts measured here are induced in the 4 weeks hypoxic brain. This suggests that both cholesterol synthesis and efflux are increased, which supports the overall maintenance of membrane cholesterol content in chronic hypoxia previously observed in this critical tissue (Chapter 2). This may mean that cholesterol turnover is stimulated even though membrane cholesterol levels remain constant. A different strategy is observed in 4 weeks hypoxic white muscle that increases *hmgcs1* expression without changing *lxr* and *cyp7a*. This suggests an increase in cholesterol synthesis, but not efflux, and supports the increase in cholesterol content of white muscle membranes (Chapter 2). The responses of 4 weeks hypoxic liver do not echo the previously observed decrease observed in overall membrane cholesterol of this tissue (Chapter 2). Briefly, 4 weeks hypoxic liver decreases *lxr* and *cyp7a* expression without changing *hmgcs1*. This suggests a decrease in cholesterol efflux without changing cholesterol synthesis. This indicates a buildup of cholesterol in this tissue in chronic hypoxia, which contradicts the decrease in membrane cholesterol content (Chap. 2). Finally, the decrease in *hmgcs1* and increase in *lxr* expression of 4 week shypoxic heart suggest an overall decrease in cholesterol content in this aerobic tissue by lowering synthesis rates and improving efflux. Taken together, the changes observed here support a role for the modulation of cholesterol metabolism in promoting hypometabolism during chronic hypoxia because of the known downregulatory effects this sterol has on several ATPases (Bastiaanse et al., 1997; Crockett and Hazel, 1997; Garcia et al., 2019; Yeagle, 1989; Yeagle et al., 1988).

Additionally, goldfish mitochondrial responses reported in chapter 4 suggest that lipid oxidation becomes dominant in the brain during chronic hypoxia. This suggestion is supported by the fact that *cpt1a* expression is only increased in the brain, but not in the other tissues. However, this contradicts the previously observed downregulation of this enzyme in the same tissue (Chapter 4). This could possibly indicate an increase in CPT expression, but a decrease in overall abundance of this enzyme. Overall, the increase in *cpt1a* expression observed here supports a hypoxia-specific lipid preference of goldfish brain.

5. Conclusion

This study investigates the effects of 1 and 4 weeks of acclimation to hypoxia on transcriptional/translational mechanisms in the goldfish. Chronic hypoxia robustly activates the oxygen sensing machinery in all tissues except 4 weeks hypoxic brain, irrespectively of acclimation duration. Goldfish also rely on transcriptional and translational silencing of hypoxic brain via hypermethylation after being transiently hypomethylated after 1 week hypoxia. This suggests that post-transcriptional modifications support metabolic suppression in this critical tissue, but require a long exposure to occur. However, there does not appear to be any support for metabolic suppression via the translational machinery in liver or white muscle because of the lack of repression in the m-TOR signalling pathway. However, other mechanisms such as AMPK-mediated signalling could be playing a role in coordinating a possible translational response that was not measured here. Thus, it could be beneficial to examine the effects of chronic hypoxia on AMPK in these tissues. Finally, this study supports to the observed changes in membrane cholesterol content and brain lipid

metabolism of hypoxic goldfish (see chapters 2 and 4). Specifically, *hmgcs1* is upregulated in both white muscle and brain which indicates an increase in cholesterol synthesis. Moreover, *lxr* and *cyp7a* are both upregulated in the 4 weeks hypoxic brain which indicates an increase in cholesterol efflux/degradation. Taken together, these changes in cholesterol biosynthesis support the observed increase in white muscle and the lack of change in brain cholesterol content of goldfish membranes after 4 weeks acclimation to hypoxia (Chapter 2). Overall, this study shows that chronic hypoxia robustly activates hypoxia sensing, suppresses transcription/translation and epigenetically supports a role for membrane remodeling in promoting metabolic suppression.

Chapter 6

General conclusions and future directions

This chapter and chapter 1 are based on a manuscript titled “Hypometabolic responses to chronic hypoxia: a potential role for membrane lipids”

Written by

Elie Farhat and Jean-Michel Weber

And published in

Metabolites

https://doi.org/10.3390/metabo11080503

Statement of contribution: I performed the literature search and wrote the manuscript. Dr. Weber edited the manuscript with me.

6.1. Evidence for hypoxia-induced membrane remodeling

The membrane restructuring effects of temperature, toxins and diet introduced in chapter 1 suggest that other environmental factors like hypoxia could also influence membrane lipid composition. This led to my first hypothesis that goldfish (Chapter 2) and naked mole-rats (NMR; chapter 3) remodel their membrane lipids in ways that promote metabolic suppression in chronic hypoxia. My results support this hypothesis because they show that goldfish (Chapter 2) and NMRs (Chapter 3) enter a hypometabolic state and undergo widespread remodeling of their membrane lipids in response to prolonged *in vivo* exposure to low O_2. Both species modulate cholesterol extensively (Fig. 6.1), but the effects of chronic hypoxia on membrane phospholipids are more pronounced in goldfish (Chapter 2) than NMRs (Chapter 3) (Fig. 6.2). Changing cholesterol abundance strongly affects the activity of membrane proteins (Bastiaanse et al., 1997; Crockett and Hazel, 1997; Garcia et al., 2019; Harayama and Riezman, 2018; Yeagle et al., 1988). Goldfish and NMRs increase cholesterol in muscle and decrease it in liver, but only NMRs lower cholesterol in the brain. These responses are intriguing because multiple studies on artificial membranes (Garcia et al., 2019; Yeagle et al., 1988) and manipulated fish membranes (Crockett and Hazel, 1997) show that changing cholesterol levels generally downregulates Na^+/K^+-ATPase. Therefore, this hypoxia-driven membrane response could contribute to metabolic suppression. Another way to downregulate Na^+/K^+-ATPase is by decreasing n-3 22:6 abundance in membrane phospholipids because this fatty acid is a known activator of the ion pump (Calhoon et al., 2015; Turner et al., 2005). Such a strategy seems to be used by the goldfish that reduces % n-3 22:6 of liver (Fig. 6.2) and gill membranes (Chapter 2). However, this

mechanism is not available to NMRs because of their intrinsically low levels of 22:6 (only 0-4% of total membrane fatty acids in normoxic animals) that leaves little to no room for a decrease in hypoxia (Chapter 3). Overall, I propose that the hypoxia-driven changes in membrane lipids observed to date could represent a novel mechanism to reduce organismal metabolic rate in stressful environments.

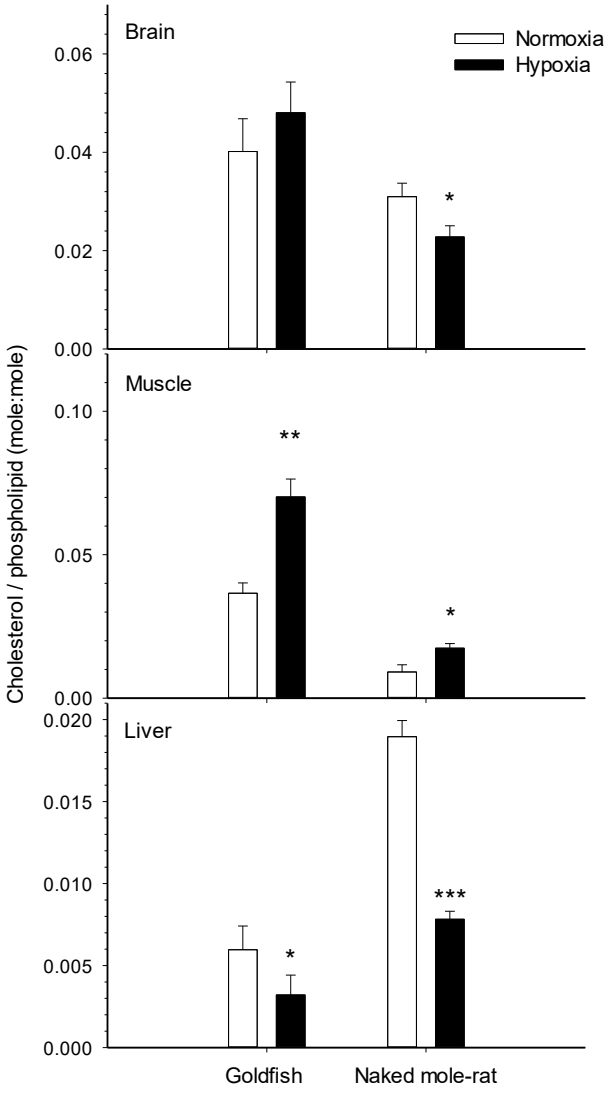

Figure 6.1. Relative membrane cholesterol in the tissues of normoxic controls and hypoxia-acclimated animals for two hypoxia-tolerant vertebrates: the goldfish (Chapter 2) and the naked-mole rat (Chapter 3). Values are means ± SEM (n = 9-16 per treatment). *$P < 0.05$, **$P < 0.01$, **$P < 0.001$ indicate significant effects of hypoxia.

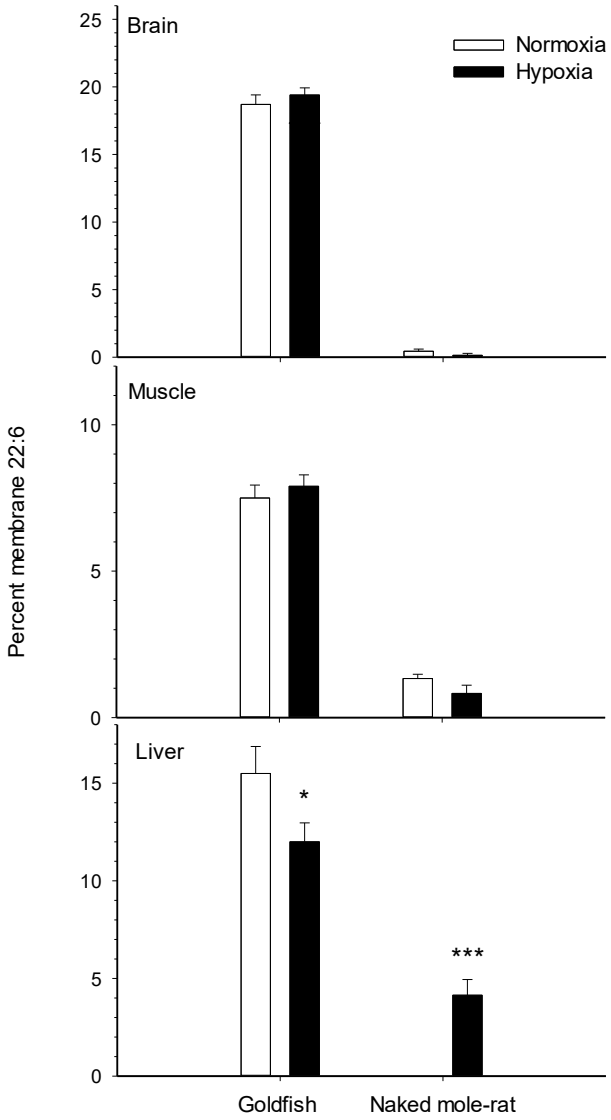

Figure 6.2. Percent docosahexaenoic acid (22:6) in membrane phospholipids in the tissues of normoxic controls and hypoxia-acclimated animals for two hypoxia-tolerant vertebrates: the goldfish (Chapter 2) and the naked-mole rat (Chapter 3). Values are means ± SEM (n = 9-14 per treatment). *$P < 0.05$, ***$P < 0.001$ indicate significant effects of hypoxia.

6.2. Hypoxia-driven changes in major enzymes

Because matching ATP supply and demand is critical to maintain energetic balance and survive low O_2 conditions, I tested the hypothesis that chronic hypoxia causes the downregulation of key enzymes involved in ATP turnover in chapters 3 (naked mole-rats) and 4 (goldfish). Summarized below are my main conclusions regarding the effects of chronic hypoxia on (i) Na^+/K^+-ATPase, (ii) glycolysis, (iii) β-oxidation and (iv) the tricarboxylic acid (TCA) cycle.

6.2.1. Na^+/K^+-ATPase

Both the goldfish (Chapter 4) and the NMR (Chapter 3) respond to chronic hypoxia by downregulating Na^+/K^+-ATPase in their brains by 40% and 77% respectively. This downregulation is echoed by a few studies performed on this ion pump at chronic hypoxia (Table 6.1). As explained in chapter 1, Na^+/K^+-ATPase is a major consumer of cellular ATP and downregulating it in a highly active organ such as the brain significantly promotes metabolic suppression. However, any decrease in ion pump activity should be matched by a similar decrease in ion channel activity so that ATP supply and demand can remain in balance. Therefore, quantifying the effects of chronic hypoxia on ion channels such as Na^+ and K^+ channels could provide support for any possible channel arrest happening in the brains of these hypoxia-tolerant champions.

Table 6.1. Effects of chronic hypoxia on the maximal activity of Na^+/K^+-ATPase in goldfish and naked mole-rats compared to other animals.

Species	Tissue	Na^+/K^+-ATPase response	Reference
Naked mole rat (*Heterocephalus glaber*)	Brain	77% ↓	Chapter 3
	Liver	41% ↑	Chapter 3
	Temporalis, heart	-	
Goldfish (*Carassius auratus*)	Brain	40% ↓	Chapter 4
	Liver, white muscle	-	
General trend (endotherms and ectotherms)	Brain, heart	↓	Table 1.1

6.2.2. Glycolysis

Glycolytic flux capacity is tissue-specific in the goldfish (Chapter 4) unlike in NMRs where the response is consistent across all tissues when exposed to chronic hypoxia (Chapter 3). Hypoxic goldfish increase glycolytic flux capacity in white muscle (by upregulating HK; Table 6.2), but decrease it in brain (by downregulating HK; Table 6.2) and in liver (by downregulating PK, Table 6.3). This unsystematic response is similar to the general tissue-specific trend observed in chronically hypoxic ectotherms (Tables 6.2 and 6.3). Naked mole-rats decrease glycolytic flux capacity in all measured tissues by downregulating PK, and this response is echoed in most chronically hypoxic endotherms (Table 6.3). However, any conclusion about NMRs downregulating glycolytic flux capacity should be taken with caution because I did not measure HK or

phosphofructokinase (PFK) activity in this animal. Moreover, Table 6.2 shows a general upregulation of HK in endotherms (opposite to PK; Table 6.3) which adds more uncertainty to my final verdict regarding the effects of chronic hypoxia on the glycolytic supply of pyruvate in the NMR (Chapter 3). Finally, apart from upregulation of LDH in NMR kidney, neither animal appears to rely on anaerobic metabolism during chronic hypoxia. Overall, chronic hypoxia generally downregulates glycolytic flux capacities in goldfish and NMRs.

Table 6.2. Effects of chronic hypoxia (minimum 1 week) on the maximal activity of hexokinase (HK) in various animals.

Species	Tissue	HK response	Reference
Goldfish (*Carassius auratus)*	Brain	12% ↓	Chapter 4
	White muscle	82% ↑	Chapter 4
	liver	-	Chapter 4
General trend (endotherms)	Gastrocnemius, soleus, heart, brain,	↑	Table 1.2
General trend (ectotherms)	Heart, brain, liver, white and red muscle, pancreas, pleopod, abdominal	↑ ↓ -	Table 1.2

Table 6.3. Effects of chronic hypoxia (minimum 1 week) on the maximal activity of pyruvate kinase (PK) in various animals.

Species	Tissue	PK response	Reference
Naked mole-rat (*Heterocephalus glaber)*	Liver, temporalis muscle, brain, heart, kidney	61-99% ↓	Chapter 3
Goldfish (*Carassius auratus)*	Liver	47% ↓	Chapter 4
	White muscle, brain	-	Chapter 4
General trend (endotherms)	Gastrocnemius, soleus, heart, brain	↓ -	Table 1.4
General trend (ectotherms)	White and red muscle, liver, heart, brain, hepatopancreas, pleopod, abdominal	↑ ↓ -	Table 1.4

Table 6.4. Effects of chronic hypoxia (minimum 1 week) on the maximal activity of lactate dehydrogenase (LDH) in various animals.

Species	Tissue	LDH response	Reference
Naked mole-rat (*Heterocephalus glaber*)	Brain, liver, temporalis	62-82% ↓	Chapter 3
	Kidney	81% ↑	Chapter 3
	Heart	-	Chapter 3
Goldfish (*Carassius auratus*)	White muscle, red muscle, liver, brain	-	Chapter 4
General trend (endotherms and ectotherms)	Gastrocnemius, heart, soleus, liver, white and red muscle, brain, hepatopancreas, pleopod, abdominal	↑ ↓ -	Table 1.5

6.2.3. β-oxidation

The response of β-oxidation presented in chapters 3 and 4 suggests a species-specific fuel strategy in chronic hypoxia. Naked mole-rats (Chapter 3) prefer to downregulate β-oxidation capacity in two tissues (Tables 6.5 and 6.7), which suggests a potential decrease in lipid oxidation. However, there does not appear to be an overall change in fuel preference in these animals mainly because they also decrease glycolytic flux capacity (Tables 6.2 and 6.3). This suggests that NMRs decrease overall aerobic supply of pyruvate from both glycolysis and β-oxidation in chronic hypoxia without favoring any particular type of fuel. In contrast, goldfish do not show a clear trend to regulating β-oxidation in chronic hypoxia because of two opposite responses seen in brain (Tables 6.5 and 6.6). However, when taking mitochondrial respiration into

account (Chapter 4), it appears that goldfish are in fact increasing reliance on lipid oxidation, in contrast to most animals that downregulate β-oxidation in chronic hypoxia (Tables 6.5 and 6.6).

Table 6.5. Effects of chronic hypoxia (minimum 1 week) on the maximal activity of carnitine palmitoyl transferase (CPT) in various animals.

Species	Tissue	CPT response	Reference
Naked mole-rat (*Heterocephalus glaber*)	Liver, temporalis muscle	89-98% ↓	Chapter 3
	Heart, kidney	-	Chapter 3
Goldfish (*Carassius auratus*)	Brain	18% ↓	Chapter 4
	Liver, white muscle	-	Chapter 4
General trend (endotherms and ectotherms)	Muscle, heart, skeletal	↓	Table 1.7

Table 6.6. Effects of chronic hypoxia (minimum 1 week) on the maximal activity of 3-hydroxyacyl-CoA dehydrogenase (HOAD) in various animals.

Species	Tissue	HOAD response	Reference
Naked mole-rat (*Heterocephalus glaber*)	Liver, temporalis musc	69-93% ↓	Chapter 3
	Brain, heart, kidney	-	Chapter 3
Goldfish (*Carassius auratus*)	Brain	70% ↑	Chapter 4
	Liver, White muscle	-	Chapter 4
General trend (endotherms and ectotherms)	Heart, skeletal, liver	↓	Table 1.8

6.2.4. TCA cycle

Goldfish and NMRs rely on different strategies to regulate flux through the TCA cycle in chronic hypoxia. Goldfish prefer to maintain CS in contrast to the general trends found in the literature (Table 6.5). However, NMRs generally downregulate CS in their tissues except in the heart where they upregulate it to possibly increase cardiac output (Chapter 3; Table 6.5). Regulating CS provides insight regarding ATP supply, fuel preference (acetyl-CoA can be supplied from glycolysis and β-oxidation) and mitochondrial abundance. This could indicate that goldfish, unlike NMRs, utilize other ways to regulate ATP supply (glycolysis and β-oxidation) and mitochondrial density during chronic hypoxia (Chapter 3).

Table 6.7. Effects of chronic hypoxia (minimum 1 week) on the maximal activity of citrate synthase (CS) in various animals.

Species	Tissue	CS response	Reference
Naked mole-rat (*Heterocephalus glaber*)	Brain, liver, temporalis, kidney	25-78% ↓	Chapter 3
	Heart	94-115% ↑	Chapter 3
Goldfish (*Carassius auratus*)	Brain, liver, white muscle	-	Chapter 4
General trend (endotherms and ectotherms)	Gastrocnemius, liver, white muscle, pleopod, pancreas, abdominal	↓	Table 1.6

6.3. Mitochondrial membranes and metabolic rate

In the fourth chapter of my thesis, I tested the hypothesis that mitochondrial respiration rates are lowered after acclimation to chronic hypoxia. I predicted the downregulation of mitochondrial respiration rates to occur in tissues that underwent extensive membrane remodeling (Chapter 2), but I did not observe a clear trend. The effects of chronic hypoxia on the lipid composition of the bilayer known to date do not deal specifically with mitochondria, but with total tissue membranes (Chapters 2 and 3). Because mitochondrial membranes often respond to stress differently than other membrane types (plasma, sarcolemma, endoplasmic reticulum), it would be interesting to investigate whether/how hypoxia affects isolated mitochondrial membranes. Diet-induced changes in membrane lipids are known to alter mitochondrial function in fish (Guderley et al., 2008; Martin et al., 2013) and in hibernating mammals (Staples and Brown, 2008). For instance, rainbow trout fed a n-3 22:6-rich diet increase state 3

(OXPHOS/phosphorylating respiration in the presence of substrates and ADP) (Guderley et al., 2008) and state 4 respiration (LEAK/nonphosphorylating respiration after ADP depletion) (Martin et al., 2013). Early studies show that the fatty acid composition of the diet has an impact on the hibernation capacity of golden-mantled ground squirrels (Frank, 1992; Frank and Storey, 1995). This interesting observation was further explored more recently in an attempt to characterize physiological mechanisms linking mitochondrial function, membrane composition, hibernation capacity, and metabolic suppression. For instance, ground squirrels and 13-mantled ground squirrels suppress mitochondrial OXPHOS respiration during torpor, especially when using succinate as a substrate (Staples, 2014). Changing the levels of n-6 18:2 in the diet of 13-lined ground squirrels can also markedly reduce OXPHOS respiration or proton leak (Gerson et al., 2008), and the authors argue that these reductions could be used to conserve energy in hibernation (Staples and Brown, 2008). They suggest that changing membrane lipid composition may be involved in reducing mitochondrial respiration capacity during torpor, although other mechanisms are also clearly involved (Chung et al., 2011). Also, cardiolipin is a major constituent of the inner mitochondrial membrane and plays a role in regulating the activities of complexes I (Paradies et al., 2002), IV (COX) (Frick et al., 2010) and V (Kraffe et al., 2007). Thus, it would be particularly interesting to find out whether chronic hypoxia affects cardiolipin abundance in mitochondrial membranes. The remodeling of membrane lipids can clearly modulate mitochondrial capacity and this mechanism could be used to promote metabolic suppression. It would thus be useful to quantify the effects of chronic hypoxia on

goldfish mitochondrial membranes, knowing that these animals decrease LEAK and OXPHOS respiration in some of their tissues (Chapter 4).

6.4. Epigenetic and molecular responses of hypoxic goldfish

Having examined the effects of chronic hypoxia on various levels, an understanding of the molecular underpinnings of hypoxia tolerance in the goldfish with lacking. Moreover, and quite surprisingly, not a lot of information currently exists on the effects of chronic hypoxia on goldfish at the transcriptional and translational level. This lead to my hypothesis that chronically hypoxic goldfish reduce overall genome transcription and translation to support metabolic suppression (Chapter 5). Indeed, goldfish respond to chronic hypoxia by robustly activating genes involved in hypoxia-sensing in all tissues except brain after 4 weeks of acclimation. Moreover, the 4 week shypoxic brain exhibits an increase in induction of transcripts involved in global DNA methylation turnover and DNA hypermethylation along with induction of the miRNA biogenesis pathway. These responses suggest a role of epigenetic posttranscriptional repression of transcription especially in hypoxic brain, supporting known neuronal ATP-saving mechanisms such as Na^+/K^+-ATPase downregulation (Chapter 4). I also investigated the effects of chronic hypoxia on mRNA targets involved in cholesterol biosynthesis and lipid metabolism to compliment my findings in chapters 2 and 4. The results support some of the responses observed in both goldfish chapters (Fig. 6.3). Briefly, the increase in white muscle membrane cholesterol abundance (Chapter 2) is complimented by an increase in expression of the mRNA *hmgcs1* that is involved in cholesterol synthesis (Chapter 5; Fig. 6.3). Moreover, the lack of change in brain membrane cholesterol abundance (Chapter 2) can be explained by the increased

expression of transcripts involved in both cholesterol synthesis and degradation/efflux (*lxr* and *cyp7a*) during chronic hypoxia (Chapter 5; Fig. 6.3). Additionally, mRNA expression of the β-oxidation enzyme *cpt1a* is increased in 4 weeks hypoxic brain (Chapter 5), supporting lipid oxidation preference of this critical tissue during similar conditions (Chapter 4). Overall, goldfish show a tissue-specific molecular response by repressing transcription/translation to promote metabolic suppression.

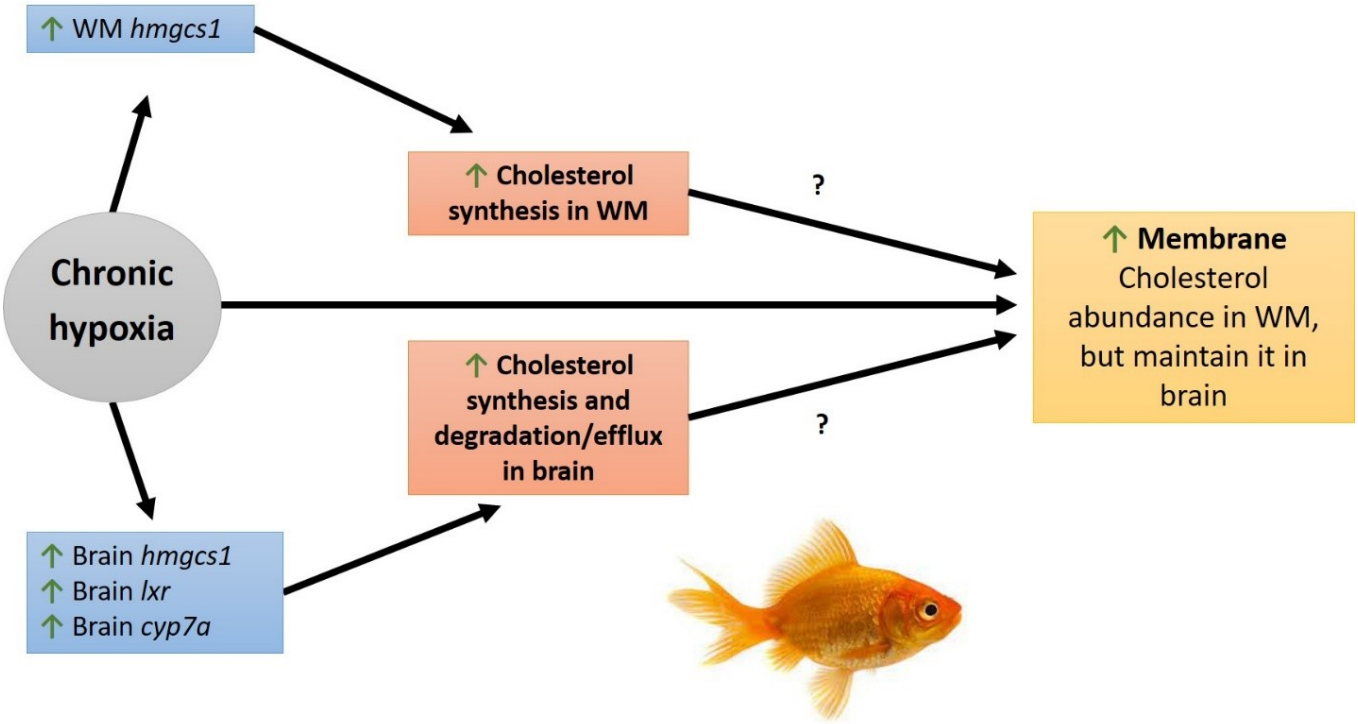

Figure 6.3. Effects of chronic hypoxia on the expression of mRNA involved in cholesterol synthesis [hydroxymethylglutaryl-CoA synthase (*hmgcs1*)] and degradation/efflux [liver X receptor (*lxr) and* cholesterol 7alpha-hydroxylase (*cyp7a*)] in goldfish white muscle (WM) and brain (Chapter 5). Cholesterol synthesis is increased in WM via an increase in *HMGCS1* expression, while both cholesterol synthesis and degradation/efflux are increased in brain via an increase in *hmgcs1*, *lxr* and *cyp7a* expression of 4 weeks hypoxic goldfish. These responses support the increase in WM, but maintenance in brain, membrane cholesterol abundance of 4 weeks hypoxic goldfish (Chapter 2).

6.5. Final remarks

Current understanding of the mechanisms that cause metabolic suppression in chronic hypoxia are summarized in Fig. 6.4. The lipid composition of membranes plays

a fundamental role in setting the metabolic capacity of cells, tissues and organisms. In chapters 2 and 3 of this thesis, I tested the hypotheses that (i) goldfish and (ii) naked mole-rats remodel their membrane lipids in ways that promote metabolic suppression in chronic hypoxia. This versatile mechanism is maybe best exemplified by birds that boost aerobic capacity before long-distance migration (natural doping in sandpipers), scaling of mass-specific metabolic rate (membrane pacemaker theory of metabolism), and various studies of metabolic suppression (hibernator mitochondria and downregulation of Na^+/K^+- ATPase in artificial membranes).

A successful hypometabolic response relies primarily on reducing ATP use whereas lowering ATP production is arguably easier to achieve and can be done secondarily. Therefore, mechanisms that downregulate ion pumps, ion channels, proton leak and transcription/translation play a strategic role in setting the tolerance of organisms for hypoxia. Therefore, I hypothesized that chronic hypoxia causes the downregulation of (i) enzymes involved in ATP turnover (Chapters 3 and 4), (ii) mitochondrial respiration (Chapter 4) and (iii) transcription/translation (Chapter 5). The results presented and discussed in this thesis suggest that hypoxia-induced suppression of metabolism is partly mediated by membrane plasticity through multiple mechanisms. Briefly, organismal acclimation to low oxygen causes widespread changes in the lipid composition of membranes in two champions of hypoxia tolerance: the goldfish and the naked mole-rat (Chapters 2 and 3). To cope with this environmental stress, these resilient animals modify their membranes in ways that support the downregulation of key enzymes directly involved in ATP turnover (Chapters 3 and 4). In hypoxia tolerant species, entering the hypometabolic state occurs together with

extensive changes in membrane cholesterol (Chapters 2 and 3), a decrease in mitochondrial density (Chapter 4), as well as the downregulation of brain $Na^{+/}K^{+}$-ATPase and acetyl-CoA supply from β-oxidation and/or glycolysis (Chapters 3 and 4). Moreover, the goldfish suppresses transcription/translation by inducing transcripts involved in DNA methylation and miRNA biogenesis (Chapter 5). However, a direct functional link between changes in membrane lipids and the downregulation of major ATP consuming processes remains to be clearly established. A common membrane signal regulating the joint inhibition of ion pumps and channels could be an exquisite way to preserve the balance between ATP supply and demand in the hypometabolic state. To further investigate how membrane restructuring and metabolic suppression could be mechanistically linked, it will be useful to mimic the membrane changes observed in vivo on artificial membranes to characterize how ion pumps and channels are affected by hypoxia.

Hibernators seem to rely on changes in mitochondrial membrane lipids to reduce proton leak and state 3 respiration as they enter torpor, and the same mechanism could be used in hypoxia (see section 6.3). Examining the effects of chronic hypoxia on the lipid composition of mitochondrial membranes is therefore an important avenue for future research. Do the hypoxia-driven changes already characterized for total tissue membranes echo those of mitochondrial membranes specifically? The membrane remodeling mechanisms presently linked to metabolic suppression include changes in cholesterol, fatty acid composition of phospholipids, and mitochondrial cardiolipin, but their relative importance is unknown.

While not as critical as reducing ATP use, lowering the rate of ATP synthesis is also required to keep matching ATP supply with demand in hypometabolic states. Maximal flux capacities of key metabolic pathways such as glycolysis, β-oxidation and the TCA cycle are affected by both chronic hypoxia and changes in membrane lipids. To what extent the downregulation of energy metabolism caused by hypoxia depends on membrane remodeling is currently unclear. To conclude, I propose that membrane restructuring is a novel physiological mechanism used by animals to suppress ATP turnover during prolonged hypoxia.

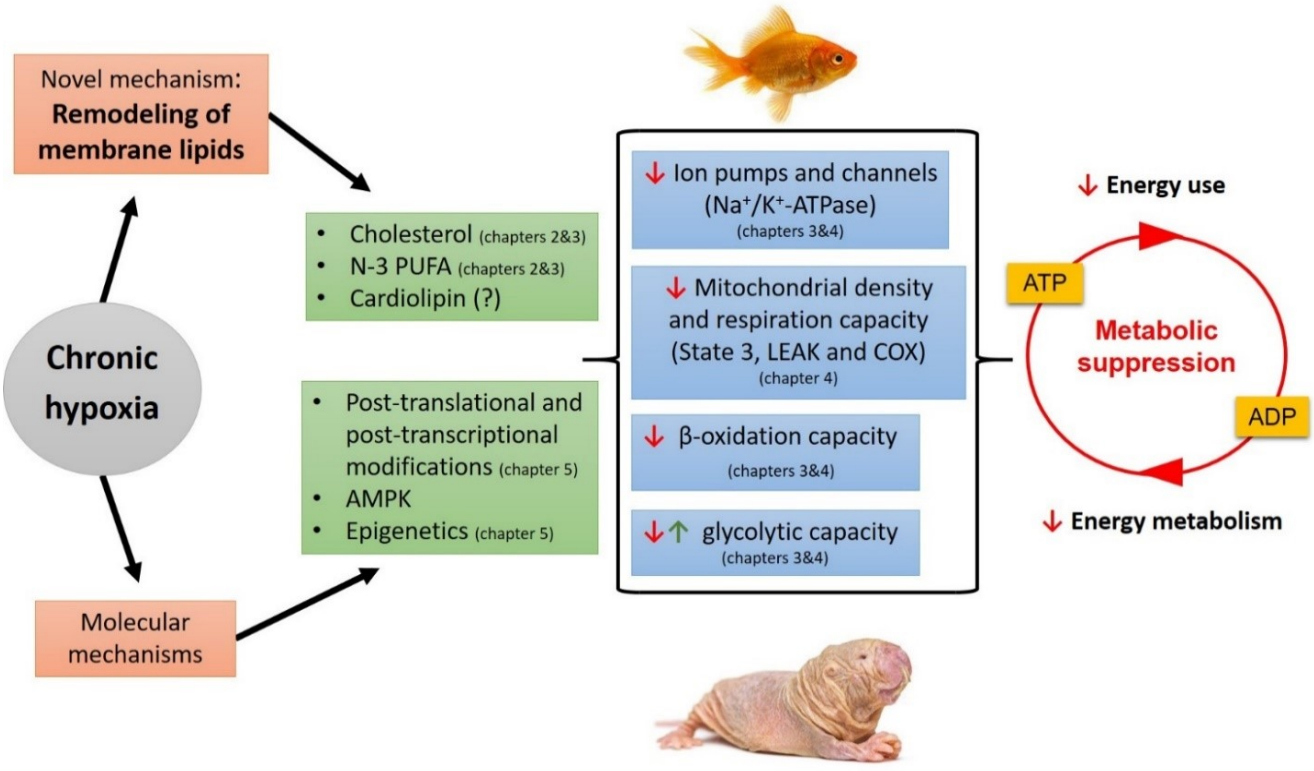

Figure 6.4. Remodeling of membrane lipids is a proposed new mechanism to promote metabolic suppression in chronic hypoxia. Prolonged in vivo exposure to low oxygen alters the relative abundance of membrane cholesterol, n-3 polyunsaturated fatty acids (PUFA), and possibly mitochondrial cardiolipin in ways that downregulate ion pumps such as Na^+/K^+-ATPase (a major ATP consumer), ion channels, and possibly mitochondrial respiration capacity [state 3 (OXPHOS in the presence of substrates and ADP) and LEAK (proton leak)]. Chronic hypoxia also causes a general reduction in cytochrome c oxidase (COX) indicating a decrease in mitochondrial density. The observed changes in membrane composition are known to modulate metabolic pathways of energy metabolism such as β-oxidation (downregulation) and glycolysis (up or downregulation). Reduction of flux through the ATP-ADP cycle can also be induced by molecular mechanisms that involve post-translational/post-transcriptional

modifications (Storey and Storey, 1990), 5’-AMP-activated protein kinase (AMPK) (Pamenter, 2014) or epigenetic changes (Storey, 2015). Membrane remodeling and molecular mechanisms work in concert to cause metabolic suppression.

Appendix A

The following appendix includes 8 tables related to chapter 2 of my thesis.

Table 1. Fatty acid composition of membrane phospholipids in brain of goldfish acclimated to normoxia or hypoxia at 13ºC. Values are mean percentages ± s.e.m. (N=13-14). Significant effects of hypoxia are indicated in bold as * ($P < 0.05$) and ** ($P < 0.01$).

	Normoxia	Hypoxia
16:0	24.8±0.22	25.2±0.24
16:1	10.7±0.41	9.4±0.62
18:0	10.0±0.19	9.5±0.80
18:1	25.2±0.39	25.9±0.86
18:2	1.5±0.13	1.2±0.16
18:3	0.5±0.35	0.0±0.0
20:2	1.9±0.06	1.8±0.05
20:4	3.0±0.07	3.2±0.05
20:5	2.0±0.05	2.0±0.06
22:6	18.0±0.7	19.4±0.53
24:0	2.4±0.15	2.4±0.11

Table 2. Fatty acid composition of membrane phospholipids in gills of goldfish acclimated to normoxia or hypoxia at 13°C. Values are mean percentages ± s.e.m. (N=13-14). Significant effects of hypoxia are indicated in bold as * ($P < 0.05$) and ** ($P < 0.01$).

	Normoxia	Hypoxia
14:0	0.0±0.0	1.0±0.25
16:0	24±0.38	25.1±0.57
16:1	5.9±0.26	6.4±0.11
18:0	8.1±0.24	8.2±0.26
18:1	26.5±0.41	27.2±0.44
18:2	10.9±0.28	10.7±0.26
20:0	1.2±0.1	1.3±0.04
20:2	4.3±0.08	4.1±0.07
20:4	3.4±0.25	3.2±0.15
20:5	3.6±0.09	3.1±0.16 **
22:3	0.0±0.0	0.4±0.4
22:5	1.7±0.06	0.9±0.15 *
22:6	9.9±0.39	8.2±0.51 **
24:0	0.5±0.13	0.2±0.11

Table 3. Fatty acid composition of membrane phospholipids in white muscle of goldfish acclimated to normoxia or hypoxia at 13°C. Values are mean percentages ± s.e.m. (N=13-14). Significant effects of hypoxia are indicated as * ($P < 0.05$) and ** ($P < 0.01$).

	Normoxia	Hypoxia
14:0	1.0±0.25	1.1±0.25
16:0	20.0±0.67	21.9±0.40 *
16:1	7.2±0.31	7.0±0.30
18:0	6.2±0.21	6.8±0.28 *
18:1	28.3±0.87	28.3±0.94
18:2	13.7±0.60	13.3±0.31
18:3	2.0±0.10	1.6±0.20
20:2	3.6±0.13	4.1±0.13 **
20:4	2.5±0.17	2.6±0.25
20:5	7.2±2.06	4.8±0.20
22:5	0.8±0.16	0.6±0.18
22:6	7.5±0.44	7.9±0.39

Table 4. Fatty acid composition of membrane phospholipids in liver of goldfish acclimated to normoxia or hypoxia at 13°C. Values are mean percentages ± s.e.m. (N=13-14). Significant effects of hypoxia are indicated in bold as * ($P < 0.05$) and ** ($P < 0.01$).

	Normoxia	Hypoxia
14:0	0.5±0.22	1.4±0.24
16:0	22.2±0.55	22.8±0.65
16:1	5.6±0.54	6.7±0.35 *
18:0	7.3±0.55	6.8±0.40
18:1	27.7±1.45	28.1±0.97
18:2	8.6±0.66	10.4±0.40 *
18:3	0.4±0.17	1.1±0.23
20:0	0.4±0.18	0.4±0.18
20:2	3.7±0.13	3.8±0.12
20:4	3.7±0.35	2.4±0.25 **
20:5	3.1±0.26	3.1±0.15
22:5	1.2±0.14	0.8±0.16
22:6	15.5±1.38	12.0±0.97 *
24:0	0.1±0.07	0.2±0.11

Table 5. Fatty acid composition of membrane phospholipids in brain of goldfish acclimated to normoxia or hypoxia at 20°C. Values are mean percentages ± s.e.m. (N=15-16). There were no significant effects of hypoxia detected ($P > 0.05$).

	Normoxia	Hypoxia
16:0	26.7±0.36	25.9±0.54
16:1	8.3±0.49	8.4±0.38 *
18:0	11.6±0.27	11.5±0.43
18:1	25.3±0.5	25.9±0.33
18:2	1.9±0.19	2.8±1.11
20:1	1.7±0.06	2.0±0.36
20:4	2.6±0.08	2.5±0.11
20:5	1.4±0.11	1.6±0.2
22:6	17.9±0.74	16.5±0.98
24:0	2.6±0.27	2.9±0.18

Table 6. Fatty acid composition of membrane phospholipids in gills of goldfish acclimated to normoxia or hypoxia at 20°C. Values are mean percentages ± s.e.m. (N=15-16). Significant effects of hypoxia are indicated in bold as * ($P < 0.05$).

	Normoxia	Hypoxia
16:0	31.2±0.67	30.5±0.77
16:1	3.5±0.19	3.5±0.15
18:0	9.1±0.28	8.8±0.3
18:1	21.7±0.6	21.5±0.55
18:2	6.2±0.27	6.6±0.34
20:0	0.0±0.0	0.3±0.2
20:1	6.0±0.27	6.7±0.31 *
20:4	3.2±0.2	2.8±0.12
20:5	2.7±0.09	2.7±0.09
22:0	2.0±0.2	2.6±0.23
22:5	1.1±0.12	0.8±0.15
22:6	12.6±0.34	12.4±0.36
24:0	0.7±0.15	0.8±0.15

Table 7. Fatty acid composition of membrane phospholipids in white muscle of goldfish acclimated to normoxia or hypoxia at 20°C. Values are mean percentages ± s.e.m. (N=15-16). There were no significant effects of hypoxia detected ($P > 0.05$).

	Normoxia	Hypoxia
16:0	31.0±0.51	30.7±0.96
16:1	1.2±0.27	1.6±0.22
18:0	10.0±0.33	10.1±0.51
18:1	14.8±0.63	14.4±0.48
18:2	7.4±0.38	7.8±0.33
20:0	0.1±0.08	0±0
20:1	5.3±0.42	6.4±0.31
20:4	3.2±0.14	2.9±0.13
20:5	6.8±0.2	6.6±0.17
22:0	0.3±0.14	0.2±0.11
22:3	0.2±0.17	0±0
22:5	1.2±0.17	1.6±0.65
22:6	18.4±0.69	17.7±0.73
24:0	0.1±0.1	0±0

Table 8. Fatty acid composition of membrane phospholipids in liver of goldfish acclimated to normoxia or hypoxia at 20°C. Values are mean percentages ± s.e.m. (N=15-16). Significant effects of hypoxia are indicated as * ($P < 0.05$) and ** ($P < 0.01$).

	Normoxia	Hypoxia
16:0	27.5±0.75	28.3±0.96
16:1	3.0±0.25	3.5±0.34
18:0	7.2±0.51	5.7±0.38 *
18:1	21.0±0.97	21.4±1.22
18:2	5.4±0.4	6.1±0.44
20:0	0.2±0.11	0.3±0.14
20:1	4.9±0.38	5.9±0.46 *
20:2	0.4±0.16	0.0±0.0 *
20:4	2.5±0.32	1.5±0.36 *
20:5	3.7±0.17	3.3±0.22
22:0	0.6±0.22	1.4±0.18
22:5	1.8±0.13	1.2±0.14 **
22:6	21.5±1.0	21.2±1.33
24:0	0.3±0.18	0.2±0.15

Appendix B

The following appendix includes 5 figures and a table related to chapter 3 of my thesis.

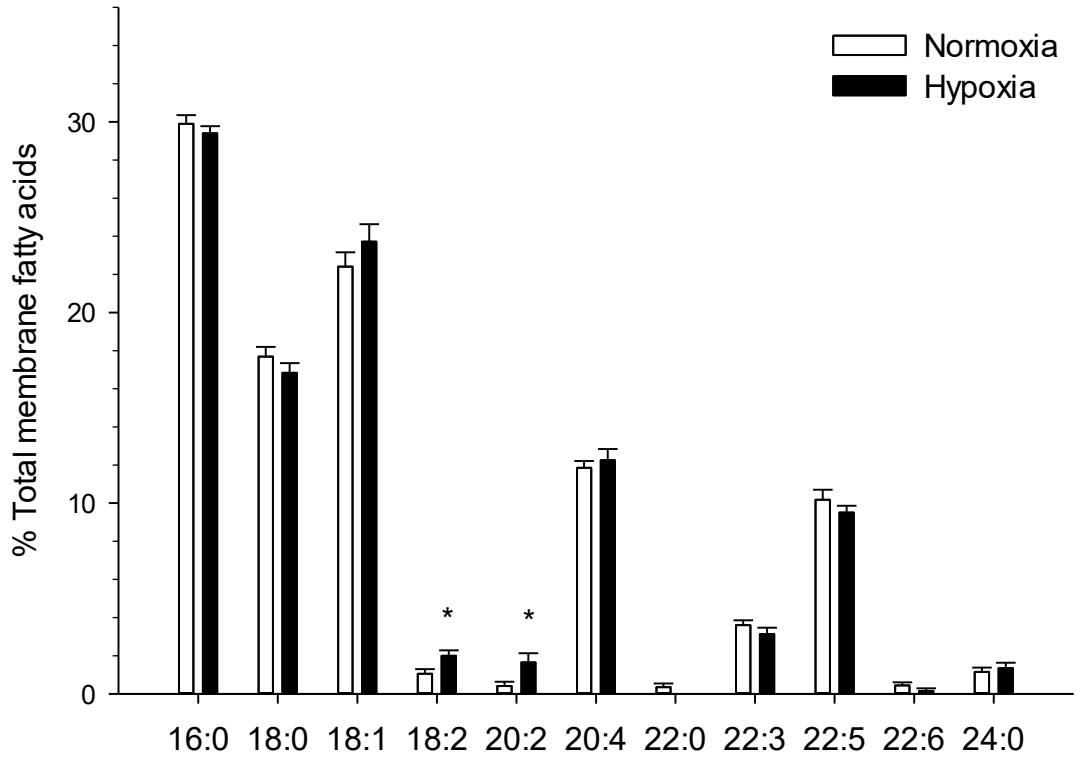

Figure 1. Fatty acid composition of membrane phospholipids in the brain of normoxic controls and hypoxia-acclimated NMRs expressed in % of total fatty acids. Values are means ± s.e.m. (N=12 in normoxia and N=9 in hypoxia). Significant effects of hypoxia are indicated as * ($P < 0.05$).

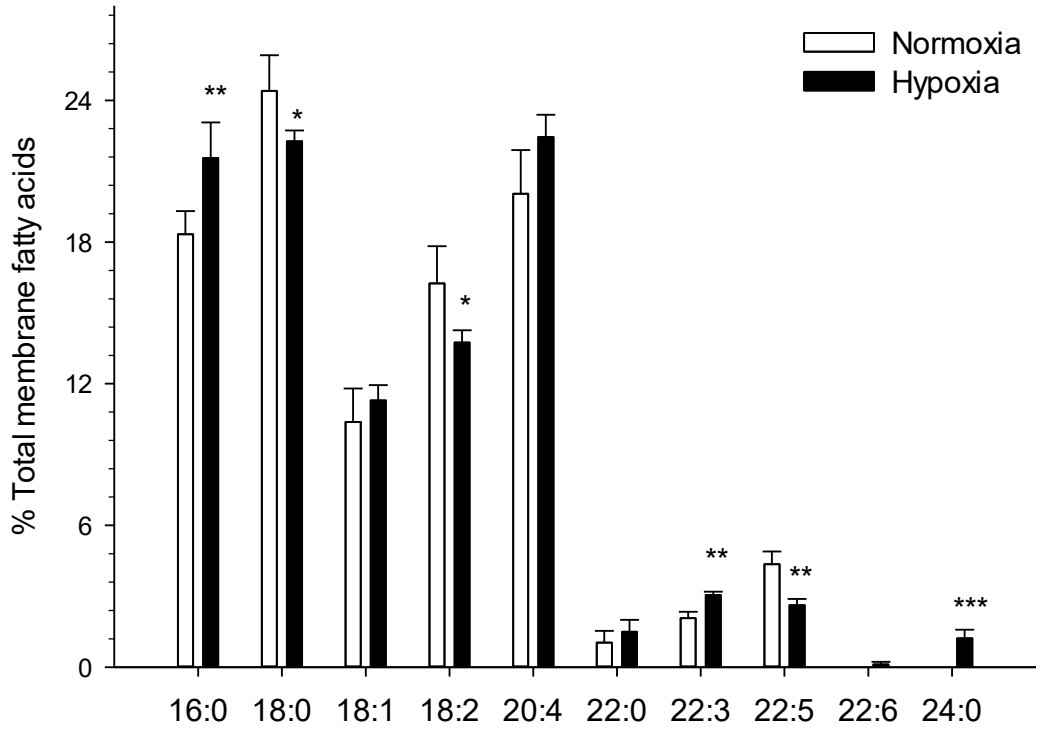

Figure 2. Fatty acid composition of membrane phospholipids in the heart of normoxic controls and hypoxia-acclimated NMRs expressed in % of total fatty acids. Values are means ± s.e.m. (N=12 in normoxia and N=9 in hypoxia). Significant effects of hypoxia are indicated as * ($P < 0.05$), ** ($P < 0.01$) and *** ($P < 0.001$).

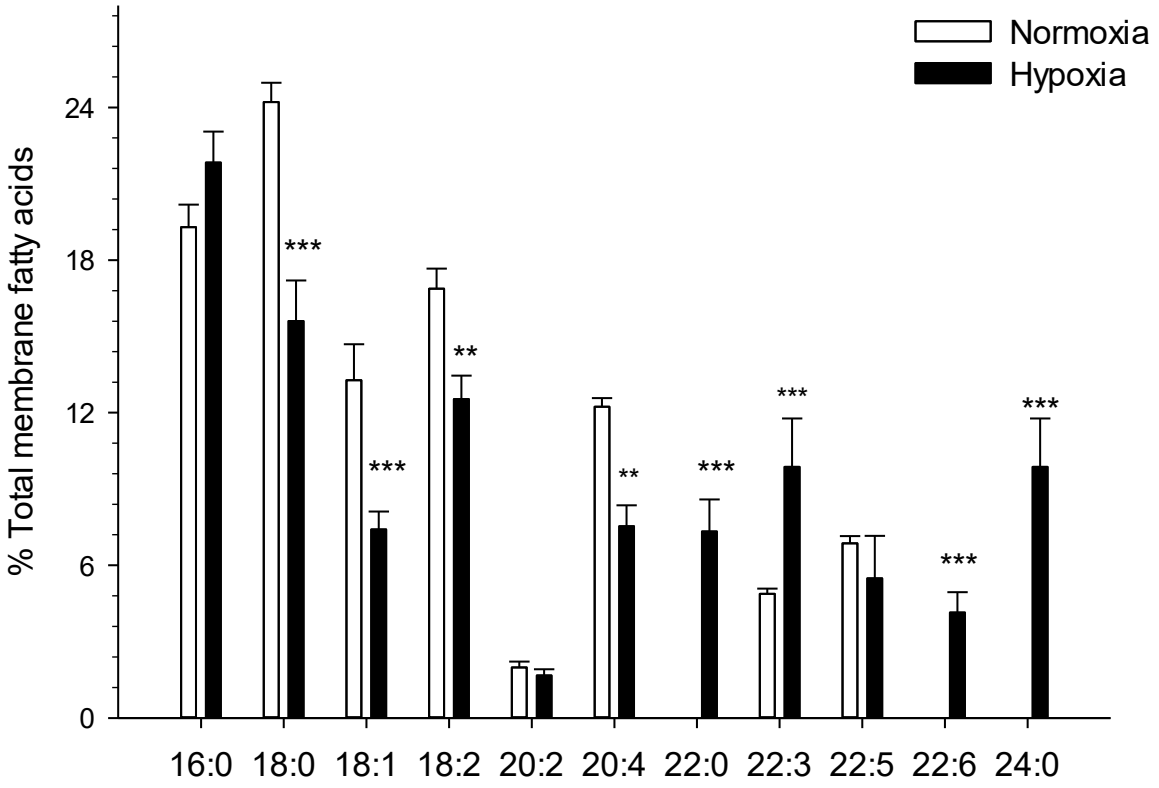

Figure 3. Fatty acid composition of membrane phospholipids in the liver of normoxic controls and hypoxia-acclimated NMRs expressed in % of total fatty acids. Values are means ± s.e.m. (N=12 in normoxia and N=9 in hypoxia). Significant effects of hypoxia are indicated as ** ($P < 0.01$) and *** ($P < 0.001$).

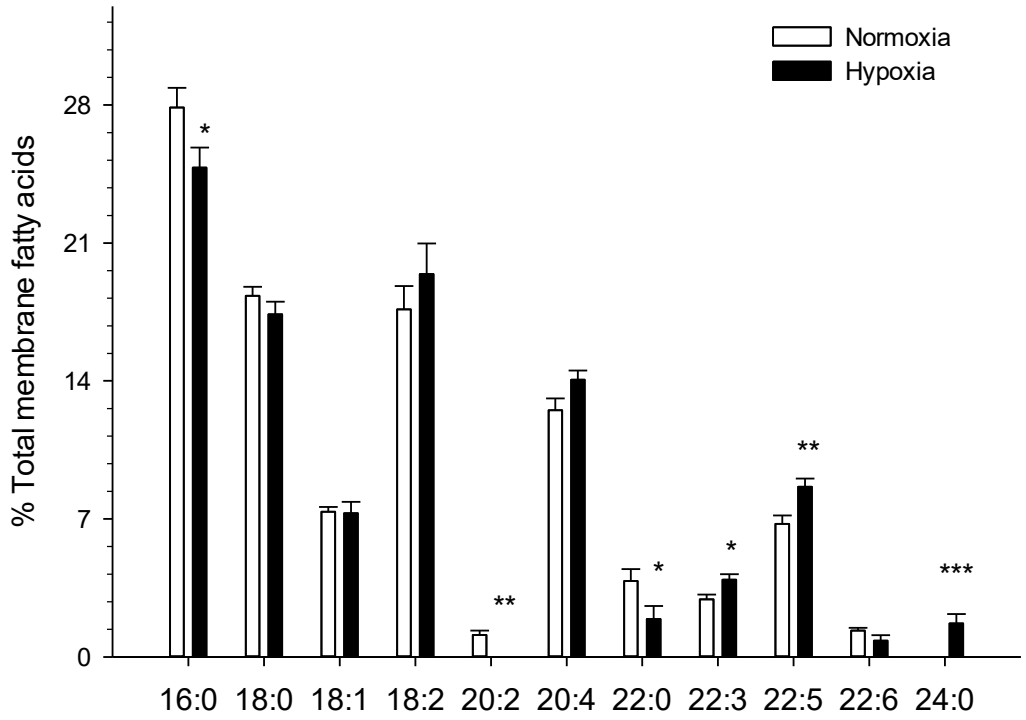

Figure 4. Fatty acid composition of membrane phospholipids in the muscle of normoxic controls and hypoxia-acclimated NMRs expressed in % of total fatty acids. Values are means ± s.e.m. (N=12 in normoxia and N=9 in hypoxia). Significant effects of hypoxia are indicated as * ($P < 0.05$), ** ($P < 0.01$) and *** ($P < 0.001$).

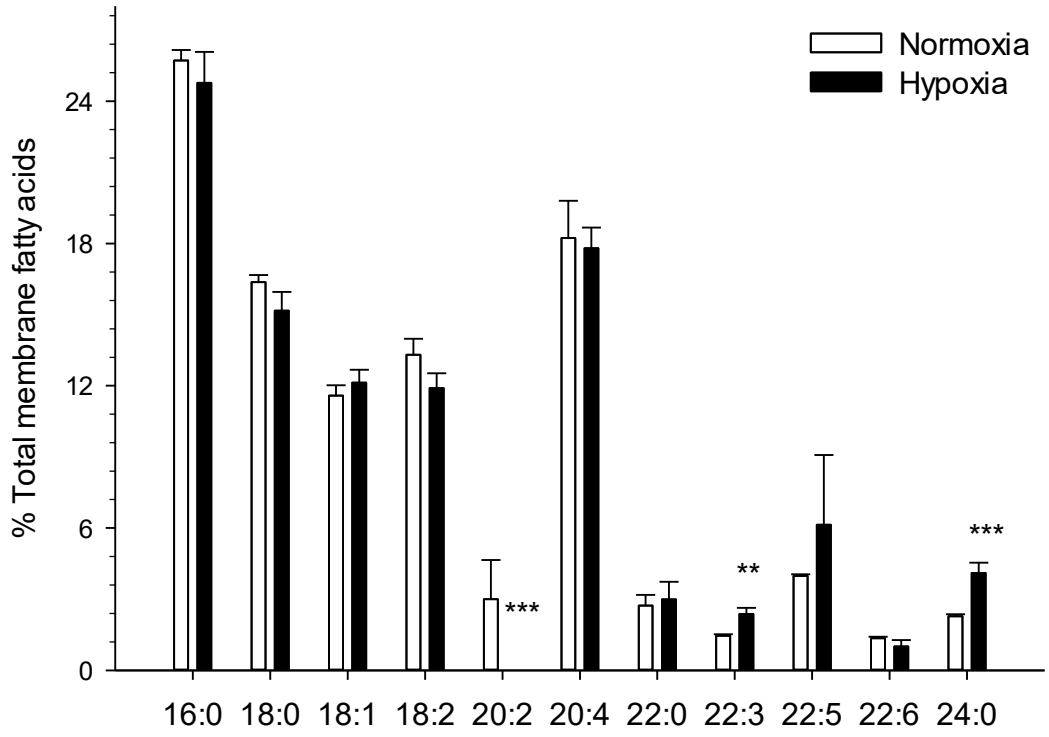

Figure 5. Fatty acid composition of membrane phospholipids in the kidney of normoxic controls and hypoxia-acclimated NMRs expressed in % of total fatty acids. Values are means ± s.e.m. (N=12 in normoxia and N=9 in hypoxia). Significant effects of hypoxia are indicated as ** ($P < 0.01$) and *** ($P < 0.001$).

Table 1. Effects of chronic hypoxia on the membrane phospholipids of naked mole-rat tissues. Double bond index (DBI), phospholipid/g_{tissue} (PL/g), saturated fatty acids (SFA), monounsaturated fatty acids (MUFA) and polyunsaturated fatty acids (PUFA) are indicated separately. Values are means ± SE (N=12 in normoxia (N) and N=9 in hypoxia (H)). Significant effects of hypoxia are indicated as * (P<0.05), ** (P<0.01) and *** (P<0.001).

	DBI		PL/g		SFA		MUFA		PUFA	
	N	H	N	H	N	H	N	H	N	H
Brain	2.8 ± 0.1	2.9 ± 0.1	37.2 ± 1.7	43.9** ± 1.8	0.49 ± 0.01	0.48 ± 0.01	0.23 ± 0.01	0.24 ± 0.01	0.28 ± 0.01	0.29 ± 0.01
Heart	3.5 ± 0.3	3.2 ± 0.2	25.2 ± 4.5	22.0 ± 1.2	0.6 ± 0.1	0.5 ± 0.02	0.2 ± 0.06	0.1 ± 0.01	0.5 ± 0.04	0.4 ± 0.04
Liver	3.4 ± 0.1	2.65* ± 0.3	64.7 ± 3.2	97.2** ± 12.4	0.44 ± 0.01	0.55* ± 0.03	0.13 ± 0.01	0.07*** ± 0.01	0.43 ± 0.01	0.38* ± 0.02
Muscle	2.92 ± 0.16	3.57* ± 0.17	17.2 ± 0.44	12.3*** ± 0.54	0.44 ± 0.02	0.32* ± 0.01	0.074 ± 0.01	0.073 ± 0.01	0.42 ± 0.01	0.47* ± 0.01
Kidney	3.14 ± 0.08	3.4 ± 0.48	22.6 ± 0.5	25.0 ± 1.72	0.47 ± 0.01	0.47 ± 0.02	0.12 ± 0.01	0.14 ± 0.02	0.42 ± 0.02	0.39* ± 0.02

Appendix C

The following appendix includes 4 figures related to chapter 4 of my thesis.

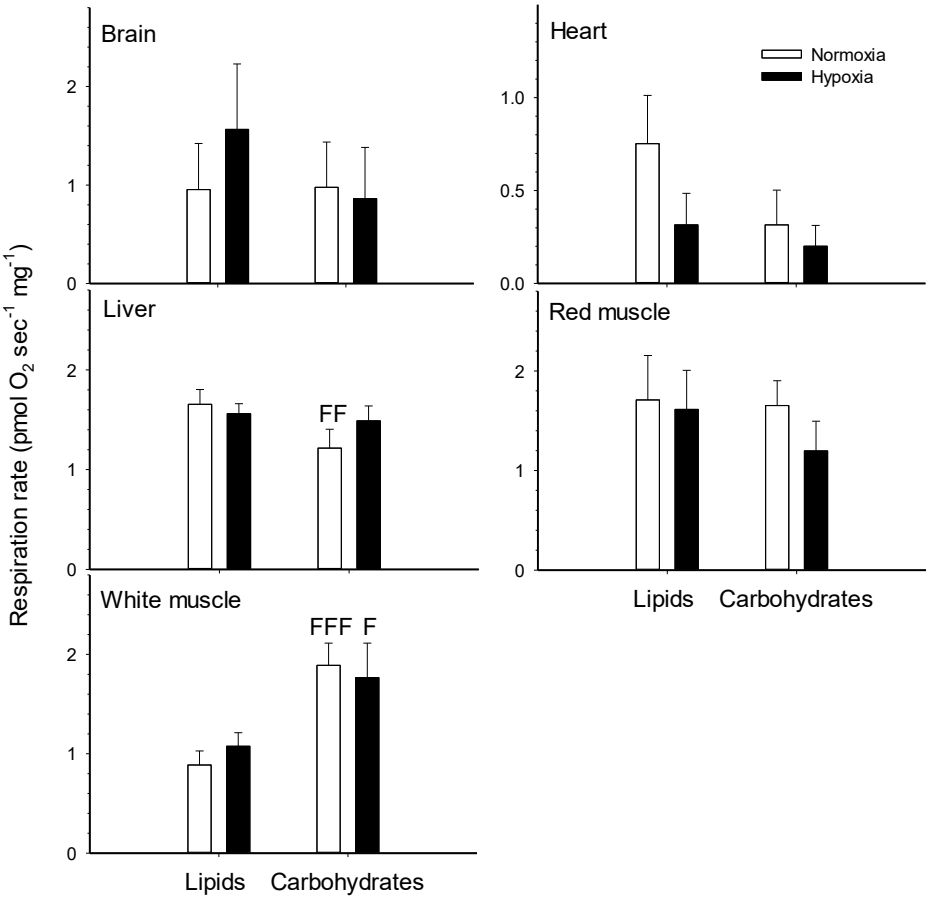

Figure 1. Mitochondrial oxidative fuel preference during LEAK respiration (non-phosphorylating) in the tissues of normoxic controls (N = 12) and hypoxia-acclimated goldfish (N = 11). Values are means ± s.e.m. Differences between fuels are indicated as F (P<0.05), FF (P<0.01) and FFF (P<0.001). There were no significant effects of hypoxia (P>0.05).

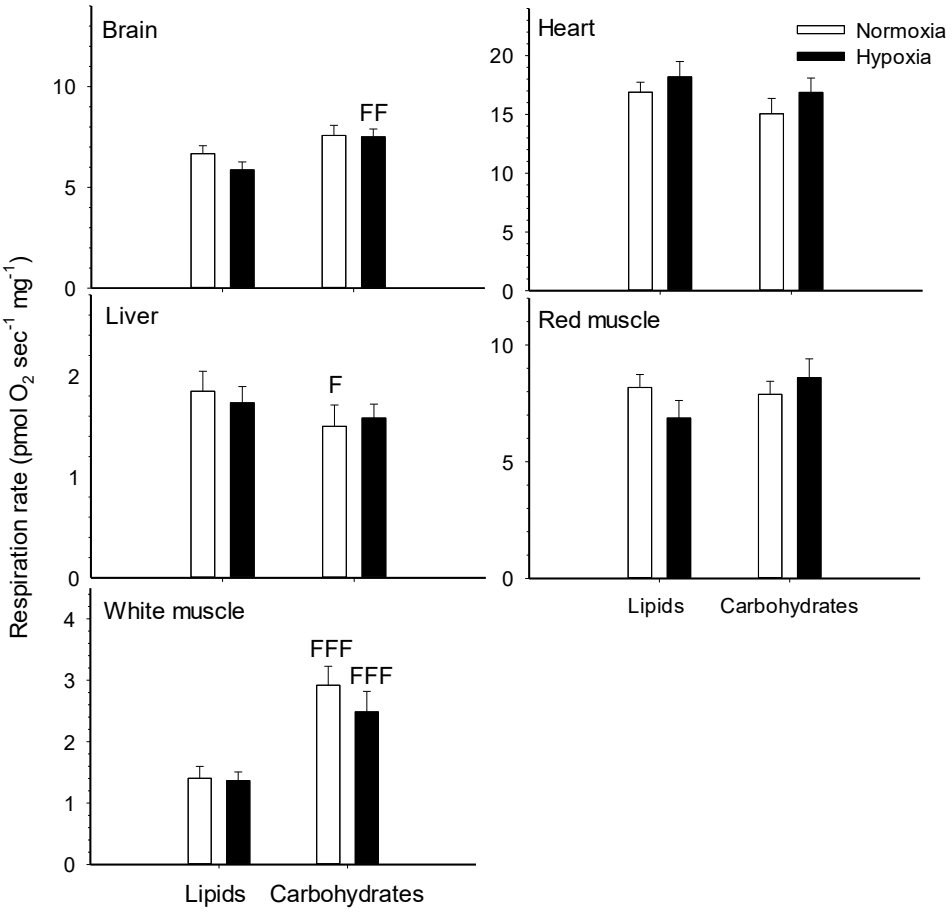

Figure 2. Mitochondrial oxidative fuel preference during state 3 respiration (OXPHOS) in the tissues of normoxic controls (N = 12) and hypoxia-acclimated (N = 11) goldfish. Values are means ± s.e.m. Differences between fuels are indicated as F (P<0.05), FF (P<0.01) and FFF (P<0.001). There were no significant effects of hypoxia (P>0.05).

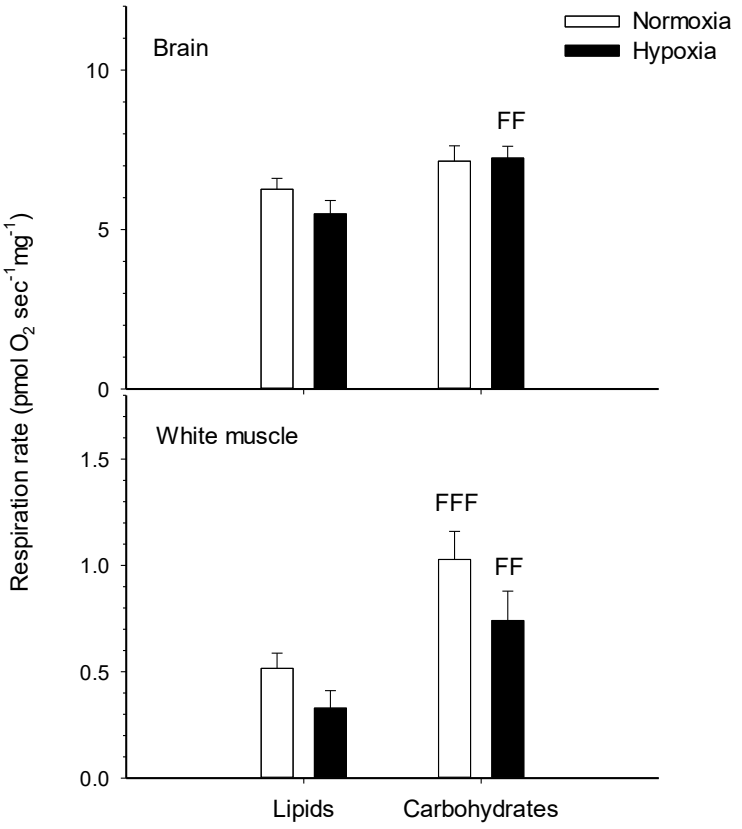

Figure 3. Mitochondrial oxidative fuel preference of aerobic scope (Calculated as OXPHOS – LEAK) in the brain and white muscle of normoxic controls (N = 12) and hypoxia-acclimated (N = 11) goldfish. Values are means ± s.e.m. Differences between fuels are indicated as FF (P<0.01) and FFF (P<0.001). There were no significant effects of hypoxia (P>0.05).

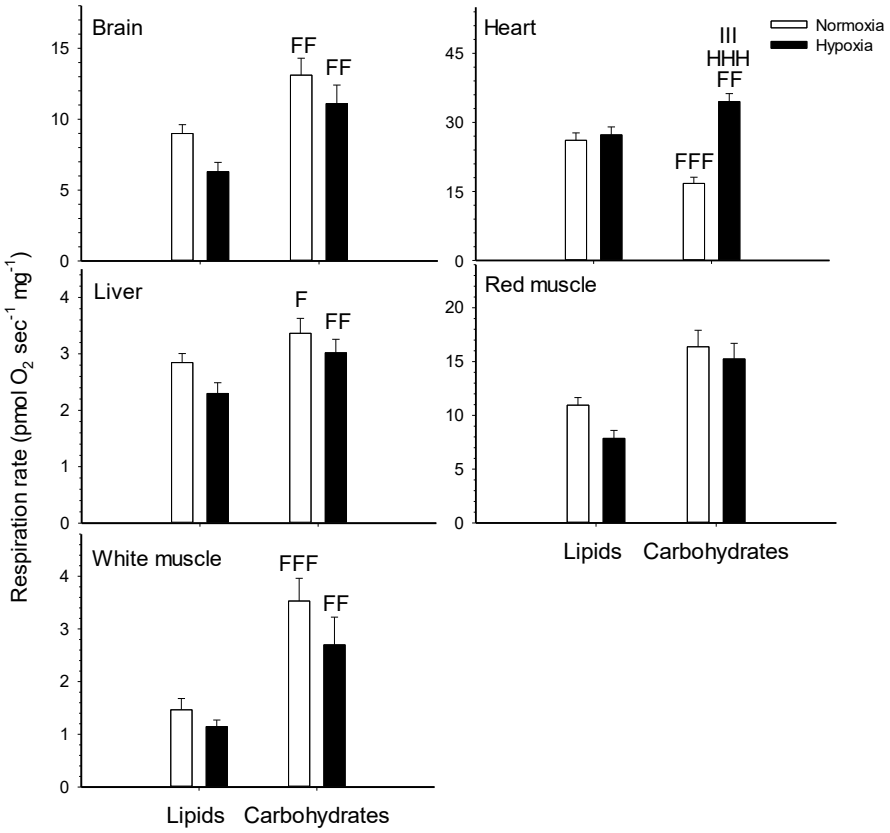

Figure 4. Mitochondrial oxidative fuel preference during the CCCP-uncoupled state in the tissues of normoxic controls (N = 12) and hypoxia-acclimated (N = 11) goldfish. Values are means ± s.e.m. Differences between fuels are indicated as F (P<0.05), FF (P<0.01) and FFF (P<0.001). Difference between oxygen levels of hypoxia is indicated as HHH (P<0.001). Significant interaction between type of fuel and oxygen is indicated as III (P<0.001).

References

Abbott, S. K., Else, P. L. and Hulbert, A. J. (2010). Membrane fatty acid composition of rat skeletal muscle is most responsive to the balance of dietary n-3 and n-6 PUFA. *British Journal of Nutrition* **103**, 522-529.

Alasnier, C., Rémignon, H. and Gandemer, G. (1996). Lipid characteristics associated with oxidative and glycolytic fibres in rabbit muscles. *Meat Science* **43**, 213-224.

Alp, P. R., Newsholme, E. A. and Zammit, V. A. (1976). Activities of citrate synthase and NAD^+-linked and $NADP^+$-linked isocitrate dehydrogenase in muscle from vertebrates and invertebrates. *Biochemical Journal* **154**, 689.

Anderson, R. L., Minton, K. W., Li, G. C. and Hahn, G. M. (1981). Temperature-induced homeoviscous adaptation of Chinese hamster ovary cells. *Biochimica et Biophysica Acta (BBA)-Biomembranes* **641**, 334-348.

Arnold, W., Giroud, S., Valencak, T. G. and Ruf, T. (2015). Ecophysiology of omega fatty acids: a lid for every jar. *Physiology* **30**, 232-240.

Bandara, K. V., Michael, M. Z. and Gleadle, J. M. (2017). MicroRNA biogenesis in hypoxia. *MicroRNA* **6**, 80-96.

Bartel, D. P. (2009). MicroRNAs: target recognition and regulatory functions. *Cell* **136**, 215-233.

Bastiaanse, E. M. L., Höld, K. M. and Van der Laarse, A. (1997). The effect of membrane cholesterol content on ion transport processes in plasma membranes. *Cardiovascular Research* **33**, 272-283.

Bell, M., Henderson, R. and Sargent, J. (1986). The role of polyunsaturated fatty acids in fish. *Comparative Biochemistry and Physiology Part B: Comparative Biochemistry* **83**, 711-719.

Benjamini, Y. and Hochberg, Y. (1995). Controlling the false discovery rate: a practical and powerful approach to multiple testing. *Journal of the Royal Statistical Society: Series B (Methodological)* **57**, 289-300.

Benzi, G., Gorini, A., Arnaboldi, R., Ghigini, B. and Villa, R. (1994). Synaptosomal non-mitochondrial ATPase activities: age-related alterations by chronic normobaric intermittent hypoxia. *Neurochemistry International* **25**, 61-67.

Berg, J., Tymoczko, J. and Stryer, L. (2007). Glycolysis and gluconeogenesis. In *Biochemistry*, pp. 433-474: Freeman WH Co. Ltd.

Best, C., Melnyk-Lamont, N., Gesto, M. and Vijayan, M. M. (2014). Environmental levels of the antidepressant venlafaxine impact the metabolic capacity of rainbow trout. *Aquatic Toxicology* **155**, 190-198.

Bickler, P. E. and Buck, L. T. (1998). Adaptations of vertebrate neurons to hypoxia and anoxia: maintaining critical Ca^{2+} concentrations. *Journal of Experimental Biology* **201**, 1141-1152.

Bickler, P. E. and Buck, L. T. (2007). Hypoxia tolerance in reptiles, amphibians, and fishes: life with variable oxygen availability. *Annual Review of Physiology* **69**, 145-170.

Block, E. R., Patel, J. M. and Edwards, D. (1989). Mechanism of hypoxic injury to pulmonary artery endothelial cell plasma membranes. *American Journal of Physiology-Cell Physiology* **257**, C223-C231.

Bourguignon, A., Rameau, A., Toullec, G., Romestaing, C. and Roussel, D. (2017). Increased mitochondrial energy efficiency in skeletal muscle after long-term fasting: its relevance to animal performance. *Journal of Experimental Biology* **220**, 2445-2451.

Boutilier, R. and St-Pierre, J. (2000). Surviving hypoxia without really dying. *Comparative Biochemistry and Physiology Part A: Molecular & Integrative Physiology* **126**, 481-490.

Boutilier, R. G. (2001). Mechanisms of cell survival in hypoxia and hypothermia. *Journal of Experimental Biology* **204**, 3171-3181.

Brown, D. and London, E. (1998). Functions of lipid rafts in biological membranes. *Annual Review of Cell and Developmental Biology* **14**, 111-136.

Buck, L. T., Land, S. C. and Hochachka, P. W. (1993). Anoxia-tolerant hepatocytes: model system for study of reversible metabolic suppression. *American Journal of Physiology-Regulatory, Integrative and Comparative Physiology* **265**, R49-R56.

Buda, C., Dey, I., Balogh, N., L.I., H., Maderspach, K., Juhasz, M., Yeo, Y. K. and Farkas, T. (1994). Structural order of membranes and composition of phospholipids in fish brain cells during thermal acclimatization. *Proceedings of the National Academy of Sciences* **91**, 8234-8238.

Bundgaard, A., Qvortrup, K., Rasmussen, L. J. and Fago, A. (2019). Turtles maintain mitochondrial integrity but reduce mitochondrial respiratory capacity in the heart after cold acclimation and anoxia. *Journal of Experimental Biology* **222**.

Bunn, H. F. and Poyton, R. O. (1996). Oxygen sensing and molecular adaptation to hypoxia. *Physiological Reviews* **76**, 839-885.

Cáceda, R., Gamboa, J. L., Boero, J. A., Monge-C, C. and Arregui, A. (2001). Energetic metabolism in mouse cerebral cortex during chronic hypoxia. *Neuroscience Letters* **301**, 171-174.

Calhoon, E. A., Ro, J. and Williams, J. B. (2015). Perspectives on the membrane fatty acid unsaturation/pacemaker hypotheses of metabolism and aging. *Chemistry and Physics of Lipids* **191**, 48-60.

Campbell, H. A., Fraser, K. P., Bishop, C. M., Peck, L. S. and Egginton, S. (2008). Hibernation in an Antarctic fish: on ice for winter. *PLoS One* **3**, e1743.

Carpenter, T. C., Schomberg, S., Nichols, C., Stenmark, K. R. and Weil, J. V. (2003). Hypoxia reversibly inhibits epithelial sodium transport but does not inhibit lung ENaC or Na-K-ATPase expression. *American Journal of Physiology-Lung Cellular and Molecular Physiology* **284**, L77-L83.

Casey, T. M., Pakay, J. L., Guppy, M. and Arthur, P. G. (2002). Hypoxia causes downregulation of protein and RNA synthesis in noncontracting mammalian cardiomyocytes. *Circulation Research* **90**, 777-783.

Chan, S. Y., Zhang, Y.-Y., Hemann, C., Mahoney, C. E., Zweier, J. L. and Loscalzo, J. (2009). MicroRNA-210 controls mitochondrial metabolism during hypoxia by repressing the iron-sulfur cluster assembly proteins ISCU1/2. *Cell Metabolism* **10**, 273-284.

Chan, Y. C., Banerjee, J., Choi, S. Y. and Sen, C. K. (2012). miR-210: The master hypoxamir. *Microcirculation* **19**, 215-223.

Chávez, J. C., Pichiule, P., Boero, J. and Arregui, A. (1995). Reduced mitochondrial respiration in mouse cerebral cortex during chronic hypoxia. *Neuroscience Letters* **193**, 169-172.

Chee, N. T., Lohse, I. and Brothers, S. P. (2019). mRNA-to-protein translation in hypoxia. *Molecular Cancer* **18**, 49.

Chen, Z., Omori, Y., Koren, S., Shirokiya, T., Kuroda, T., Miyamoto, A., Wada, H., Fujiyama, A., Toyoda, A. and Zhang, S. (2019). De novo assembly of the goldfish (Carassius auratus) genome and the evolution of genes after whole-genome duplication. *Science Advances* **5**, eaav0547.

Cheviron, Z. A., Bachman, G. C., Connaty, A. D., McClelland, G. B. and Storz, J. F. (2012). Regulatory changes contribute to the adaptive enhancement of thermogenic capacity in high-altitude deer mice. *Proceedings of the National Academy of Sciences* **109**, 8635-8640.

Cheviron, Z. A., Connaty, A. D., McClelland, G. B. and Storz, J. F. (2014). Functional genomics of adaptation to hypoxic cold-stress in high-altitude deer mice: transcriptomic plasticity and thermogenic performance. *Evolution* **68**, 48-62.

Chiang, J. Y. and Ferrell, J. M. (2020). Up to date on cholesterol 7α-hydroxylase (CYP7A1) in bile acid synthesis. *Liver Research*.

Chung, D., Dzal, Y. A., Seow, A., Milsom, W. K. and Pamenter, M. E. (2016). Naked mole rats exhibit metabolic but not ventilatory plasticity following chronic sustained hypoxia. *Proceedings of the Royal Society B: Biological Sciences* **283**, 20160216.

Chung, D., Lloyd, G. P., Thomas, R. H., Guglielmo, C. G. and Staples, J. F. (2011). Mitochondrial respiration and succinate dehydrogenase are suppressed early during entrance into a hibernation bout, but membrane remodeling is only transient. *Journal of Comparative Physiology B: Biochemical, Systemic, and Environmental Physiology* **181**, 699-711.

Cockburn, J. J. B., Abrescia, N. G. A., Grimes, J. M., Sutton, G. C., Diprose, J. M., Benevides, J. M., Thomas, G. J., Bamford, J. K. H., Bamford, D. H. and Stuart, D. I. (2004). Membrane structure and interactions with protein and DNA in bacteriophage PRD1. *Nature* **432**, 122-125.

Cook, D. G., Iftikar, F. I., Baker, D. W., Hickey, A. J. and Herbert, N. A. (2013). Low-O_2 acclimation shifts the hypoxia avoidance behaviour of snapper (Pagrus auratus) with only subtle changes in aerobic and anaerobic function. *Journal of Experimental Biology* **216**, 369-378.

Cornelius, F. (1995). Cholesterol modulation of molecular activity of reconstituted shark Na^+,K^+-ATPase. *BBA - Biomembranes* **1235**, 205-212.

Cornelius, F. (2008). Cholesterol-dependent interaction of polyunsaturated phospholipids with Na, K-ATPase. *Biochemistry* **47**, 1652-1658.

Cossins, A., Bowler, K. and Prosser, C. (1981). Homeoviscous adaptation and its effect upon membrane-bound proteins. *Journal of Thermal Biology* **6**, 183-187.

Cossins, A. R., Friedlander, M. J. and Prosser, C. L. (1977). Correlations between behavioral temperature adaptations of goldfish and the viscosity and fatty acid composition of their synaptic membranes. *Journal of Comparative Physiology A: Neuroethology, Sensory, Neural, and Behavioral Physiology* **120**, 109-121.

Costa, L. E., Boveris, A., Koch, O. R. and Taquini, A. C. (1988). Liver and heart mitochondria in rats submitted to chronic hypobaric hypoxia. *American Journal of Physiology-Cell Physiology* **255**, C123-C129.

Crockett, E. and Hazel, J. (1995). Cholesterol levels explain inverse compensation of membrane order in brush border but not homeoviscous adaptation in basolateral membranes from the intestinal epithelia of rainbow trout. *Journal of Experimental Biology* **198**, 1105-1113.

Crockett, E. L. (1998). Cholesterol function in plasma membranes from ectotherms: membrane-specific roles in adaptation to temperature. *American Zoologist* **38**, 291-304.

Crockett, E. L. and Hazel, J. R. (1997). Cholesterol affects physical properties and (Na^+, K^+)-ATPase in basolateral membranes of renal and intestinal epithelia from thermally acclimated rainbow trout. *Journal of Comparative Physiology B* **167**, 344-351.

D'Avanzo, N. (2016). Lipid regulation of sodium channels. In *Current Topics in Membranes*, vol. 78, pp. 353-407. Amsterdam, Netherlands: Elsevier.

D'Anna, F., Van Dyck, L., Xiong, J., Zhao, H., Berrens, R. V., Qian, J., Bieniasz-Krzywiec, P., Chandra, V., Schoonjans, L. and Matthews, J. (2020). DNA methylation repels binding of hypoxia-inducible transcription factors to maintain tumor immunotolerance. *Genome Biology* **21**, 1-36.

Daneshrad, Z., Garcia-Riera, M., Verdys, M. and Rossi, A. (2000). Differential responses to chronic hypoxia and dietary restriction of aerobic capacity and enzyme levels in the rat myocardium. *Molecular and Cellular Biochemistry* **210**, 159-166.

Dawson, N. J., Lyons, S. A., Henry, D. A. and Scott, G. R. (2018). Effects of chronic hypoxia on diaphragm function in deer mice native to high altitude. *Acta Physiologica* **223**.

Demel, R. A. and De Kruyff, B. (1976). The function of sterols in membranes. *Biochimica et Biophysica Acta (BBA)-Reviews on Biomembranes* **457**, 109-132.

Diaz, R. J. and Rosenberg, R. (2008). Spreading dead zones and consequences for marine ecosystems. *Science* **321**, 926-929.
Dietrich, C., Bagatolli, L., Volovyk, Z., Thompson, N., Levi, M., Jacobson, K. and Gratton, E. (2001). Lipid rafts reconstituted in model membranes. *Biophysical Journal* **80**, 1417-1428.
DiMauro, S. and Moraes, C. T. (1993). Mitochondrial encephalomyopathies. *Archives of Neurology* **50**, 1197-1208.
Dotson, R. J., Smith, C. R., Bueche, K., Angles, G. and Pias, S. C. (2017). Influence of cholesterol on the oxygen permeability of membranes: insight from atomistic simulations. *Biophysical Journal* **112**, 2336-2347.
Drynan, L., Quant, P. A. and Zammit, V. A. (1996). Flux control exerted by mitochondrial outer membrane carnitine palmitoyltransferase over β-oxidation, ketogenesis and tricarboxylic acid cycle activity in hepatocytes isolated from rats in different metabolic states. *Biochemical Journal* **317**, 791-795.
Du, S. N., Mahalingam, S., Borowiec, B. G. and Scott, G. R. (2016). Mitochondrial physiology and reactive oxygen species production are altered by hypoxia acclimation in killifish (Fundulus heteroclitus). *Journal of Experimental Biology* **219**, 1130-1138.
Dukhande, V. V., Sharma, G. C., Lai, J. C. K. and Farahani, R. (2011). Chronic hypoxia-induced alterations of key enzymes of glucose oxidative metabolism in developing mouse liver are mTOR dependent. *Molecular and Cellular Biochemistry* **357**, 189-197.
Dutta, A., Vats, P., Singh, V. K., Sharma, Y. K., Singh, S. N. and Singh, S. B. (2009). Impairment of mitochondrial β-oxidation in rats under cold-hypoxic environment. *International Journal of Biometeorology* **53**, 397.
Eckert, G. P., Igbavboa, U., Müller, W. E. and Wood, W. G. (2003). Lipid rafts of purified mouse brain synaptosomes prepared with or without detergent reveal different lipid and protein domains. *Brain Research* **962**, 144-150.
Else, P. and Wu, B. (1999). What role for membranes in determining the higher sodium pump molecular activity of mammals compared to ectotherms? *Journal of Comparative Physiology B* **169**, 296-302.
Erecińska, M. and Silver, I. A. (1994). Ions and energy in mammalian brain. *Progress in Neurobiology* **43**, 37-71.
Faulkes, C. G., Eykyn, T. R. and Aksentijevic, D. (2019). Cardiac metabolomic profile of the naked mole-rat—glycogen to the rescue. *Biology Letters* **15**, 20190710.
Fernandez, M. I. G., Ceccarelli, D. and Muscatello, U. (2004). Use of the fluorescent dye 10-N-nonyl acridine orange in quantitative and location assays of cardiolipin: a study on different experimental models. *Analytical Biochemistry* **328**, 174-180.
Forbes, J. L., Kostyniuk, D. J., Mennigen, J. A. and Weber, J.-M. (2019). Unexpected effect of insulin on glucose disposal explains glucose intolerance of rainbow trout. *American Journal of Physiology-Regulatory, Integrative and Comparative Physiology* **316**, R387-R394.
Frank, C. L. (1992). The influence of dietary fatty acids on hibernation by golden-mantled ground squirrels (*Spermophilus lateralis*). *Physiological Zoology.* **65**, 906-920.
Frank, C. L. (2002). Short-term variations in diet fatty acid composition and torpor by ground squirrels. *Journal of Mammalogy* **83**, 1013-1019.
Frank, C. L. and Storey, K. B. (1995). The optimal depot fat composition for hibernation by golden-mantled ground squirrels (*Spermophilus lateralis*). *Journal of Comparative Physiology B.* **164**, 536-542.
Frick, N. T., Bystriansky, J. S., Ip, Y. K., Chew, S. F. and Ballantyne, J. S. (2010). Cytochrome c oxidase is regulated by modulations in protein expression and mitochondrial membrane phospholipid composition in estivating African lungfish. *American Journal of Physiology-Regulatory, Integrative and Comparative Physiology* **298**, R608-R616.

Galbes, O., Goret, L., Caillaud, C., Mercier, J., Obert, P., Candau, R. and Py, G. (2008). Combined effects of hypoxia and endurance training on lipid metabolism in rat skeletal muscle. *Acta Physiologica* **193**, 163-173.

Garcia, A., Lev, B., Hossain, K. R., Gorman, A., Pham, T. H. N., Cornelius, F., Allen, T. W. and Clarke, R. J. (2019). Cholesterol depletion inhibits Na^+, K^+-ATPase activity in a near-native membrane environment. *Journal of Biological Chemistry* **294**, 5956-5969.

Gerber, L., Clow, K. A., Katan, T., Emam, M., Leeuwis, R. H., Parrish, C. C. and Gamperl, A. K. (2019). Cardiac mitochondrial function, nitric oxide sensitivity and lipid composition following hypoxia acclimation in sablefish. *Journal of Experimental Biology* **222**.

Gerson, A. R., Brown, J. C. L., Thomas, R., Bernards, M. A. and Staples, J. F. (2008). Effects of dietary polyunsaturated fatty acids on mitochondrial metabolism in mammalian hibernation *Journal of Experimental Biology* **211**, 2689-2699.

Gesser, H., Johansen, K. and Maloiy, G. (1977). Tissue metabolism and enzyme activities in the rodent Heterocephalus glaber, a poor temperature regulator. *Comparative Biochemistry and Physiology. B, Comparative Biochemistry* **57**, 293-296.

Giroud, S., Stalder, G., Gerritsmann, H., Kübber-Heiss, A., Kwak, J., Arnold, W. and Ruf, T. (2018). Dietary lipids affect the onset of hibernation in the garden dormouse (Eliomys quercinus): implications for cardiac function. *Frontiers in Physiology* **9**, 1235.

Glitsch, H. G. (2001). Electrophysiology of the sodium-potassium-ATPase in cardiac cells. *Physiological Reviews* **81 (4)**, 1791-1826.

Gomez, C. R. and Richards, J. G. (2018). Mitochondrial responses to anoxia exposure in red eared sliders (Trachemys Scripta). *Comparative Biochemistry and Physiology Part - B: Biochemistry and Molecular Biology* **224**, 71-78.

Gonzalez, A., Odjélé, A. and Weber, J.-M. (2013). PCB-153 and temperature cause restructuring of goldfish membranes: Homeoviscous response to a chemical fluidiser. *Aquatic Toxicology* **144-145**, 11-18.

Gonzalez, A., Pagé, B. and Weber, J.-M. (2015). Membranes as a possible pacemaker of metabolism in cypriniform fish: does phylogeny matter? *Journal of Experimental Biology.* **218**, 2563-2572.

Guderley, H., Kraffe, E., Bureau, W. and Bureau, D. P. (2008). Dietary fatty acid composition changes mitochondrial phospholipids and oxidative capacities in rainbow trout red muscle. *Journal of Comparative Physiology B* **178**, 385-399.

Guglielmo, C. G., Haunerland, N. H., Hochachka, P. W. and Williams, T. D. (2002). Seasonal dynamics of flight muscle fatty acid binding protein and catabolic enzymes in a migratory shorebird. *American Journal of Physiology-Regulatory, Integrative and Comparative physiology.* **282**, R1405-R1413.

Guo, W., Xie, W., Lei, T. and Hamilton, J. A. (2005). Eicosapentaenoic acid, but not oleic acid, stimulates β-oxidation in adipocytes. *Lipids* **40**, 815-821.

Gustavsson, M., Traaseth, N. J. and Veglia, G. (2011). Activating and deactivating roles of lipid bilayers on the Ca^{2+}-ATPase/phospholamban complex. *Biochemistry* **50**, 10367-10374.

Hadj-Moussa, H., Logan, S. M., Seibel, B. A. and Storey, K. B. (2018). Potential role for microRNA in regulating hypoxia-induced metabolic suppression in jumbo squids. *Biochimica et Biophysica Acta (BBA)-Gene Regulatory Mechanisms* **1861**, 586-593.

Hadj-Moussa, H. and Storey, K. B. (2020). The OxymiR response to oxygen limitation: a comparative microRNA perspective. *Journal of Experimental Biology* **223**.

Hadj-Moussa, H., Pamenter, M. E. and Storey, K. B. (2020). Hypoxic naked mole–rat brains use microRNA to coordinate hypometabolic fuels and neuroprotective defenses. *Journal of Cellular Physiology*.

Han, J., Lee, Y., Yeom, K.-H., Nam, J.-W., Heo, I., Rhee, J.-K., Sohn, S. Y., Cho, Y., Zhang, B.-T. and Kim, V. N. (2006). Molecular basis for the recognition of primary microRNAs by the Drosha-DGCR8 complex. *Cell* **125**, 887-901.

Harayama, T. and Riezman, H. (2018). Understanding the diversity of membrane lipid composition. *Nature Reviews Molecular Cell Biology*.
Hardie, D. G., Scott, J. W., Pan, D. A. and Hudson, E. R. (2003). Management of cellular energy by the AMP-activated protein kinase system. *FEBS Letters* **546**, 113-120.
Hatzimichael, E., Dasoula, A., Shah, R., Syed, N., Papoudou-Bai, A., Coley, H. M., Dranitsaris, G., Bourantas, K. L., Stebbing, J. and Crook, T. (2010). The prolyl-hydroxylase EGLN3 and not EGLN1 is inactivated by methylation in plasma cell neoplasia. *European Journal of Haematology* **84**, 47-51.
Hazel, J. R. (1995). Thermal adaptation in biological membranes: Is homeoviscous adaptation the explanation? *Annual Review of Physiology* **57**, 19-42.
He, L. and Hannon, G. J. (2004). MicroRNAs: small RNAs with a big role in gene regulation. *Nature Reviews Genetics* **5**, 522-531.
Heather, L. C., Cole, M. A., Tan, J.-J., Ambrose, L. J., Pope, S., Abd-Jamil, A. H., Carter, E. E., Dodd, M. S., Yeoh, K. K. and Schofield, C. J. (2012). Metabolic adaptation to chronic hypoxia in cardiac mitochondria. *Basic Research in Cardiology* **107**, 268.
Heckmann, L.-H., Sørensen, P. B., Krogh, P. H. and Sørensen, J. G. (2011). NORMA-Gene: A simple and robust method for qPCR normalization based on target gene data. *BMC Bioinformatics* **12**, 250.
Hickey, A. J. R., Renshaw, G. M. C., Speers-Roesch, B., Richards, J. G., Wang, Y., Farrell, A. P. and Brauner, C. J. (2012). A radical approach to beating hypoxia: depressed free radical release from heart fibres of the hypoxia-tolerant epaulette shark (Hemiscyllum ocellatum). *Journal of Comparative Physiology B* **182**, 91-100.
Hochachka, P., Stanley, C., Matheson, G., McKenzie, D., Allen, P. and Parkhouse, W. (1991). Metabolic and work efficiencies during exercise in Andean natives. *Journal of Applied Physiology* **70**, 1720-1730.
Hochachka, P. W. (1986). Defense strategies against hypoxia and hypothermia. *Science* **231**, 234-241.
Hochachka, P. W., Buck, L. T., Doll, C. J. and Land, S. C. (1996). Unifying theory of hypoxia tolerance: Molecular/metabolic defense and rescue mechanisms for surviving oxygen lack. *Proceedings of the National Academy of Sciences* **93**, 9493-9498.
Holtze, S., Braude, S., Lemma, A., Koch, R., Morhart, M., Szafranski, K., Platzer, M., Alemayehu, F., Goeritz, F. and Hildebrandt, T. B. (2018). The microenvironment of naked mole-rat burrows in East Africa. *African Journal of Ecology* **56**, 279-289.
Hossein-Javaheri, N. and Buck, L. T. (2021). GABA receptor inhibition and severe hypoxia induce a paroxysmal depolarization shift in goldfish neurons. *Journal of Neurophysiology* **125**, 321-330.
Hulbert, A. J. (2003). Life, death and membrane bilayers. *Journal of Experimental Biology* **206**, 2303-2311.
Hulbert, A. J. (2007). Membrane fatty acids as pacemakers of animal metabolism. *Lipids* **42**, 811-819.
Hulbert, A. J. and Else, P. L. (1999). Membranes as possible pacemakers of metabolism. *Journal of Theoretical Biology* **199**, 257-274.
Hulbert, A. J. and Else, P. L. (2000). Mechanisms underlying the cost of living in animals. *Annual Review of Physiology* **62**, 207-235.
Hulbert, A. J. and Else, P. L. (2005). Membranes and the setting of energy demand. *Journal of Experimental Biology* **208**, 1593-1599.
Hulbert, A. J., Faulks, S. C. and Buffenstein, R. (2006). Oxidation-resistant membrane phospholipids can explain longevity differences among the longest-living rodents and similarly-sized mice. *The Journals of Gerontology Series A: Biological Sciences and Medical Sciences* **61**, 1009-1018.

Hutter, J., Piper, H. and Spieckerman, P. (1985). Effect of fatty acid oxidation on efficiency of energy production in rat heart. *American Journal of Physiology-Heart and Circulatory Physiology* **249**, H723-H728.
Hylland, P., Milton, S., Pek, M., Nilsson, G. E. and Lutz, P. L. (1997). Brain Na^+/K^+-ATPase activity in two anoxia tolerant vertebrates: crucian carp and freshwater turtle. *Neuroscience Letters* **235**, 89-92.
Ivan, M. and Kaelin Jr, W. G. (2017). The EGLN-HIF O_2-sensing system: multiple inputs and feedbacks. *Molecular Cell* **66**, 772-779.
Ivy, C. M., Sprenger, R. J., Bennett, N. C., van Jaarsveld, B., Hart, D. W., Kirby, A. M., Yaghoubi, D., Storey, K. B., Milsom, W. K. and Pamenter, M. E. (2019). The hypoxia tolerance of 8 related African mole-rat species rivals that of naked mole-rats, despite divergent ventilatory and metabolic strategies in severe hypoxia. *Acta Physiologica*, e13436.
Ježková, J., Nováková, O., Kolář, F., Tvrzická, E., Neckář, J. and Novák, F. (2002). Chronic hypoxia alters fatty acid composition of phospholipids in right and left ventricular myocardium. *Molecular and Cellular Biochemistry* **232**, 49-56.
Jibb, L. A. and Richards, J. G. (2008). AMP-activated protein kinase activity during metabolic rate depression in the hypoxic goldfish, Carassius auratus. *Journal of Experimental Biology* **211**, 3111-3122.
Johnston, I. A. and Bernard, L. M. (1982). Ultrastructure and metabolism of skeletal muscle fibres in the tench: Effects of long-term acclimation to hypoxia. *Cell and Tissue Research* **227**, 179-199.
Kang, J. X. and Leaf, A. (1996). Evidence that free polyunsaturated fatty acids modify Na^+ channels by directly binding to the channel proteins. *Proceedings of the National Academy of Sciences* **93**, 3542-3546.
Katz, A. M., Messineo, F. C. and Herbette, L. (1982). Ion channels in membranes. *Circulation* **65 (1 Pt 2)**, I2-10.
Kennedy, S. L., Stanley, W. C., Panchal, A. R. and Mazzeo, R. S. (2001). Alterations in enzymes involved in fat metabolism after acute and chronic altitude exposure. *Journal of Applied Physiology* **90**, 17-22.
Kim, E. B., Fang, X., Fushan, A. A., Huang, Z., Lobanov, A. V., Han, L., Marino, S. M., Sun, X., Turanov, A. A., Yang, P. et al. (2011). Genome sequencing reveals insights into physiology and longevity of the naked mole rat. *Nature* **479**, 223-227.
Kimelberg, H. K. and Papahadjopoulos, D. (1974). Effects of phospholipid acyl chain fluidity, phase transitions, and cholesterol on (Na^++ K^+)-stimulated adenosine triphosphatase. *Journal of Biological Chemistry* **249**, 1071-1080.
Kolwicz, S. C., Jr and Tian, R. (2011). Glucose metabolism and cardiac hypertrophy. *Cardiovascular Research* **90**, 194-201.
Kraffe, E., Marty, Y. and Guderley, H. (2007). Changes in mitochondrial oxidative capacities during thermal acclimation of rainbow trout *Oncorhynchus mykiss*: roles of membrane proteins, phospholipids and their fatty acid compositions. *Journal of Experimental Biology* **210**, 149-165.
Kumosani, T. A. and Moselhy, S. S. (2010). Modulatory effect of cod-liver oil on Na^+-K^+ ATPase in rats' brain. *Human & Experimental Toxicology* **30**, 267-274.
Kuznetsov, A. V., Strobl, D., Ruttmann, E., Königsrainer, A., Margreiter, R. and Gnaiger, E. (2002). Evaluation of mitochondrial respiratory function in small biopsies of liver. *Analytical Biochemistry* **305**, 186-194.
Kuznetsov, A. V., Veksler, V., Gellerich, F. N., Saks, V., Margreiter, R. and Kunz, W. S. (2008). Analysis of mitochondrial function in situ in permeabilized muscle fibers, tissues and cells. *Nature Protocols* **3**, 965.

Larsen, S., Kraunsøe, R., Gram, M., Gnaiger, E., Helge, J. W. and Dela, F. (2014). The best approach: homogenization or manual permeabilization of human skeletal muscle fibers for respirometry? *Analytical Biochemistry* **446**, 64-68.

Larsen, S., Nielsen, J., Hansen, C. N., Nielsen, L. B., Wibrand, F., Stride, N., Schroder, H. D., Boushel, R., Helge, J. W., Dela, F. et al. (2012). Biomarkers of mitochondrial content in skeletal muscle of healthy young human subjects. *The Journal of Physiology* **590**, 3349-3360.

Lau, D. S., Connaty, A. D., Mahalingam, S., Wall, N., Cheviron, Z. A., Storz, J. F., Scott, G. R. and McClelland, G. B. (2017). Acclimation to hypoxia increases carbohydrate use during exercise in high-altitude deer mice. *American Journal of Physiology-Regulatory, Integrative and Comparative Physiology* **312**, R400-R411.

le Moine, C. M. R., Morash, A. J. and McClelland, G. B. (2011). Changes in HIF-1α protein, pyruvate dehydrogenase phosphorylation, and activity with exercise in acute and chronic hypoxia. *American Journal of Physiology-Regulatory Integrative and Comparative Physiology* **301**, R1098-R1104.

Lee, A. G. (2004). How lipids affect the activities of integral membrane proteins. *Biochimica et Biophysica Acta (BBA) - Biomembranes* **1666**, 62-87.

Lee, A. G. (2011). Biological membranes: the importance of molecular detail. *Trends in Biochemical Sciences* **36**, 493-500.

Lee, S. D. and Tontonoz, P. (2015). Liver X receptors at the intersection of lipid metabolism and atherogenesis. *Atherosclerosis* **242**, 29-36.

Levitan, I., Fang, Y., Rosenhouse-Dantsker, A. and Romanenko, V. (2010). Cholesterol and ion channels. In *Cholesterol Binding and Cholesterol Transport Proteins:*, pp. 509-549. New York, USA: Springer.

Lewis, R. and McElhaney, R. N. (1992). The mesomorphic phase behavior of lipid bilayers. *The Structure of Biological Membranes* **2**.

Li, J., Xu, X., Li, W. and Zhang, X. (2018). Effects of acute and chronic hypoxia on the locomotion and enzyme of energy metabolism in Chinese shrimp Fenneropenaeus chinensis. *Marine and Freshwater Behaviour and Physiology* **51**, 275-291.

Li, Y., Ge, M., Ciani, L., Kuriakose, G., Westover, E. J., Dura, M., Covey, D. F., Freed, J. H., Maxfield, F. R. and Lytton, J. (2004). Enrichment of endoplasmic reticulum with cholesterol inhibits sarcoplasmic-endoplasmic reticulum calcium ATPase-2b activity in parallel with increased order of membrane lipids. *Journal of Biological Chemistry* **279**, 37030-37039.

Lighton, J. R. (2018). Measuring metabolic rates: a manual for scientists: Oxford University Press.

Liu, L., Cash, T. P., Jones, R. G., Keith, B., Thompson, C. B. and Simon, M. C. (2006). Hypoxia-induced energy stress regulates mRNA translation and cell growth. *Molecular Cell* **21**, 521-531.

Low, P. A., Schmelzer, J., Ward, K. and Yao, J. (1986). Experimental chronic hypoxic neuropathy: relevance to diabetic neuropathy. *American Journal of Physiology-Endocrinology And Metabolism* **250**, E94-E99.

Lui, M. A., Mahalingam, S., Patel, P., Connaty, A. D., Ivy, C. M., Cheviron, Z. A., Storz, J. F., McClelland, G. B. and Scott, G. R. (2015). High-altitude ancestry and hypoxia acclimation have distinct effects on exercise capacity and muscle phenotype in deer mice. *American Journal of Physiology-Regulatory, Integrative and Comparative Physiology* **308**, R779-R791.

Lutz, P. L. and Storey, K. B. (2010). Adaptations to variations in oxygen tension by Vertebrates and Invertebrates. In *Comprehensive Physiology*, pp. 1479-1522. New Jersey, USA: John Wiley & Sons, Inc.

Madden, T. D., King, M. D. and Quinn, P. J. (1981). The modulation of Ca^{2+}-ATPase activity of sarcoplasmic reticulum by membrane cholesterol. The effect of enzyme coupling. *Biochimica et Biophysica Acta (BBA) - Biomembranes* **641**, 265-269.

Magnoni, L. and Weber, J. M. (2007). Endurance swimming activates trout lipoprotein lipase: plasma lipids as a fuel for muscle. *Journal of Experimental Biology* **210**, 4016-4023.
Mahalingam, S., McClelland, G. B. and Scott, G. R. (2017). Evolved changes in the intracellular distribution and physiology of muscle mitochondria in high-altitude native deer mice. *The Journal of Physiology* **595**, 4785-4801.
Mahfouz, M. E., Hegazi, M. M., El-Magd, M. A. and Kasem, E. A. (2015). Metabolic and molecular responses in Nile tilapia, Oreochromis niloticus during short and prolonged hypoxia. *Marine and Freshwater Behaviour and Physiology* **48**, 319-340.
Maillet, D. and Weber, J.-M. (2006). Performance-enhancing role of dietary fatty acids in a long-distance migrant: The semipalmated sandpiper. *Journal of Experimental Biology* **209**, 2686-2695.
Maillet, D. and Weber, J.-M. (2007). Relationship between n-3 PUFA content and energy metabolism in the flight muscles of a migrating shorebird: evidence for natural doping. *Journal of Experimental Biology* **210**, 413-420.
Mairbäurl, H., Wodopia, R., Eckes, S., Schulz, S. and Bärtsch, P. (1997). Impairment of cation transport in A549 cells and rat alveolar epithelial cells by hypoxia. *American Journal of Physiology-Lung Cellular and Molecular Physiology* **273**, L797-L806.
Malthankar-Phatak, G. H., Patel, A. B., Xia, Y., Hong, S., Chowdhury, G. M., Behar, K. L., Orina, I. A. and Lai, J. C. (2008). Effects of continuous hypoxia on energy metabolism in cultured cerebro-cortical neurons. *Brain Research* **1229**, 147-154.
Martens, J. R., Navarro-Polanco, R., Coppock, E. A., Nishiyama, A., Parshley, L., Grobaski, T. D. and Tamkun, M. M. (2000). Differential targeting of Shaker-like potassium channels to lipid rafts. *Journal of Biological Chemistry* **275**, 7443-7446.
Martin, N., Bureau, D. P., Marty, Y., Kraffe, E. and Guderley, H. (2013). Dietary lipid quality and mitochondrial membrane composition in trout: responses of membrane enzymes and oxidative capacities. *Journal of Comparative Physiology B* **183**, 393-408.
Martínez, M. L., Landry, C., Boehm, R., Manning, S., Cheek, A. O. and Rees, B. B. (2006). Effects of long-term hypoxia on enzymes of carbohydrate metabolism in the Gulf killifish, Fundulus grandis. *Journal of Experimental Biology* **209**, 3851-3861.
Mas-Oliva, J. and Santiago-Garcia, J. (1990). Cholesterol effect on thermostability of the (Ca^{2+}, Mg^{2+})-ATPase from cardiac muscle sarcolemma. *Biochemistry International* **21**, 233-241.
Matuleviciute, R., Cunha, P. P., Johnson, R. S. and Foskolou, I. P. (2021). Oxygen regulation of TET enzymes. *The FEBS Journal* **n/a**.
McClelland, G., Dalziel, A., Fragoso, N. and Moyes, C. (2005). Muscle remodeling in relation to blood supply: implications for seasonal changes in mitochondrial enzymes. *Journal of Experimental Biology* **208**, 515-522.
McClelland, G. B., Hochachka, P. W. and Weber, J.-M. (1998). Carbohydrate utilization during exercise after high-altitude acclimation: A new perspective. *Proceedings of the National Academy of Sciences* **95**, 10288-10293.
McCormick, S. D. (1993). Methods for Nonlethal Gill Biopsy and Measurement of Na^+, K^+-ATPase Activity. *Canadian Journal of Fisheries and Aquatic Sciences* **50**, 656-658.
McElroy, G. S. and Chandel, N. S. (2017). Mitochondria control acute and chronic responses to hypoxia. *Experimental Cell Research* **356**, 217-222.
Mennigen, J. A., Martyniuk, C. J., Seiliez, I., Panserat, S. and Skiba-Cassy, S. (2014). Metabolic consequences of microRNA-122 inhibition in rainbow trout, Oncorhynchus mykiss. *BMC Genomics* **15**, 1-20.
Metzen, E., Stiehl, D. P., Doege, K., Marxsen, J. H., Hellwig-Bürgel, T. and Jelkmann, W. (2005). Regulation of the prolyl hydroxylase domain protein 2 (phd2/egln-1) gene: identification of a functional hypoxia-responsive element. *Biochemical Journal* **387**, 711-717.

Morash, A. J., Kotwica, A. O. and Murray, A. J. (2013). Tissue-specific changes in fatty acid oxidation in hypoxic heart and skeletal muscle. *American Journal of Physiology-Regulatory, Integrative and Comparative Physiology* **305**, R534-R541.
Murphy, M. G. (1990). Dietary Fatty Acids and Membrane Protein Function. *The Journal of Nutritional Biochemistry* **1**, 68-79.
Nagahuedi, S., Popesku, J. T., Trudeau, V. L. and Weber, J.-M. (2009). Mimicking the natural doping of migrant sandpipers in sedentary quails: effects of dietary n-3 fatty acids on muscle membranes and PPAR expression. *Journal of Experimental Biology* **212**, 1106-1114.
Nallamshetty, S., Chan, S. Y. and Loscalzo, J. (2013). Hypoxia: a master regulator of microRNA biogenesis and activity. *Free Radical Biology and Medicine* **64**, 20-30.
Nikel, K. E., Shanishchara, N. K., Ivy, C. M., Dawson, N. J. and Scott, G. R. (2018). Effects of hypoxia at different life stages on locomotory muscle phenotype in deer mice native to high altitudes. *Comparative Biochemistry and Physiology Part - B: Biochemistry and Molecular Biology* **224**, 98-104.
Nikinmaa, M. and Rees, B. B. (2005). Oxygen-dependent gene expression in fishes. *American Journal of Physiology-Regulatory, Integrative and Comparative Physiology* **288**, R1079-R1090.
Nilsson, G. E. (2010). Surviving without any oxygen. In *Respiratory Physiology of Vertebrates: Life with and without oxygen*, (ed. G. E. Nilsson), pp. 300-328. Cambridge UK: Cambridge University Press.
Ortega, A. and Mas-Oliva, J. (1984). Cholesterol effect on enzyme activity of the sarcolemmal (Ca2++ Mg2+)-ATPase from cardiac muscle. *Biochimica et Biophysica Acta (BBA)-Biomembranes* **773**, 231-236.
Paajanen, V. and Vornanen, M. (2003). Effects of chronic hypoxia on inward rectifier K^+ current (IK1) in ventricular myocytes of crucian carp (Carassius carassius) heart. *Journal of Membrane Biology* **194**, 119-127.
Palmer, B. F. and Clegg, D. J. (2014). Oxygen sensing and metabolic homeostasis. *Molecular and Cellular Endocrinology* **397**, 51-58.
Palomer, E., Martín-Segura, A., Baliyan, S., Ahmed, T., Balschun, D., Venero, C., Martin, M. G. and Dotti, C. G. (2016). Aging triggers a repressive chromatin state at Bdnf promoters in hippocampal neurons. *Cell Reports* **16**, 2889-2900.
Pamenter, M. E. (2014). Mitochondria: a multimodal hub of hypoxia tolerance. *Canadian Journal of Zoology* **92**, 569-589.
Pamenter, M. E., Dzal, Y. A. and Milsom, W. K. (2015). Adenosine receptors mediate the hypoxic ventilatory response but not the hypoxic metabolic response in the naked mole rat during acute hypoxia. *Proceedings of the Royal Society of London B: Biological Sciences* **282**, 20141722.
Pamenter, M. E., Dzal, Y. A., Thompson, W. A. and Milsom, W. K. (2019). Do naked mole rats accumulate a metabolic acidosis or an oxygen debt in severe hypoxia? *Journal of Experimental Biology* **222**, jeb191197.
Pamenter, M. E., Gomez, C. R., Richards, J. G. and Milsom, W. K. (2016). Mitochondrial responses to prolonged anoxia in brain of red-eared slider turtles. *Biology Letters* **12**, 20150797.
Pamenter, M. E., Lau, G. Y., Richards, J. G. and Milsom, W. K. (2018). Naked mole rat brain mitochondria electron transport system flux and H+ leak are reduced during acute hypoxia. *Journal of Experimental Biology* **221**.
Paradies, G., Petrosillo, G., Pistolese, M. and Ruggiero, F. M. (2002). Reactive oxygen species affect mitochondrial electron transport complex I activity through oxidative cardiolipin damage. *Gene* **286**, 135-141.

Park, T. J., Reznick, J., Peterson, B. L., Blass, G., Omerbašić, D., Bennett, N. C., Kuich, P. H. J. L., Zasada, C., Browe, B. M., Hamann, W. et al. (2017). Fructose-driven glycolysis supports anoxia resistance in the naked mole-rat. *Science* **356**, 307-311.

Pastoris, O., Dossena, M., Foppa, P., Arnaboldi, R., Gorini, A., Villa, R. and Benzi, G. (1995). Modifications by chronic intermittent hypoxia and drug treatment on skeletal muscle metabolism. *Neurochemical Research* **20**, 143-150.

Pelster, B. and Egg, M. (2018). Hypoxia-inducible transcription factors in fish: expression, function and interconnection with the circadian clock. *Journal of Experimental Biology* **221**.

Pescador, N., Cuevas, Y., Naranjo, S., Alcaide, M., Villar, D., Landázuri, M. O. and Del Peso, L. (2005). Identification of a functional hypoxia-responsive element that regulates the expression of the egl nine homologue 3 (egln3/phd3) gene. *Biochemical Journal* **390**, 189-197.

Pesta, D. and Gnaiger, E. (2012). High-resolution respirometry: OXPHOS protocols for human cells and permeabilized fibers from small biopsies of human muscle. In *Mitochondrial Bioenergetics*, pp. 25-58: Springer.

Pierce, B. J., McWilliams, S. R., O'Connor, T. P., Place, A. R. and Guglielmo, C. G. (2005). Effect of dietary fatty acid composition on depot fat and exercise performance in a migrating songbird, the red-eyed vireo. *Journal of Experimental Biology* **208**, 1277-1285.

Pillet, M., Dupont-Prinet, A., Chabot, D., Tremblay, R. and Audet, C. (2016). Effects of exposure to hypoxia on metabolic pathways in northern shrimp (Pandalus borealis) and Greenland halibut (Reinhardtius hippoglossoides). *Journal of Experimental Marine Biology and Ecology* **483**, 88-96.

Pocock, R. (2011). Invited review: decoding the microRNA response to hypoxia. *Pflügers Archiv-European Journal of Physiology* **461**, 307-315.

Poveda, J. A., Giudici, A. M., Renart, M. L., Molina, M. L., Montoya, E., Fernández-Carvajal, A., Fernández-Ballester, G., Encinar, J. A. and González-Ros, J. M. (2014). Lipid modulation of ion channels through specific binding sites. *Biochimica et Biophysica Acta (BBA) - Biomembranes* **1838**, 1560-1567.

Quinlan, C. L., Perevoschikova, I. V., Goncalves, R. L., Hey-Mogensen, M. and Brand, M. D. (2013). The determination and analysis of site-specific rates of mitochondrial reactive oxygen species production. In *Methods in Enzymology*, vol. 526, pp. 189-217. Amsterdam, Netherlands: Elsevier.

Raynard, R. and Cossins, A. (1991). Homeoviscous adaptation and thermal compensation of sodium pump of trout erythrocytes. *American Journal of Physiology-Regulatory, Integrative and Comparative Physiology* **260**, R916-R924.

Regan, M. D., Gill, I. S. and Richards, J. G. (2017). Calorespirometry reveals that goldfish prioritize aerobic metabolism over metabolic rate depression in all but near-anoxic environments. *Journal of Experimental Biology* **220**, 564-572.

Reynolds, A. M., Lee, R. E. and Costanzo, J. P. (2014). Membrane adaptation in phospholipids and cholesterol in the widely distributed, freeze-tolerant wood frog, Rana sylvatica. *Journal of Comparative Physiology B* **184**, 371-383.

Richards, J. G. (2009). Metabolic and molecular responses of fish to hypoxia. In *Fish Physiology*, vol. 27 eds. J. G. Richards A. P. Farrell and C. J. Brauner), pp. 443-485: Academic Press.

Richards, J. G. (2011). Hypoxia | Metabolic rate suppression as a mechanism for surviving hypoxia. In *Encyclopedia of Fish Physiology*, (ed. A. P. Farrell), pp. 1764-1770. San Diego: Academic Press.

Richards, J. G., Farrell, A. P. and Brauner, C. J. (2009). Hypoxia. In *Fish Physiology*, vol. 27 eds. A. P. Farrell and C. J. Brauner), pp. 528. London: Academic Press.

Robertson, J. C. and Hazel, J. R. (1995). Cholesterol content of trout plasma membranes varies with acclimation temperature. *American Journal of Physiology - Regulatory, Integrative and Comparative Physiology* **269**, R1113-R1119.

Rodriguez, E., Weber, J.-M., Pagé, B., Roubik, D. W., Suarez, R. K. and Darveau, C.-A. (2015). Setting the pace of life: Membrane composition of flight muscle varies with metabolic rate of hovering orchid bees. *Proceedings of the Royal Society B: Biological Sciences* **282**, 20142232.

Rolfe, D. F. S. and Brown, G. C. (1997). Cellular energy utilization and molecular origin of standard metabolic rate in mammals. *Physiological Reviews* **77**, 731-758.

Ruf, T. and Arnold, W. (2008). Effects of polyunsaturated fatty acids on hibernation and torpor: a review and hypothesis. *American Journal of Physiology-Regulatory, Integrative and Comparative Physiology* **294**, R1044-1052.

Salin, K., Auer, S. K., Rudolf, A. M., Anderson, G. J., Selman, C. and Metcalfe, N. B. (2016). Variation in metabolic rate among individuals is related to tissue-specific differences in mitochondrial leak respiration. *Physiological and Biochemical Zoology* **89**, 511-523.

Schippers, M.-P., Ramirez, O., Arana, M., Pinedo-Bernal, P. and McClelland, Grant B. (2012). Increase in carbohydrate utilization in high-altitude Andean mice. *Current Biology* **22**, 2350-2354.

Schmidt-Rohr, K. (2020). Oxygen Is the high-energy molecule powering complex multicellular life: Fundamental corrections to traditional bioenergetics. *ACS Omega* **5**, 2221-2233.

Seebacher, F., Brand, M. D., Else, P. L., Guderley, H., Hulbert, A. J. and Moyes, C. D. (2010). Plasticity of oxidative metabolism in variable climates: Molecular mechanisms. *Physiological and Biochemical Zoology* **83**, 721-732.

Seebacher, F., Murray, S. and Else, P. (2009). Thermal acclimation and regulation of metabolism in a reptile (Crocodylus porosus): the importance of transcriptional mechanisms and membrane composition. *Physiological and Biochemical Zoology* **82**, 766-775.

Seibel, B. A. (2011). Critical oxygen levels and metabolic suppression in oceanic oxygen minimum zones. *Journal of Experimental Biology* **214**, 326-336.

Seibel, B. A., Häfker, N. S., Trübenbach, K., Zhang, J., Tessier, S. N., Pörtner, H.-O., Rosa, R. and Storey, K. B. (2014). Metabolic suppression during protracted exposure to hypoxia in the jumbo squid, Dosidicus gigas, living in an oxygen minimum zone. *Journal of Experimental Biology* **217**, 2555-2568.

Seibel, B. A., Luu, B. E., Tessier, S. N., Towanda, T. and Storey, K. B. (2017). Metabolic suppression in the pelagic crab, Pleuroncodes planipes, in oxygen minimum zones. *Comparative Biochemistry and Physiology Part B: Biochemistry and Molecular Biology*.

Sellner, P. A. and Hazel, J. R. (1982). Time course of changes in fatty acid composition of gills and liver from rainbow trout (Salmo gairdneri) during thermal acclimation. *Journal of Experimental Zoology Part A: Ecological Genetics and Physiology* **221**, 159-168.

Semenza, G. L. (2001a). HIF-1 and mechanisms of hypoxia sensing. *Current Opinion in Cell Biology* **13**, 167-171.

Semenza, G. L. (2001b). HIF-1, O_2, and the 3 PHDs: how animal cells signal hypoxia to the nucleus. *Cell* **107**, 1-3.

Semenza, G. L. (2007). Life with oxygen. *Science* **318**, 62-64.

Sepúlveda, M. R., Berrocal-Carrillo, M., Gasset, M. and Mata, A. M. (2006). The plasma membrane Ca^{2+}-ATPase isoform 4 is localized in lipid rafts of cerebellum synaptic plasma membranes. *Journal of Biological Chemistry* **281**, 447-453.

Serocki, M., Bartoszewska, S., Janaszak-Jasiecka, A., Ochocka, R. J., Collawn, J. F. and Bartoszewski, R. (2018). miRNAs regulate the HIF switch during hypoxia: a novel therapeutic target. *Angiogenesis* **21**, 183-202.

Shoubridge, E. and Hochachka, P. (1980). Ethanol: novel end product of vertebrate anaerobic metabolism. *Science* **209**, 308-309.

Simons, K. and Ikonen, E. (1997). Functional rafts in cell membranes. *Nature* **387**, 569.

Simons, K. and Sampaio, J. L. (2011). Membrane organization and lipid rafts. *Cold Spring Harbor Perspectives in Biology* **3**, a004697.

Simons, K. and Toomre, D. (2000). Lipid rafts and signal transduction. *Nature Reviews Molecular Cell Biology* **1**, 31-39.
Singer, S. J. and Nicolson, G. L. (1972). The fluid mosaic model of the structure of cell membranes. *Science* **175**, 720-731.
Smith, M. and Kemp, P. (1971). Parallel temperature-induced changes in membrane fatty acids and in the transport of amino acids by the intestine of goldfish (Carassius auratus L. *Comparative Biochemistry and Physiology Part B: Comparative Biochemistry* **39**, 357-365.
Soengas, J. L. and Aldegunde, M. (2002). Energy metabolism of fish brain. *Comparative Biochemistry and Physiology Part B: Biochemistry and Molecular Biology* **131**, 271-296.
Sokolova, I. (2018). Mitochondrial adaptations to variable environments and their role in animals' stress tolerance. *Integrative and Comparative Biology* **58**, 519-531.
Solaini, G., Baracca, A., Lenaz, G. and Sgarbi, G. (2010). Hypoxia and mitochondrial oxidative metabolism. *Biochimica et Biophysica Acta (BBA) - Bioenergetics* **1797**, 1171-1177.
Spector, A. A. and Yorek, M. A. (1985). Membrane lipid composition and cellular function. *Journal of Lipid Research* **26 (9)**, 1015-1035.
St-Pierre, J., Brand, M. D. and Boutilier, R. G. (2000a). Mitochondria as ATP consumers: cellular treason in anoxia. *Proceedings of the National Academy of Sciences* **97**, 8670-8674.
St-Pierre, J., Tattersall, G. J. and Boutilier, R. G. (2000b). Metabolic depression and enhanced O_2 affinity of mitochondria in hypoxic hypometabolism. *American Journal of Physiology-Regulatory, Integrative and Comparative Physiology* **279**, R1205-R1214.
Staples, J. F. (2014). Metabolic suppression in mammalian hibernation: The role of mitochondria. *Journal of Experimental Biology* **217**, 2032-2036.
Staples, J. F. and Brown, J. C. L. (2008). Mitochondrial metabolism in hibernation and daily torpor: a review. *Journal of Comparative Physiology B* **178**, 811-827.
Storey, K. B. (1997). Metabolic regulation in mammalian hibernation: enzyme and protein adaptations. *Comparative Biochemistry and Physiology Part A: Physiology* **118**, 1115-1124.
Storey, K. B. (2015). Regulation of hypometabolism: insights into epigenetic controls. *Journal of Experimental Biology* **218**, 150-159.
Storey, K. B. and Storey, J. M. (1990). Metabolic rate depression and biochemical adaptation in anaerobiosis, hibernation and estivation. *The Quarterly Review of Biology* **65**, 145-174.
Storey, K. B. and Storey, J. M. (2004). Metabolic rate depression in animals: transcriptional and translational controls. *Biological Reviews* **79**, 207-233.
Storey, K. B. and Storey, J. M. (2007). Tribute to PL Lutz: putting life onpause'–molecular regulation of hypometabolism. *Journal of Experimental Biology* **210**, 1700-1714.
Stramma, L., Johnson, G. C., Sprintall, J. and Mohrholz, V. (2008). Expanding oxygen-minimum zones in the tropical oceans. *Science* **320**, 655-658.
Subczynski, W. K., Hyde, J. S. and Kusumi, A. (1991). Effect of alkyl chain unsaturation and cholesterol intercalation on oxygen transport in membranes: a pulse ESR spin labeling study. *Biochemistry* **30**, 8578-8590.
Sukhum, K. V., Freiler, M. K., Wang, R. and Carlson, B. A. (2016). The costs of a big brain: extreme encephalization results in higher energetic demand and reduced hypoxia tolerance in weakly electric African fishes. *Proceedings of the Royal Society B: Biological Sciences* **283**, 20162157.
Templeman, N. M., Beaudry, J. L., Le Moine, C. M. R. and McClelland, G. B. (2010). Chronic hypoxia- and cold-induced changes in cardiac enzyme and gene expression in CD-1 mice. *Biochimica et Biophysica Acta (BBA) - General Subjects* **1800**, 1248-1255.
Tillman, T. S. and Cascio, M. (2003). Effects of membrane lipids on ion channel structure and function. *Cell Biochemistry and Biophysics* **38**, 161-190.
Tocher, D. R., Leaver, M. J. and Hodgson, P. (1998). Recent advances in the biochemistry and molecular biology of fatty acyl desaturases. *Progress in Lipid Research* **37**, 73-117.

Turk, H. F. and Chapkin, R. S. (2013). Membrane lipid raft organization is uniquely modified by n-3 polyunsaturated fatty acids. *Prostaglandins, Leukotrienes and Essential Fatty Acids (PLEFA)* **88**, 43-47.

Turner, N., Else, P. L. and Hulbert, A. (2003). Docosahexaenoic acid (DHA) content of membranes determines molecular activity of the sodium pump: implications for disease states and metabolism. *Naturwissenschaften* **90**, 521-523.

Turner, N., Haga, K. L., Hulbert, A. J. and Else, P. L. (2005). Relationship between body size, Na^+-K^+-ATPase activity, and membrane lipid composition in mammal and bird kidney. *American Journal of Physiology-Regulatory, Integrative and Comparative Physiology* **288**, R301-R310.

Valencak, T. G. and Ruf, T. (2007). N−3 polyunsaturated fatty acids impair lifespan but have no role for metabolism. *Aging Cell* **6**, 15-25.

Van den Thillart, G., Berge-Henegouwen, M. and Kesbeke, F. (1983). Anaerobic metabolism of goldfish, *Carassius auratus* (L.): ethanol and CO_2 excretion rates and anoxia tolerance at 20, 10, and 5 ^oC. *Comparative Biochemistry and Physiology Part A: Physiology* **76**, 295-300.

van den Thillart, G., Kesbeke, F. and van Waarde, A. (1980). Anaerobic energy-metabolism of goldfish,Carassius auratus (L.). *Journal of Comparative Physiology* **136**, 45-52.

van den Thillart, G. and Smit, H. (1984). Carbohydrate metabolism of goldfish (Carassius auratus L.) - Effects of long-term hypoxia-acclimation on enzyme patterns of red muscle, white muscle and liver. *Journal of Comparative Physiology B* **154**, 477-486.

van Ginneken, V. J., Snelderwaard, P., van der Linden, R., van der Reijden, N., van den Thillart, G. E. and Kramer, K. (2004). Coupling of heart rate with metabolic depression in fish: a radiotelemetric and calorimetric study. *Thermochimica acta* **414**, 1-10.

van Raaij, M. T. M., Bakker, E., Nieveen, M. C., Zirkzee, H. and van den Thillart, G. E. E. J. M. (1994). Energy status and free fatty acid patterns in tissues of common carp (Cyprinus carpio, L.) and rainbow trout (Oncorhynchus mykiss, L.) during severe oxygen restriction. *Comparative Biochemistry and Physiology Part A: Physiology* **109**, 755-767.

Van Waversveld, J., Addink, A. and van den Thillart, G. (1989). The anaerobic energy metabolism of goldfish determined by simultaneous direct and indirect calorimetry during anoxia and hypoxia. *Journal of Comparative Physiology B* **159**, 263-268.

Velasco, C., Draxl, A., Wiethuchter, A., Eigentler, A. and Gnaiger, E. (2012). Mitochondrial respiration in permeabilized fibres versus homogenate from trout heart and liver. *Mitochondrial Physiology Network* **17**, 1-12.

Vock, C., Döring, F. and Nitz, I. (2008). Transcriptional regulation of HMG-CoA synthase and HMG-CoA reductase genes by human ACBP. *Cellular Physiology and Biochemistry* **22**, 515-524.

Wang, J., Zhang, D., Du, J., Zhou, C., Li, Z., Liu, X., Ouyang, G. and Xiao, W. (2017). Tet1 facilitates hypoxia tolerance by stabilizing the HIF-α proteins independent of its methylcytosine dioxygenase activity. *Nucleic Acids Research* **45**, 12700-12714.

Waskova-Arnostova, P., Kasparova, D., Elsnicova, B., Novotny, J., Neckar, J., Kolar, F. and Zurmanova, J. (2014). Chronic hypoxia enhances expression and activity of mitochondrial creatine kinase and hexokinase in the rat ventricular myocardium. *Cellular Physiology and Biochemistry* **33**, 310-320.

Weber, J.-M. (2009). The physiology of long-distance migration: extending the limits of endurance metabolism. *Journal of Experimental Biology* **212**, 593-597.

Weber, J.-M. (2011). Metabolic fuels: regulating fluxes to select mix. *Journal of Experimental Biology* **214**, 286-294.

Weber, J.-M. (2016). Revealing how goldfish defy anoxia. *Journal of Experimental Biology* **219**, 1422-1423.

Weber, J.-M. and Haman, F. (2004). Oxidative fuel selection: adjusting mix and flux to stay alive. In *Animals and Environments*, vol. International Congress Series 1275 eds. S. Morris and A. Vosloo), pp. 22-31. Amsterdam: Elsevier.

Wilkie, M. P., Pamenter, M. E., Alkabie, S., Carapic, D., Shin, D. S. H. and Buck, L. T. (2008). Evidence of anoxia-induced channel arrest in the brain of the goldfish (Carassius auratus). *Comparative Biochemistry and Physiology Part C: Toxicology & Pharmacology* **148**, 355-362.

Wodopia, R., Ko, H. S., Billian, J., Wiesner, R., Bärtsch, P. and Mairbäurl, H. (2000). Hypoxia decreases proteins involved in epithelial electrolyte transport in A549 cells and rat lung. *American Journal of Physiology-Lung Cellular and Molecular Physiology* **279**, L1110-L1119.

Wu, B. J., Else, P. L., Storlien, L. H. and Hulbert, A. J. (2001). Molecular activity of Na^+/K^+-ATPase from different sources is related to the packing of membrane lipids. *Journal of Experimental Biology* **204**, 4271-4280.

Wu, B. J., Hulbert, A. J., Storlien, L. H. and Else, P. L. (2004). Membrane lipids and sodium pumps of cattle and crocodiles: an experimental test of the membrane pacemaker theory of metabolism. *American Journal of Physiology-Regulatory, Integrative and Comparative Physiology.* **287**, R633-R641.

Yeagle, P. L. (1983). Cholesterol modulation of ($Na^+ + K^+$)-ATPase ATP hydrolyzing activity in the human erythrocyte. *Biochimica et Biophysica Acta (BBA) - Biomembranes* **727**, 39-44.

Yeagle, P. L. (1989). Lipid regulation of cell membrane structure and function. *The FASEB journal* **3**, 1833-1842.

Yeagle, P. L. (2012). The structure of biological membranes. Boca Raton, FL: CRC Press.

Yeagle, P. L., Young, J. and Rice, D. (1988). Effects of cholesterol on sodium-potassium ATPase ATP hydrolyzing activity in bovine kidney. *Biochemistry* **27**, 6449-6452.

Yoshida, M., Muneyuki, E. and Hisabori, T. (2001). ATP synthase — a marvellous rotary engine of the cell. *Nature Reviews Molecular Cell Biology* **2**, 669-677.

Young, J. B. and Landsberg, L. (1977). Suppression of sympathetic nervous system during fasting. *Science* **196**, 1473-1475.

Zammit, V. A., Beis, I. and Newsholme, E. A. (1978). Maximum activities and effects of fructose bisphosphate on pyruvate kinase from muscles of vertebrates and invertebrates in relation to the control of glycolysis. *Biochemical Journal* **174**, 989.

Zammit, V. A. and Newsholme, E. A. (1976). The maximum activities of hexokinase, phosphorylase, phosphofructokinase, glycerol phosphate dehydrogenases, lactate dehydrogenase, octopine dehydrogenase, phosphoenolpyruvate carboxykinase, nucleoside diphosphatekinase, glutamate-oxaloacetate transaminase and arginine kinase in relation to carbohydrate utilization in muscles from marine invertebrates. *Biochemical Journal* **160**, 447.

Zehmer, J. K. and Hazel, J. R. (2004). Membrane order conservation in raft and non-raft regions of hepatocyte plasma membranes from thermally acclimated rainbow trout. *Biochimica et Biophysica Acta (BBA)-Biomembranes* **1664**, 108-116.

Zehmer, J. K. and Hazel, J. R. (2005). Thermally induced changes in lipid composition of raft and non-raft regions of hepatocyte plasma membranes of rainbow trout. *Journal of Experimental Biology* **208**, 4283-4290.

Zhou, B., Wu, R., Randall, D., Lam, P., Ip, Y. and Chew, S. (2000). Metabolic adjustments in the common carp during prolonged hypoxia. *Journal of Fish Biology* **57**, 1160-1171.